

**HYDROGEOLOGICAL AND HYDROCHEMICAL
CHARACTERISATION OF THE AREA AROUND THE KUSILE
POWER STATION, MPUMALANGA**

ANDILE E DLAMINI

Submitted in fulfilment of the academic requirements of

Master of Science in Hydrogeology

Discipline of Geological Sciences

College of Agriculture, Engineering and Science

University of KwaZulu-Natal

Durban

South Africa

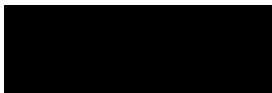
Supervisor: Prof Molla Demlie

February 2022

PREFACE

The research contained in this dissertation was completed by the candidate while based in the Discipline of Geological Sciences, School of Agricultural, Earth and Environmental Sciences of the College of Agriculture, Engineering and Science, University of KwaZulu-Natal, Westville Campus, South Africa. The research was financially supported by JG Afrika and the school through Prof. Molla Demlie.

The contents of this work have not been submitted in any form to another university and, except where the work of others is acknowledged in the text, the results reported are due to investigations by the candidate.



Signed: Andile Dlamini

Date: 27 February 2022

DECLARATION 1: PLAGIARISM

I, Andile Eugene Dlamini, declare that:

(i) the research reported in this dissertation, except where otherwise indicated or acknowledged, is my original work;

(ii) this dissertation has not been submitted in full or in part for any degree or examination to any other university;

(iii) this dissertation does not contain other persons' data, pictures, graphs or other information, unless specifically acknowledged as being sourced from other persons;

(iv) this dissertation does not contain other persons' writing, unless specifically acknowledged as being sourced from other researchers. Where other written sources have been quoted, then:

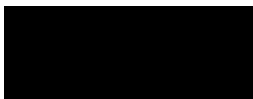
a) their words have been re-written but the general information attributed to them has been referenced;

b) where their exact words have been used, their writing has been placed inside quotation marks, and referenced;

(v) where I have used material for which publications followed, I have indicated in detail my role in the work;

(vi) this dissertation is primarily a collection of material, prepared by myself, published as journal articles or presented as a poster and oral presentations at conferences. In some cases, additional material has been included;

(vii) this dissertation does not contain text, graphics or tables copied and pasted from the Internet, unless specifically acknowledged, and the source being detailed in the dissertation and in the References sections.



Signed: Andile Eugene Dlamini

Date: 27 February 2022

DECLARATION 2: PUBLICATIONS

- Dlamini AE and Demlie, M. (2020). Integrated hydrogeological, hydrochemical and environmental isotope investigation of the area around the Kusile Power Station, Mpumalanga, South Africa. Journal of African Earth Sciences 172:103958. DOI: [10.1016/j.jafrearsci.2020.103958](https://doi.org/10.1016/j.jafrearsci.2020.103958).

Conferences Attended

1. Dlamini A.E., Demlie, M., Schapers, M., and Butler, M. (2019). Integrated hydrogeological, hydrochemical and environmental isotope investigation of the area around the Kusile Power Station, Mpumalanga, South Africa. Oral presentation at the 16th Biennial Groundwater Division Conference and Exhibition (GWD) in Port Elizabeth., 21 to 23 October 2019.


Signed: Andile Eugene Dlamini

Date: 27 February 2022

ABSTRACT

South Africa is a water-stressed country where the security of water supply has become a key strategic issue and a driver for continued and sustained economic growth and service delivery to the people of the country. Urbanisation at a rapid pace, mounting need for new energy, climate change, and swelling demands for water resources are some of the problems faced by South Africa. The construction and operations of the Kusile Power Station may release contaminants to the environment that may result in pollution of water resources. Therefore, monitoring both surface and groundwater quality and analysing the observed data are crucial for planning, resource allocation, and conservation decisions. This study investigates the hydrogeological conditions around the Kusile coal-fired power station located in quaternary catchment B20F in the Mpumalanga province of South Africa. The main aim of the research is to improve understanding of the prevailing hydrochemistry, surface water and groundwater quality and to identify the most influential processes responsible for the hydrochemical composition of groundwater and its spatial variability in the area. Hydrogeological, hydrochemical and environmental isotope ($\delta^2\text{H}$, $\delta^{18}\text{O}$, ^3H) data collected from a series of field measurements and sampling campaigns was collated, analysed and interpreted to conceptualize the hydrogeological and hydrochemical conditions of the study area. Multivariate statistical analyses including principal component analysis (PCA) and hierarchical cluster analysis (HCA) were used to evaluate the major hydrochemical processes controlling the hydrochemistry of groundwater within the study area. Furthermore, the non-parametric Mann-Kendall method was used to analyse trends in the groundwater levels together with the hydrochemical data from the year 2008 to 2018.

The results indicate that groundwater in the catchment occurs in secondary weathered and fractured aquifers made up of the Ecca Group, and fractured aquifers of the Dwyka and Pretoria Groups mainly in unconfined conditions. Borehole yields from both secondary aquifer systems range from 0.1 to 2 L/s. The weathered and fractured aquifer has a median hydraulic conductivity (K) of 0.04 m/day, while the fractured aquifers are characterised by low K values that range from 0.002 to 0.01 m/day. The mean annual groundwater recharge in the area is about 60 mm or 9% of the mean annual precipitation (MAP). The depth to groundwater level in the study area ranges from near ground surface to as deep as 23 m below ground level (b.g.l.) and the general groundwater flow direction follows the topographic gradient. Hydrochemical data

analysis of water samples collected from 25 boreholes, 6 springs, and 19 surface water points show electrical conductivity (EC) values below 700 $\mu\text{S}/\text{cm}$ and pH values ranging from 5.2 to 9.6. The dominant hydrochemical facies is Mg-HCO₃ indicating a shallow circulating less evolved recharge area groundwater. The PCA analysis identified three factors that explain the hydrochemical composition, namely the main ions' contribution to water salinity (EC), redox processes and carbonate buffering on the pH of the system. The HCA grouped the hydrochemical data into two main clusters, where Cluster-1 contains mainly surface water samples that are dominated by Ca-Mg-SO₄ water-type while Cluster-2 is dominated by Mg-HCO₃ water type. Cluster-2 is further classified into two distinct sub-clusters, in which the first subcluster (Cluster C-2-1) is characterised by groundwater samples that have low Cl⁻ and K⁺ concentrations and are located in the recharge area, while the second subcluster (Cluster C-2-2) represents groundwater samples with some hydrochemical evolution from the first, characterized by a relatively higher major ion concentration and EC values and located downstream of Cluster-2-1 samples. Environmental isotope data indicates that groundwater in the study area is recharged from local rainfall and the average residence time of groundwater in the various aquifers is relatively short, ranging from 7 to 36 years. The similarity in isotopic signature between surface water and groundwater samples in the studied catchment indicate groundwater-surface water interactions. The observed high sulphate concentrations in some groundwater and surface water samples indicate that the coal mining activities taking place within the catchment and the coal-fired power plant operations have impacted the water resources. However, due to natural carbonate buffering reactions, the pH of the high sulphate groundwater and surface water is neutral to alkaline and the EC is moderately low. From the results of the Mann-Kendall trend test and Sen's slope estimate, majority of the boreholes show decreasing groundwater level trends at a rate of decline of 0.35 m/year. It appears that the primary drivers of groundwater level decline are attributed to climate change effects on recharge and anthropogenic activities including coal mining in the area. The general long-term hydrochemical time-series data reveals a general decrease in the water quality of the study area attributed to the coal mining activities and operations at the Kusile Power Station. Increasing trends in EC, total alkalinity, Cl, K, and SO₄ were observed while pH, turbidity, Ca, Mg and Na showed decreasing trends during the period of analysis.

Key words/Phrases: Environmental isotopes; Hydrochemistry; Multivariate statistical analyses; Kusile coal-fired power station; South Africa.

ACKNOWLEDGMENTS

It is through the support of a lot of people that this work became a success, I would like to extend my sincere gratitude to all those that supported me during this journey.

I would like to thank my supervisor, Prof. Demlie Molla for allowing me the opportunity to undertake this study under his guidance. His patience, encouragement and support made this project possible.

I would like to thank the Hydrogeology team of JG Afrika that I worked with while collecting the research data, especially Mr Mark Schapers, Robert Schapers, Gary Ainsworth, Ndukenhle Mbatha, Sduduzo Ndokweni, Andile Gumede. I want to offer my warm thanks to Bheki Sibande for making the field trips memorable.

I wish to thank the South African Weather Service for supplying me with weather data. I am grateful to Eskom for permitting me to use some of the existing data. To Mike Butler of iThemba Labs, thank you for the isotope data analysis. Special thanks to UKZN for covering the cost of analysis of some of the water samples.

To my friends Zizipho, Matsatsi and Malume; thank you for your support and being pillars of strength during tough times.

Finally, I would like to thank my family, my parents Musa and Lungile Dlamini. I am grateful to my siblings Hlonie, Smiso, Tay, Wandi, Piwo, and Malindi. Thank you for your unwavering support, inspiration, and unconditional love.

TABLE OF CONTENTS

	<u>Page</u>
PREFACE	ii
DECLARATION 1: PLAGIARISM.....	iii
ABSTRACT	v
ACKNOWLEDGMENTS.....	vii
TABLE OF CONTENTS.....	viii
LIST OF TABLES.....	xii
LIST OF FIGURES.....	xiv
Chapter 1 : INTRODUCTION.....	17
1.1 Background and Rationale to the research.....	17
1.2 Problem Statement.....	18
1.3 Aims and Objectives.....	19
1.4 Outline of the dissertation/thesis structure.....	19
Chapter 2 : DESCRIPTION OF THE STUDY AREA.....	21
2.1 Location and Climate.....	21
2.2 Topography and Drainage.....	23
2.3 Geological Setting.....	23
2.3.1 Regional Geology.....	23
2.3.2 Local Geology.....	24
2.4 Hydrogeological setting.....	26
2.4.1 Weathered and fractured Aquifer.....	27
2.4.2 Fractured Aquifers.....	28
2.4.3 Groundwater Potential Zones.....	28
Chapter 3 : LITERATURE REVIEW.....	32

3.1 Introduction.....	32
3.2 Groundwater quality	33
3.2.1 Factors influencing Groundwater Quality	33
3.2.2 Hydrochemical composition of groundwater	34
3.3 Hydrochemical Data Analysis	36
3.3.1 Graphical Analysis	36
3.3.2 Univariate and Bivariate Statistical Analysis	38
Descriptive Statistics	38
Correlation Analysis.....	39
3.3.3 Multivariate Statistical Analysis	40
Factor Analysis.....	41
Hierarchical Cluster Analysis (HCA)	41
3.3.4 Time Series Trend Analysis	41
3.4 Environmental Isotopes.....	43
3.5 Development of Hydrogeological Conceptual Models	45
3.6 Previous Works in the study area.....	46
Chapter 4 : MATERIALS AND METHODS	49
4.1 Desktop study	49
4.2 Water quality monitoring network in the study area	49
4.3 Fieldwork (Sampling and Hydrocensus)	50
4.3.1 Equipment used	51
4.3.2 Field measurements	52
4.4 Quality assurance	52
4.5 Laboratory analysis.....	53
4.6 Accuracy of chemical analysis	53

4.7 Groundwater recharge.....	53
4.8 Software used for data analysis	54
Chapter 5 : RESULTS AND DISCUSSION.....	56
5.1 Introduction.....	56
5.2 Hydrogeological characteristics of the study area	56
5.2.1 Groundwater recharge	56
5.2.2 Groundwater levels and groundwater flow direction	61
5.3 Hydrogeochemical Characteristics	63
5.3.1 Descriptive Statistics and Correlation Matrices of hydrochemical data	64
5.3.2 Spatial distribution of pH and EC	69
5.3.3 Hydrochemical Facies	71
5.3.4 Hydrogeochemical Processes Controlling Major Solute Compositions	79
5.3.5 Multivariate Statistical Analysis	83
Factor Analysis.....	83
Hierarchical Cluster Analysis (HCA)	86
5.4 Saturation Index	90
5.5 Environmental Isotopes (² H, ¹⁸ O, ³ H) analyses	91
5.6 Groundwater levels and hydrochemical data trend analysis.....	96
5.6.1 Groundwater level trend analysis	96
5.6.2 Hydrochemical data trend analysis	101
5.7 Hydrogeological conceptual model for the study area	107
Chapter 6 : CONCLUSIONS AND RECOMMENDATIONS.....	110
6.1 Conclusion	110
6.2 Recommendations.....	111
REFERENCES	112

APPENDIX A: FIELD MEASURED PARAMETERS AND CALCULATED ELECTRONEUTRALITY.....	122
APPENDIX B: LABORATORY MEASURED PHYSICAL AND CHEMICAL PARAMETERS OF THE SURFACE WATER AND GROUNDWATER SAMPLES.....	124
APPENDIX C: LABORATORY MEASURED CONCENTRATIONS OF TRACE ELEMENTS	127
APPENDIX D: IONIC RATIOS USED IN HYDROCHEMICAL PROCESSES.....	130
APPENDIX E: GRAPHS OF VARIATIONS IN GROUNDWATER LEVELS.....	132
APPENDIX F: TREND ANALYSIS OF HYDROCHEMICAL DATA	138

LIST OF TABLES

<u>Tables</u>	<u>Page</u>
Table 2.1: Summary of geological units with associated aquifer types in the study area (modified from Zitholele, 2014).....	30
Table 3.1: Groundwater chemical composition divided into major and minor ions, trace constituents and dissolved gases (after Hiscock, 2005).	35
Table 3.2: Guilford's rule of thumb for interpreting correlation coefficient (adapted from Guilford, 1973).....	40
Table 3.3: Features of a conceptual Model (modified after Middlemis, 2001).	46
Table 5.1: Results of groundwater recharge estimated using the CMB method.....	57
Table 5.2: Recharge estimation using qualified guesses approach following van Tonder and Xu (2000).	58
Table 5.3: Estimation of groundwater recharge using the WTF method for the period of 2014 to 2017.....	60
Table 5.4: Descriptive statistics of the hydrochemical variables measured within the study area (all values are reported in mg/L unless and otherwise stated).	66
Table 5.5: Comparison of a statistical summary of physicochemical data of groundwater and surface water in the study area.	67
Table 5.6: Pearson's correlation matrix of hydrochemical variables analysed in the study area.	69
Table 5.7: Classification of the water in the study area based on the Piper diagram.....	73
Table 5.8: Classification of water based on the Durov diagram (after Lloyd and Heathcoat, 1985).....	78
Table 5.9: Results of principal component factor analysis of the hydrochemical data.....	85

Table 5.10: Mean concentrations of the major chemical parameters for the different clusters. All values in mg/l unless otherwise stated. 87

Table 5.11: PhreeqC saturation indices for minerals present within the study area: anhydrite, aragonite, calcite, dolomite, gypsum, and halite. 90

Table 5.12: Environmental isotope (^2H , ^{18}O , ^3H) analysis results of surface and groundwater samples. 94

Table 5.13: Results of the MK test and Sen's Slope Estimator for groundwater levels within the study area. Bold sample points are not statistically significant at 95% 100

Table 5.14: Mann-Kendal Z statistics for hydrochemical data. All results in mg/L unless indicated. Bold numbers indicate significance at 95%. 103

Table 5.15: Sen's slope values for hydrochemical data. All results in mg/L unless indicated. 105

LIST OF FIGURES

<u>Figures</u>	<u>Page</u>
Figure 2-1: Location map of the studied catchment along with surface and groundwater sampling points.	21
Figure 2-2: Mean monthly rainfall, S-Pan Evaporation rate, minimum and maximum temperatures measured at the Witbank weather station (data sourced from SAWS, 2018 and DWS, 2017; Meteorological Station: B2E001).....	22
Figure 2-3: Topography and Drainage.	23
Figure 2-4: Geological map of the study area (modified after Department of Mines, 1978; Department of Mineral and Energy Affairs, 1986).). The A-A' line indicates the cross-section direction of the proposed conceptual model.	26
Figure 2-5: Hydrogeological map of the study area (modified from DWAF, 1999).	28
Figure 2-6: Aeromagnetic total intensity map with mapped geological lineaments (Data sourced from Council for Geoscience).	29
Figure 3-1: An overview of processes that affect the water quality (Appelo and Postma, 2005).	34
Figure 3-2: Piper Trilinear Diagram (modified from Al-Kalbani et al., 2017).....	37
Figure 3-3: Durov diagram (Durov, 1948).....	38
Figure 4-1: Location of data collection sites.	50
Figure 4-2: Location of groundwater and surface water sampling locations within the study area.	51
Figure 5-1: Interpolated depth to groundwater levels of the study area.....	62
Figure 5-2: Correlation between surface topography and potentiometric heads. (Compiled from all available recorded water level data).....	62

Figure 5-3: Map showing the hydraulic head pattern, groundwater flow direction, groundwater depth within the study area.....	63
Figure 5-4: Box plots of chemical parameters used in descriptive statistics of all the water samples. Plots of Al and Mn were excluded due to their low concentrations.....	68
Figure 5-5: Spatial distribution of pH in the study area.....	70
Figure 5-6: Spatial distribution of EC in the study area.....	71
Figure 5-7: Piper Plot reflecting major hydrochemical water types.....	73
Figure 5-8: Spatial distribution of the hydrochemical water types in the study area.....	74
Figure 5-9: Stiff diagrams showing the various distinct shapes for the samples in the study area for borehole samples.....	75
Figure 5-10: Stiff diagrams showing the various distinct shapes for the samples in the study area for surface water samples and springs.....	76
Figure 5-11: Durov diagram showing mixing and reverse ion exchange as hydrochemical processes involved.....	77
Figure 5-12: Gibb's diagrams depicting the mechanism of controlling groundwater quality in the study area (a) TDS versus $Cl^-/(Cl^-+HCO_3^-)$. and (b) TDS versus $(Na^+ + K^+)/ (Na^+ + K^+ + Ca^{2+})$	79
Figure 5-13: Scatter plot of Ca^{2+}/Mg^{2+}	80
Figure 5-14: Relationship between $(Ca + Mg)$ vs. (HCO_3+SO_4)	81
Figure 5-15: Na vs. Cl scatter diagram suggesting that Na may be derived from silicate weathering.....	82
Figure 5-16: Scatter plots of main cations (a) and main anions (b) vs TDS of groundwater analysed in the study area (the regression coefficient for Na^+ , Ca^{2+} , Mg^{2+} , Cl^- , SO_4^{2-} and HCO_3^- against TDS are 0.46, 0.82, 0.89, 0.46, 0.92 and 0.25, respectively).....	83

Figure 5-17: Scree plot used to identify the three factors with eigenvalues greater than 1. The dashed line indicates eigenvalues equal to 1, and represents the ‘factorial scree’ line used in this study.	84
Figure 5-18: Principal component analyses plot of the variables in rotated space.	85
Figure 5-19: Stiff diagrams showing the average compositions of each cluster (a) Cluster 1, (b) Cluster C-2-1 and (c) Cluster C-2-2.	88
Figure 5-20: HCA Dendrogram of the hydrochemical samples for the study area.	89
Figure 5-22: Stable environmental isotope ($\delta^{18}\text{O}$ and $\delta^2\text{H}$) plot of water samples for the study area along with GMWL and the Pretoria LMWL.	92
Figure 5-23: Plot of $\delta^{18}\text{O}$ versus EC values of the water samples within the study area.	93
Figure 5-24: Boreholes considered for trend analysis within the monitoring network.	98
Figure 5-25: Selected time-series graphs of groundwater levels. An increasing trend in groundwater levels for (a) Borehole DWBH-06 and (b) decreasing trend in groundwater levels for Borehole 10490-21.	99
Figure 5-26: Selected time-series graphs displaying trends of the hydrochemical data. (a) an increasing trend of pH in borehole KP05 and (b) an increasing trend of turbidity in borehole 10490-27.	102
Figure 5-27: Well to well log geological cross-section from A-A.	108
Figure 5-28: Conceptual hydrogeological model of the study catchment based on a southeast-northwest cross-section line.	109

CHAPTER 1 : INTRODUCTION

1.1 Background and Rationale to the research

South Africa is a water-stressed country, where the security of water supply has become a key strategic issue and a driver for continued and sustained economic growth and service delivery to the people of the country (Manders et al., 2009). According to WWF-SA (2017), physical water scarcity in South Africa will be a reality by 2025. Therefore, studying, monitoring, conserving and managing the water resources of the country, including groundwater resources are crucial for future water security.

A third of the world population is estimated to be dependent on groundwater resources for various purposes (Marghade et al., 2010), with more than half of drinking water being supplied from groundwater (Harter, 2003). In South Africa, the contribution of groundwater to the total water supply is estimated between 13% and 15% (Mpenyana-Monyatsi et al., 2012). In most rural areas of the country, including Mpumalanga, groundwater is primarily used for domestic purposes without treatment (Mpenyana-Monyatsi et al., 2012).

Groundwater quantity and quality monitoring is the starting point for planning, allocation, and conservation decisions (Mechlem, 2016). However, the International Groundwater Resources Assessment Centre (IGRAC, 2008), states that organised groundwater quantity and quality monitoring is either minimal or lacking in many countries of the world. The consequences of not monitoring groundwater resources will result in degradation of the resource either due to over-abstraction or contamination (Goussard, 2017), which may result in, among others, the following:

- Declining groundwater levels and depletion of groundwater reserves,
- Reductions in stream/spring baseflow or flows to sensitive ecosystems such as wetlands,
- Reduced access to groundwater water for drinking water supply and irrigation,
- Use restrictions due to deterioration of groundwater quality,
- Increased costs of pumping and treatment,
- Subsidence and foundation damage.

Groundwater monitoring programmes are used to check the status of water resources and how well pollution control measures are working. The development and implementation of water resources monitoring programmes are very important to readily identify and mitigate any

potential sources of contamination and are therefore the first line of prevention (Barnes and Vermeulen, 2012).

Similarly, the construction and operational activities of the Kusile Coal-fired Power Station (KPS) located in the Mpumalanga Province of South Africa may pollute surface and groundwater resources around the area. The main possible sources of groundwater contamination around the KPS include fly ash disposal, coal stockpiling, domestic and other solid waste, sewage, general surface run-off from the power station and waste water dams. Other minor groundwater pollution potential related to the construction and operation of the power station include heavy machinery oil leaks, grease and related wastes. Considering all these possible sources of groundwater pollution associated with power stations, the KPS has been running a surface water and groundwater monitoring programme since 2008, where surface and groundwater sampling has been conducted on a monthly basis. The purpose of the monitoring programme is to detect any changes and/or deterioration of water quality from construction and operational activities at the site. However, the monitored data has not been systematically integrated and interpreted to understand the state of the surface and groundwater quality around the footprint area of the KPS.

Thus, this M.Sc. study envisages to understand the impact of the KPS construction and operational activities on the surrounding groundwater resources systematically interpreting the monitored data complemented with new data generated in this study. The study is undertaken by characterising the prevailing hydrogeological and hydrochemical characteristics of the area around the KPS including the origin, recharge, flow conditions and identification of the dominant hydrochemical facies and the most influential variables responsible for the observed groundwater chemistry in the area. The results will help in advocating for effective and sustainable management and protection of water resources against contamination around the footprint areas of the KPS.

1.2 Problem Statement

The construction and operations at the KPS releases waste to the environment that may result in groundwater pollution. The KPS has been monitoring surface water and groundwater quality since 2008 on a monthly basis. However, the monitored data has not been systematically integrated and interpreted to understand the state of the surface and groundwater quality around

the footprint area of the KPS. Furthermore, the hydrogeology of the area around the KPS is poorly understood.

1.3 Aims and Objectives

The main aim of the research project is to study the groundwater quality around the KPS and its evolution through time to understand the impact of the construction and operation of the coal-fired power station on the water resources.

The specific objectives of the research are to:

- Estimate the groundwater recharge rate in the study area.
- Classify and characterise the groundwater hydrochemically and identify the most critical hydrogeochemical processes controlling the groundwater chemistry using an integrated approach.
- Identify significant trends in groundwater levels and hydrochemical parameters
- Develop a conceptual hydrogeological model representing the hydrogeological regime based on all data collected.

1.4 Outline of the dissertation/thesis structure

The thesis is divided into six chapters with each chapter briefly summarised as follows:

Chapter 1 introduces the study by presenting the background, rationale, problem statement, aims and objectives of the research.

Chapter 2 describes the study area with reference to its location, climatic conditions, topography and drainage patterns, geological setting, and hydrogeology.

Chapter 3 presents the literature review that describe water quality and factors affecting water quality, and the different tools and methods used to assess hydrochemical data. In addition, approaches and methods employed in developing hydrogeological conceptual models are discussed. Relevant previous works conducted within the study area are reviewed as well.

Chapter 4 elaborates on the research methodology together with approaches employed during data collection, analysis and interpretations.

Chapter 5 reports on the main results obtained during the course of the study and discussions. The hydrogeological, hydrochemical, and isotope characteristics of the area are reported. Based on the results and interpretations, a conceptual hydrogeological model is proposed.

Chapter 6 presents the main findings emanating from the research and some recommendations are made.

CHAPTER 2 : DESCRIPTION OF THE STUDY AREA

2.1 Location and Climate

South Africa has been divided into 1946 quaternary catchments by the Department of Water and Sanitation (DWS). These quaternary catchments are the basic units for water resources assessment and management. The study area is located in quaternary catchment B20F, having a surface area of 505 square kilometres. This catchment lies within the borders of the provinces of Mpumalanga and Gauteng. The Kusile Power Station is located within this quaternary catchment as shown in Figure 2-1. The Kusile Power Station is one of the three power stations under construction by South Africa's power utility, Eskom. The power station lies on a 2500 ha land of Klipfontein 566 JR and Hartbeestfontein 537 JR which is under the jurisdiction of the Victor Khanye Local Municipality in Nkangala District of Mpumalanga Province. It is located approximately 25 km north of Ogies, 40 km north of Bronkhorstspuit and 50 km west of the town of Emalahleni.

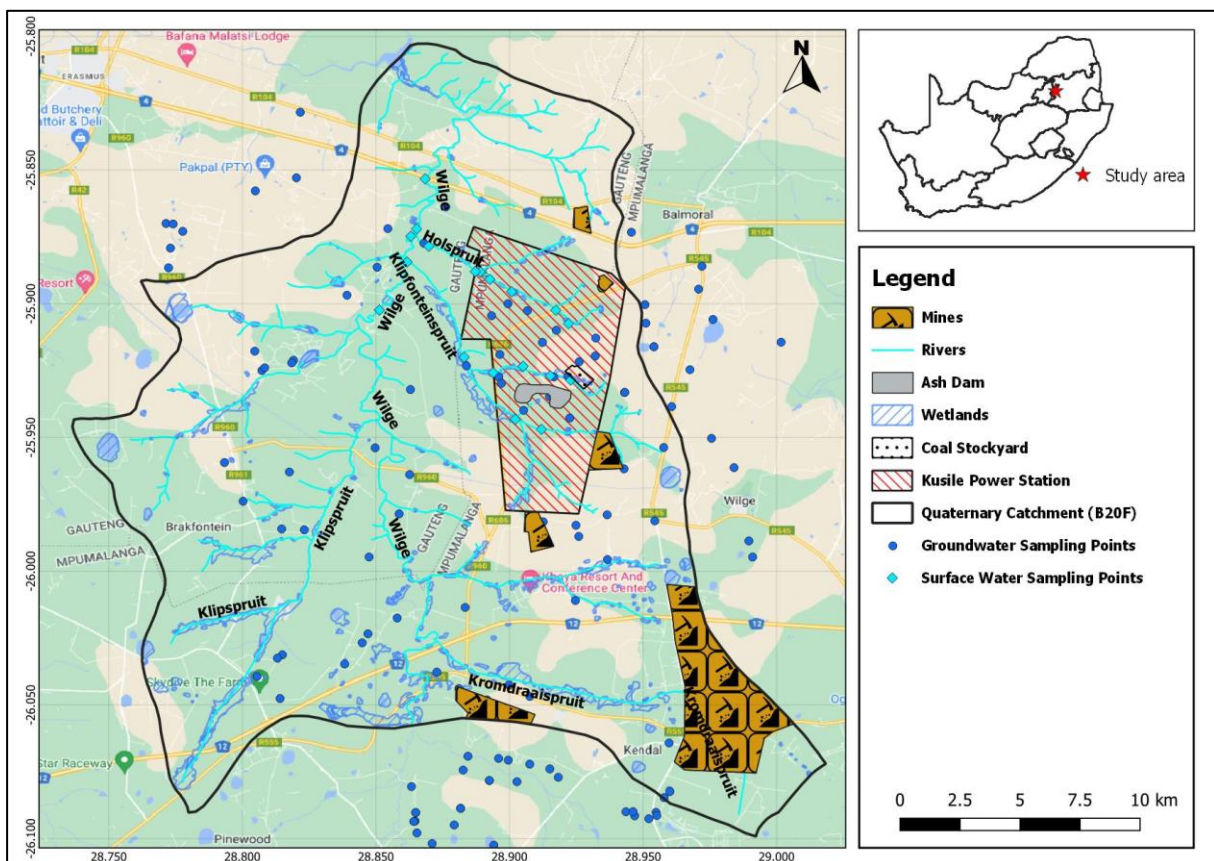


Figure 2-1: Location map of the studied catchment along with surface and groundwater sampling points.

The study area is characterised by moderate summers and cold winters with average daytime summer and winter temperatures of 25°C and 20°C, respectively, which is typical of the South African Highveld climate (DWS, 2017). The climate of the study area is controlled mainly by the movement of air masses linked to the seasonal migration of the Inter-Tropical Convergence Zone (ITCZ) (Banks et al., 2011). The study area is characterised by strong seasonal rainfall variations with most rain occurring in the summer period (October to April), with maximum rainfall occurring in the period from November to January (Figure 2.2). The winter months are generally cool and dry. The mean annual precipitation of the area is about 644 mm as measured from the Witbank weather station (SAWS, 2018). The mean annual S-Pan evaporation is 1523 mm/a (DWS, 2017). The average monthly S-Pan evaporation for the period 1968 to 2017 as recorded from the B2E001 meteorological station is shown in Figure 2-2.

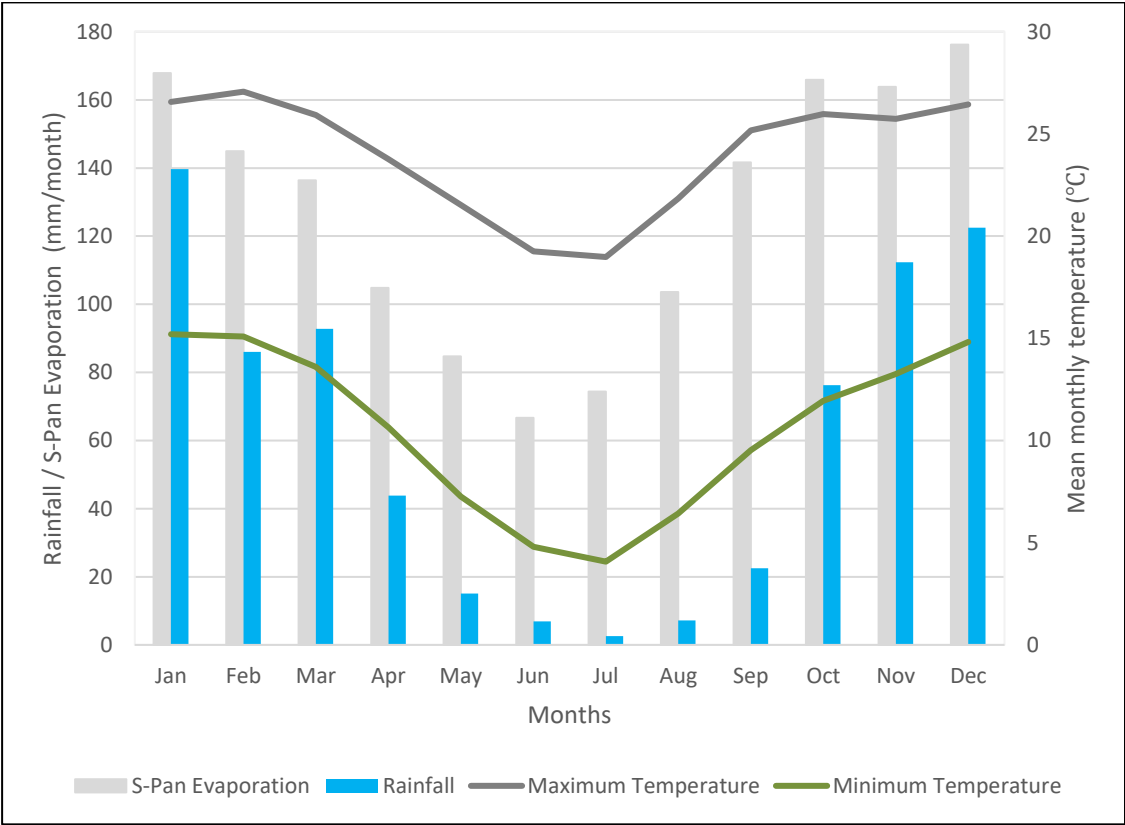


Figure 2-2: Mean monthly rainfall, S-Pan Evaporation rate, minimum and maximum temperatures measured at the Witbank weather station (data sourced from SAWS, 2018 and DWS, 2017; Meteorological Station: B2E001).

2.2 Topography and Drainage

The surface topography around the study area consists of a gently undulating plateau of the Highveld region with gently sloping hills. The highest point of the area has an altitude of 1633 meters above mean sea level (m amsl) on the south-eastern section of the site. The lowest point is 1374 m amsl on the northern area of the site (Figure 2-3). The B20F quaternary catchment falls drained by the Wilge River which is part of the Upper Olifants Water Management Area (WMA). The Klipfonteinspruit and Holfonteinspruit are the major perennial tributaries of the Wilge River. The Wilge River flows in a northerly direction and drains into the Olifants River.

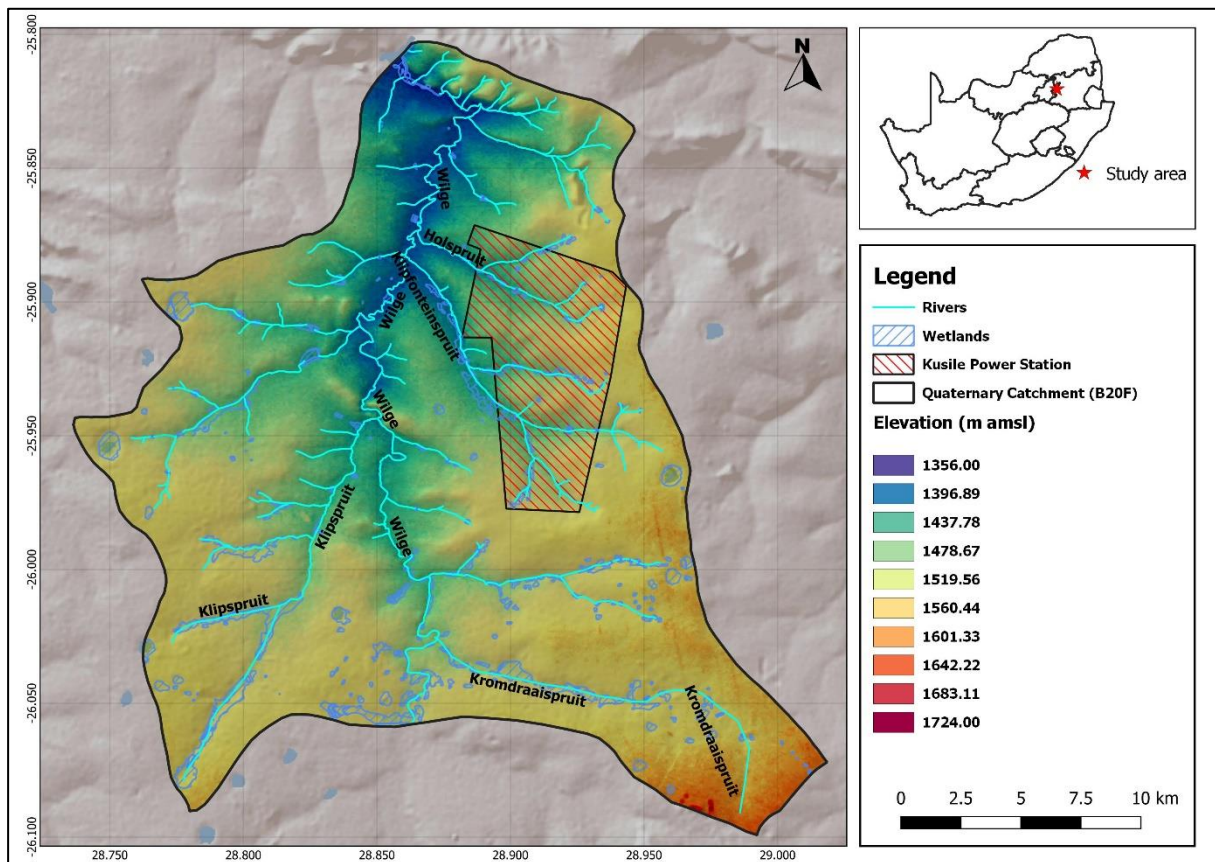


Figure 2-3: Topography and Drainage.

2.3 Geological Setting

2.3.1 Regional Geology

The regional geology (from oldest to youngest) of the study area comprises of the Pretoria Group, Rooiberg Group, Waterberg Group, the Karoo Supergroup, and Quaternary Sediments. These rocks have been intruded by diabase dykes and sills of Proterozoic to Phanerozoic age.

The Pretoria Group consists of mainly mudrocks alternating with quartzitic sandstones, subordinate conglomerates, diamictites and carbonate rocks. All these rocks have undergone low-grade metamorphism (Eriksson et al., 2006). The Pretoria Group is overlain by the Rooiberg Group which is made up of a suite of Precambrian magmatic rocks that are part of the Bushveld Magmatic Province (BMP). These volcanics have a thickness of up to 400 m and are characterised by thin interbedded, laterally extensive sedimentary strata. There are four Formations within this Group: the Dullstroom Formation at the base of the succession, the Damwal Formation, Kwaggasnek Formation, and the younger Schrikkloof Formation (Eriksson et al., 2006).

The Rooiberg Group is unconformably overlain by the Waterberg Group which is subdivided into three subgroups; the Nylstroom, Matlabas and Kransberg Subgroups. The Waterberg Group is typically represented by dark greyish red rocks, with the red colour signifying oxidation of haematite in the early diagenetic history of the rock. All three Subgroups display an upward-fining sequence. In the study area, the Waterberg Group is represented by the Wilge River Formation. The Wilge River Formation comprises mostly of red-bed sandstones, while conglomerate interbeds and mudrocks are least common (Eriksson et al., 2006).

The Waterberg Group is overlain unconformably by the Karoo Supergroup. The deposition period of the Karoo Supergroup ranges from Late Carboniferous to Middle Jurassic, attaining a total cumulative thickness of nearly 12 km (Johnson et al., 2006). The Karoo Supergroup is grouped into five successive Groups (from bottom to top); the Dwyka Group; Ecca Group; Beaufort Group; Stormberg Group; and the Drakensburg Group.

2.3.2 Local Geology

The geology of the area around the Kusile Power Station comprises of sedimentary rocks of the Pretoria Group and the Karoo Supergroup sediments. These have been intruded by diabase dykes and sills (Figure 2-4). The oldest rocks in the study area are sediments of the Pretoria Group, of which the Dasport Formation is the basement rock which is overlain by the Silverton Formation (Department of Mines, 1978; Department of Mineral and Energy Affairs, 1986). The Dasport Formation comprises mainly mature quartz arenites and subordinate mudrocks. However, least common are immature sandstones, pebbly arenites and conglomerates. These sediments are presumed to have been deposited in shallow marine and fluvial environments, indicative of the commencement of a main marine transgression event, accountable for the

deposition of the overlying Silverton Formation. The Silverton Formation made up of shale (carbonaceous in places), hornfels, and chert (Department of Mines, 1978; Department of Mineral and Energy Affairs, 1986).

The Pretoria Group in the study area is unconformably overlain by the Karoo Supergroup sediments comprising of the Dwyka tillite and the Eccca Group sediments (shale, shaly sandstone, grit, sandstone, conglomerate, coal in places near base and top). These rocks have been intruded by diabase dykes (Department of Mines, 1978; Department of Mineral and Energy Affairs, 1986). The Dwyka Group was reported to be deposited by glacial processes eroded from the underlying rocks (Johnson et al., 2006), the evidence of which are the presence of stratified glacial pavements. The Dwyka Group comprises mostly diamictite (tillite) which is generally massive with little jointing, but it is stratified in places. With subordinate rock types of conglomerate, sandstone, rhythmite and mudrock (Woodford and Chevallier 2002).

The Vryheid Formation of the Eccca Group occurs in the study. It comprises of mudrock, rhythmite, siltstone and fine- to coarse-grained sandstone (pebbly in places) and is known to contain up to five economic coal seams. The lithofacies in the Formation are typically upward-coarsening deltaic cycles (Woodford and Chevallier 2002).

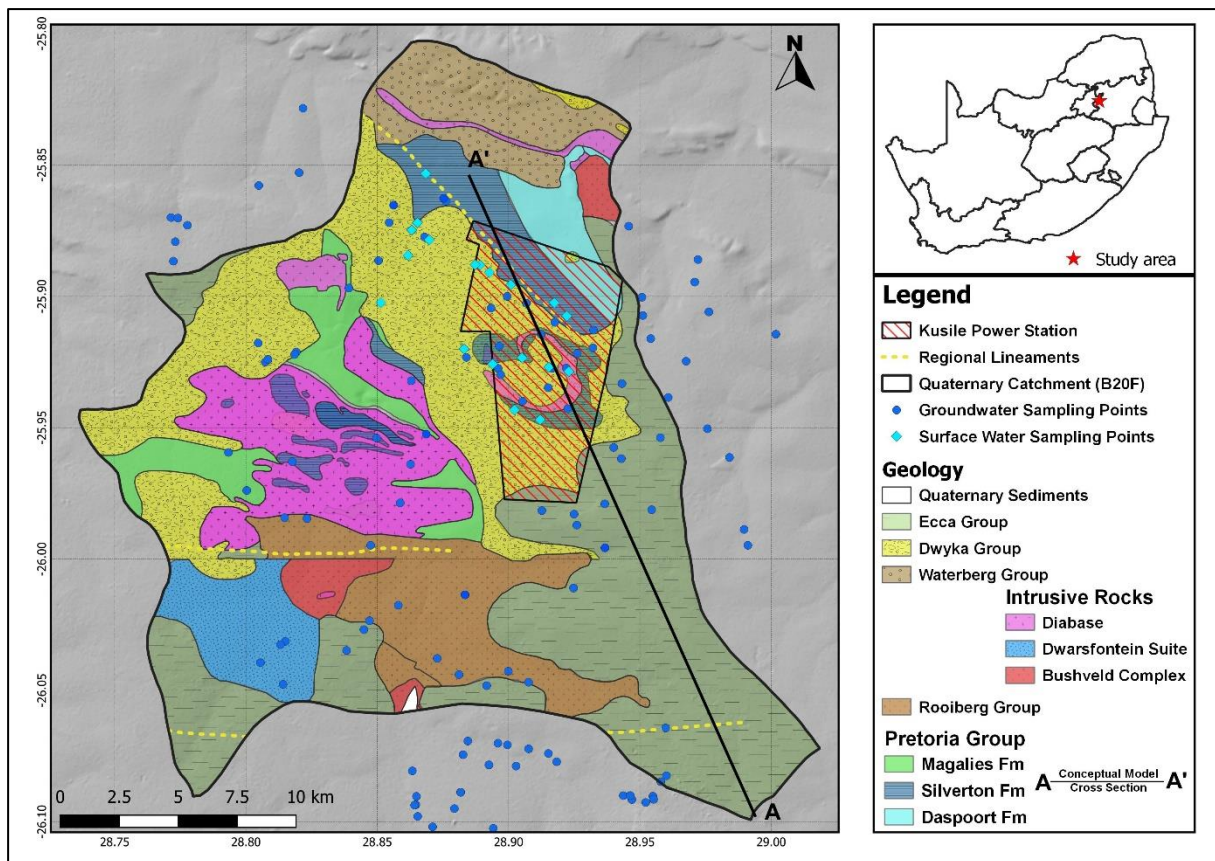


Figure 2-4: Geological map of the study area (modified after Department of Mines, 1978; Department of Mineral and Energy Affairs, 1986.). The A-A' line indicates the cross-section direction of the proposed conceptual model.

2.4 Hydrogeological setting

The regional geohydrological characteristics within the study area are expected to be controlled by the host geology. The southern and central extents of the study area is predominantly underlain by consolidated sediments of the Karoo Supergroup (Dwyka and Ecca Groups) and the Wilge Formation is limited to the northern part. The Pretoria Group is sparsely distributed, diabase intrusions are in the central areas and the intrusive rocks of the Dwarsfontein Suite and the Bushveld Complex are predominantly limited to the south-central parts. Based on Zitholele (2014), the relationship between the study area's geology and aquifer systems is summarised in Table 2.1.

Based on a review of the 1:500 000 Sheet 2526 national hydrogeological map (DWAf, 1999) and existing hydrogeological data, two aquifer types are recognised in the study area (Figure 2-5). These are intergranular and fractured aquifers, and fractured aquifers (Banks et al., 2011).

A large portion of the southern part of the study area has median borehole yields that range from 0.1 to 0.5 l/s, while a small portion on the northern part has yields in the range from 0.5 to 2 l/s. The overall groundwater electrical conductivity (EC) is less than 70 mS/m. The hydrogeological characteristics of the various aquifers that occur in the study area are described below.

2.4.1 Weathered and fractured Aquifer

In an intergranular and fractured aquifer type, groundwater is contained in intergranular interstices and fractures. Rocks of the Pretoria Group, Rooiberg Group, Bushveld Complex, and the Karoo Supergroup all display characteristics of the intergranular and fractured system (DWAF, 1999).

Weathering depths of the sandstones and shales of the Vryheid Formation is between 5 and 12 m below the surface (Banks et al., 2011). However, in certain areas, they may be as thin as 0.2 m and as thick as 50 m. This weathered zone forms the upper aquifer and groundwater frequently found within a few metres below the surface. The lower boundary of this aquifer tends to be the fractured zone (Banks et al., 2011). Dolerite dykes, paleo-topographic highs in the bedrock, and areas where the surface topography cuts below the groundwater table at streams result in the groundwater to discharge at the surface, giving rise to shallow water levels, springs and seepage zones (Hodgson and Krantz, 1998). The weathered and fractured aquifers in the study area gets small percentage of rainfall recharge and the aquifer is significantly utilised for various purposes. The estimated annual recharge ranges between 1 and 3% of the mean annual precipitation (MAP) (Banks et al., 2011). Due to the limited recharge thickness, the aquifer tends to be low yielding with typical compressor yields of one litre per second. High yielding boreholes may be expected if the aquifer is thick due to significant bedrock fracturing, where borehole yields can be as high as 5 L/s (Banks et al., 2011).

On a few occasions where drilling has intersected the basement below the Karoo Supergroup, and when intersected, this aquifer is regarded as insignificant for several reasons, including its great depth, low yielding fractures, inferior water quality with elevated concentrations of fluoride associated with the granitic rocks, and Low recharge characteristics of this aquifer because of the overlying impermeable Dwyka tillite (Banks et al., 2011). Generally, fresh tillite is considered to have a very low permeability, evidenced in instances where boreholes have been drilled (Hodgson and Krantz, 1998).

2.4.2 Fractured Aquifers

The fractured aquifers are limited to the northern part of the study area that is underlain by the Wilge River Formation of the Waterberg Group. The fractured aquifer is arranged into two borehole yield classes: b2 with borehole yields of 0.5-2.0 l/s and b3 with borehole yields of 0.5-2.0 l/s (DWAF, 1999). Groundwater occurrence is controlled by contacts between lithologies and these contacts are either open, weathered, or fractured.

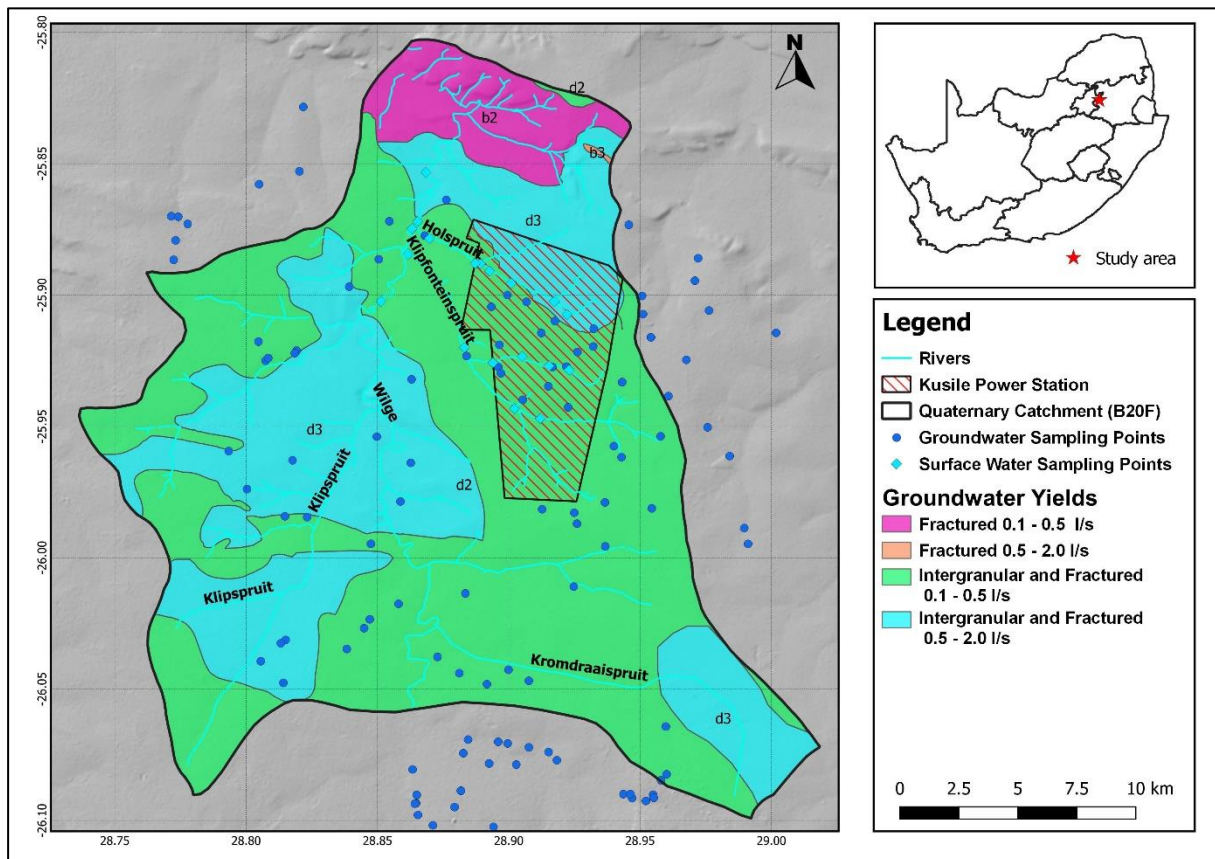


Figure 2-5: Hydrogeological map of the study area (modified from DWAF, 1999).

2.4.3 Groundwater Potential Zones

The total aeromagnetic data (Figure 2-6) in the study area was collected in 1977 at a flight height of 150m with a line spacing of 1km (Ledwaba et al., 2009). Lineaments have a close relationship with groundwater flow and yield as lineaments are typically underlain by zones of localised weathering, high permeability and porosity (Mabee et al., 2009). The regional lineaments were mapped from the existing regional geology maps, while the localised lineaments were digitized from the Advanced Spaceborne Thermal Emission and Reflection Radiometer (ASTER) Digital Elevation Model (DEM). The most prominent linear feature is

northwest to southeast trending with a noticeable aeromagnetic signature on the northern part of the study, this corresponds with the regional lineament from the geology maps. Southwest of the study area is a low to moderate magnetism, corresponding to Dwarsfontein Suite which comprises of pyroxenite, gabbro, and anorthosite. The central part with high magnetism is underlain by diabase and granitic rocks of the Lebowa Granite Suite of the Bushveld Complex.

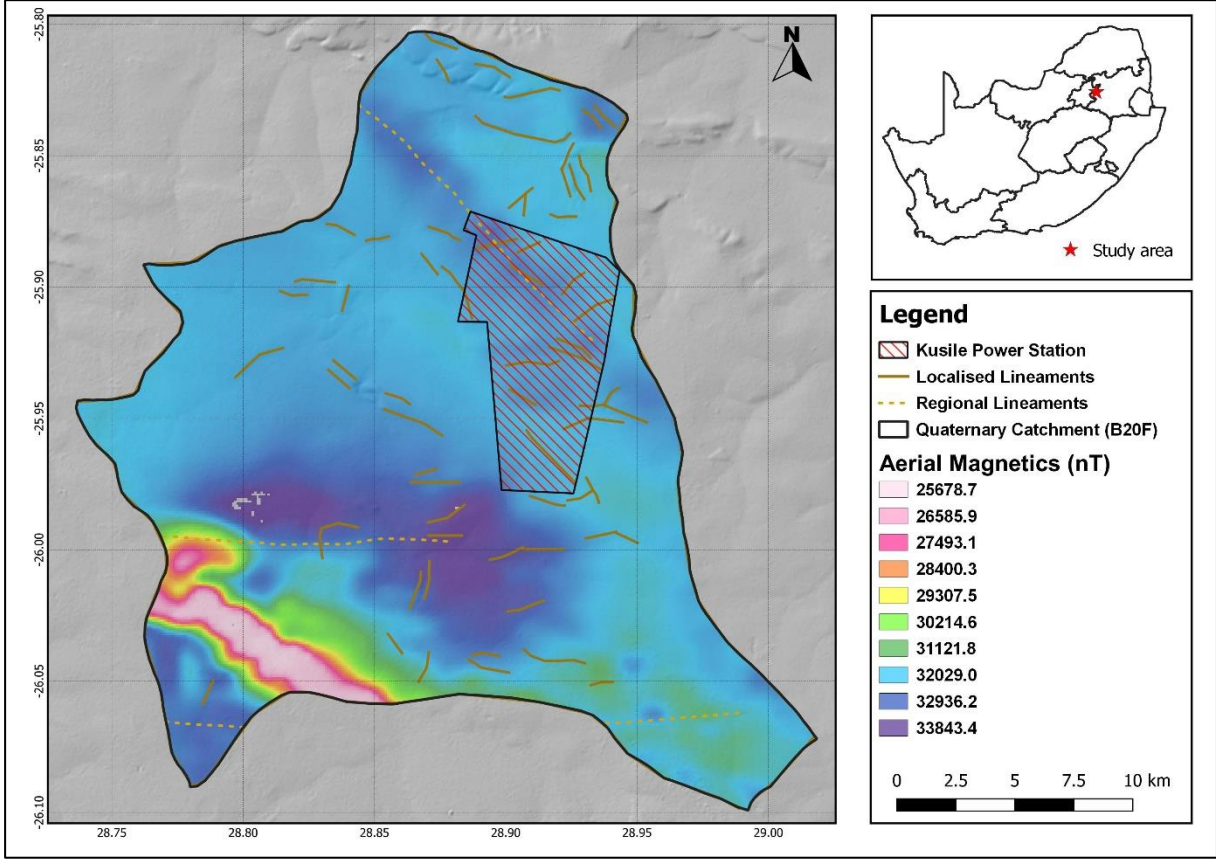


Figure 2-6: Aeromagnetic total intensity map with mapped geological lineaments (Data sourced from Council for Geoscience).

Table 2.1: Summary of geological units with associated aquifer types in the study area (modified from Zitholele, 2014).

Geology		Aquifer Type	Groundwater Occurrence	Maximum borehole yield (l/s)	Range of water level (m bgl)
Karoo Supergroup	Ecca Group (Vryheid Fm)	Intergranular and fractured aquifer	Weathered and fractured sedimentary rocks not associated with dolerite intrusion, indurated and jointed sedimentary rocks alongside dykes, narrow weathered and fractured dolerite dykes, weathered dolerite sills and jointed sedimentary rocks, weathered and fractured upper contact-zones of dolerite sills, weathered and fractured lower contacts-zones, and coal seams.	12.60	5-25
	Dwyka Group		Upper weathered tillite	4.4	-
Rooiberg Group	Loskop Formation	Intergranular and fractured aquifer	Fractures associated with the intrusion of acidic lava, contact zones between its different sediments.	4.4	10 and 30
Pretoria Group	Rayton Formation	Intergranular and fractured aquifer	Zones of its different quartzite horizons and shale beds		20
	Magaliesberg Formation		Fractures, contact zones with diabase sills, faults and associated shear zones	9.30	10 and 40

	Silverton Formation		Shale brecciated (jointed) zones, contacts zones between intrusive diabase sheets and the shale.	20.0	10 - 80
	Daspoort Formation		Faults; shear zones; contact zones of intrusive diabase sills with shale and quartzite horizons; occasional joints in fresh diabase		10 and 30

CHAPTER 3 : LITERATURE REVIEW

3.1 Introduction

Due to rapid population growth, industrial development and increasing use of chemicals, water pollution has become an everyday problem despite several mitigation measures being taken (Satyanarayana et al., 2013). Deterioration of groundwater quality and decline in its quantity has been caused by increased population, unplanned land-use practices and high water supply demands (Singh et al., 2017). The extensive discharge of industrial waste, sewage sludge, and solid waste disposals into the environment are resulting in the pollution of water resources, affecting both developed and developing countries (Karmegam et al., 2010; Satyanarayana et al., 2013). According to Satyanarayana et al., (2013), 50% of the population in developing countries suffers from one or more water related diseases, and 50% of diseases in developing countries are caused by contaminated water. Marghade et al., (2010) states that the current groundwater pollution problems are primarily from short-term exploitation and mismanagement of water resources.

Pollution of surface and groundwater is very common in mining and industrial areas (Tiwary and Sinha, 2006). Power generation in South Africa relies mostly on coal-fired power stations which release considerable amounts of fly ash into the environment. The prevention of groundwater pollution from these fly ash deposits requires proper management of the ash (Moolman, 2011). Leaching of pollutants in coal ash is more prevalent at wet ash ponds where the coal ash is mixed with water. This mixing of the ash and water promotes the leaching of heavy metals, eventually seeping into groundwater (Ailun et al., 2010). The quality of groundwater is dependent, among other factors, on the quality of the recharge water, atmospheric precipitation, inland surface water and subsurface geochemical processes (Suma et al., 2015).

Assessing the hydrochemical composition of water does not only involve analysis of hydrochemical parameters in the laboratory and evaluating them against known water quality standards to reach some conclusions but also helps understand the geochemical evolution of the groundwater, which is vital for assessing and analysing the hydrogeochemistry of the groundwater system. Water chemistry is characterised by multivariable data; therefore, its interpretation requires complex statistical modelling for its full assessment (Manoj et al., 2013). Some of the multivariate data analysis methods that can be used for the characterisation and

classification of groundwater may include factor analysis, cluster analysis (CA) and discriminant analysis (DA) (Manoj et al., 2013).

3.2 Groundwater quality

3.2.1 Factors influencing Groundwater Quality

Kresic (2009) defines water quality as the chemical, physical, biological, and radiological conditions of a surface water or groundwater system. In its natural environment, the quality of groundwater is influenced by the sum of soil-modified atmospheric inputs in addition to water-rock interaction taking place at the soil–bedrock interface and from longer-term reactions taking place along flow paths in the saturated zone (Edmunds and Shand, 2008). According to Fianko et al., (2010), the mineralogy of the aquifer matrix and the residence time controls the extent of the water-rock interaction. Biological, physical and chemical processes can modify the chemistry of groundwater. Figure 3-1 illustrates the various processes that generally influence groundwater chemistry including cation exchange, dissolution of the weathered mantle, and mixing with existing water within the unsaturated zone during recharge, flow path, climatic conditions, geological formations and anthropogenic activities.

Generally, almost all groundwater is derived from precipitation (rain, snowmelt, etc) that infiltrates through the soil into the flow systems in the underlying geologic materials. The thin biologically active soil zone has unique and powerful capabilities to modify the water chemistry during infiltration. As groundwater flows from recharge to discharge zones along flow lines, these hydrogeochemical processes alter its chemistry (Saikia and Sarma, 2011).

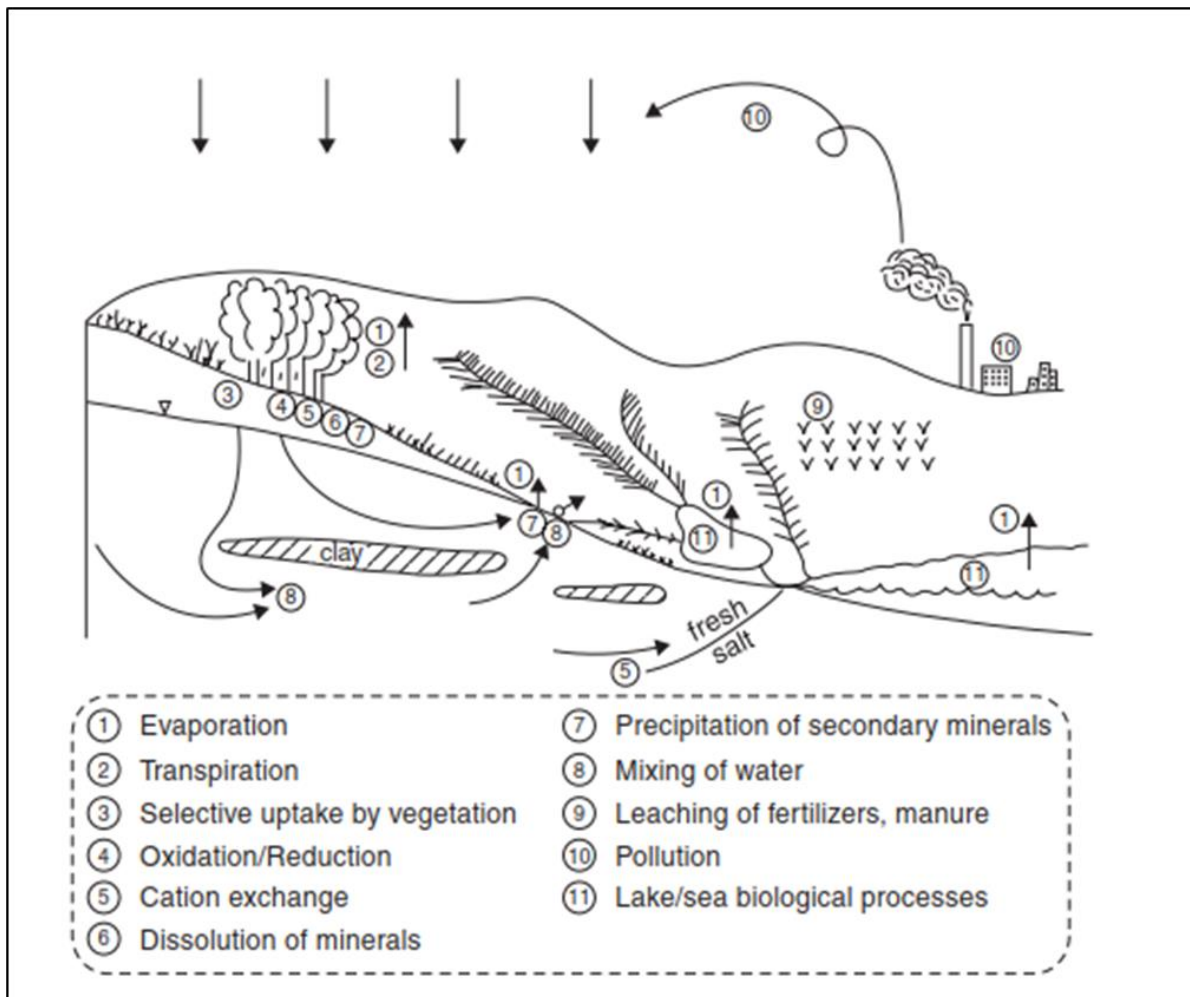


Figure 3-1: An overview of processes that affect the water quality (Appelo and Postma, 2005).

3.2.2 Hydrochemical composition of groundwater

The hydrochemical composition of groundwater is mainly dominated by macro constituents and micro constituents (Tikhomirov, 2016). Inorganic constituents in water with concentrations greater than 5 mg/l are classified as major constituents, those with concentrations ranging from 0.01 to 10 mg/L are minor constituents, and trace constituents are those parameters that occur dissolved in water with concentrations < 0.01 mg/l (Domenico and Schwartz, 1998). The six major dissolved ions in groundwater include sodium (Na^+), calcium (Ca^{2+}), magnesium (Mg^{2+}), chloride (Cl^-), bicarbonate (HCO_3^-) and sulphate (SO_4^{2-}), which typically comprise over 90% of the total dissolved ions composition (Table 3.1). This composition is irrespective of whether the water is dilute rainwater or has a salinity greater than seawater (Hiscock, 2005).

Table 3.1: Groundwater chemical composition divided into major and minor ions, trace constituents and dissolved gases (after Hiscock, 2005).

Groundwater composition					
Major ions (dissolved concentration > 5 mg/l)					
Bicarbonate	Sodium	Chloride	Calcium	Sulphate	Magnesium
Minor ions (dissolved concentrations from 0.01 to 10.0 mg/l)					
Nitrate	Potassium	Carbonate	Strontium	Fluoride	Iron
Phosphate	Boron				
Trace constituents (dissolved concentration < 0.1 mg/l)					
Aluminium	Manganese	Arsenic	Nickel	Barium	Phosphate
Radium	Cadmium	Selenium	Caesium	Silica	Chromium
Cobalt	Thorium	Gold	Tin	Iodide	Titanium
Uranium	Lithium	Vanadium	Zinc	Bromide	Silver
Lead					
Dissolved gases (trace to 10 mg/l)					
Nitrogen	Methane	Oxygen	Hydrogen sulphide	Carbon dioxide	Nitrous oxide

Other water quality indicators include Electrical Conductivity (EC), Total Dissolved Solids (TDS), pH, and alkalinity. Water contains electrolytes that are dissolved in it and these electrolytes occur in ionic forms and conduct electrical current (Kresic, 2007). The electrical conductivity of water equals the inverse of the electrical resistance across a 1 cm cube of water. Electrical conductivity is measured in siemens (S) or micro siemens (μS), it is temperature-dependent, and most readings are corrected to the equivalent reading at 25°C. The more dissolved ions in water, the greater will be its electrical conductivity (EC) (Fitts, 2002). Therefore, the EC of water is a direct measurement of the concentration of the number of dissolved ions in the water under consideration.

TDS expresses the degree of salinity of groundwater and expresses the sum of dissolved constituents' concentration in a water sample. It is measured by evaporating a water sample to dryness or calculated from the measured EC or from the sum of dissolved constituents. When

TDS is analysed in the laboratory, a known volume of a water sample is evaporated to dryness and the mass of the dry residue left divided by the volume of the original water sample gives the TDS (Fitts, 2002).

The hydrogen-ion activity or pH is a measure of the acidity or alkalinity of groundwater. Measurement of pH is important as it controls many of the chemical reactions involving groundwater. The pH scale is from 1 to 14, where 0 is a pure acid while a pH of 14 indicates a strongly alkaline solution (Kresic, 2007). It is important to note that the alkalinity of a solution is the capacity of solutes to react with and neutralise acids and the acidity of a solution is the opposite. The alkalinity is due to dissolved carbon dioxide species, bicarbonate, and carbonate for natural waters. It is a widely accepted practice to report alkalinity in terms of an equivalent amount of calcium carbonate.

3.3 Hydrochemical Data Analysis

3.3.1 Graphical Analysis

Several graphical hydrochemical data analysis and visualization methods have been developed to interpret hydrochemical and water quality data and illustrate its characteristics. These methods include, among others, Piper, Durov, Stiff, Gibbs, Wilcox, Chandha diagrams (Al-Kalbani et al., 2017).

Piper's Trilinear Plots

Piper diagrams use milliequivalents percentages of the major cations and anions which are plotted in separate triangles and projected to a central diamond field. The diamond field provides the overall character of the water (Figure 3-2). Piper diagrams help to evaluate water types/hydrochemical facies which provide a preliminary clue about the complex subsurface hydrochemical processes. Hydrochemical facies provide enough information on the chemical quality of water, especially its origin (Kumar, 2013). It further provides insight into changes in water quality that may be due to rock-water interaction or any type of anthropogenic influence (Sadashivaiah et al., 2008).

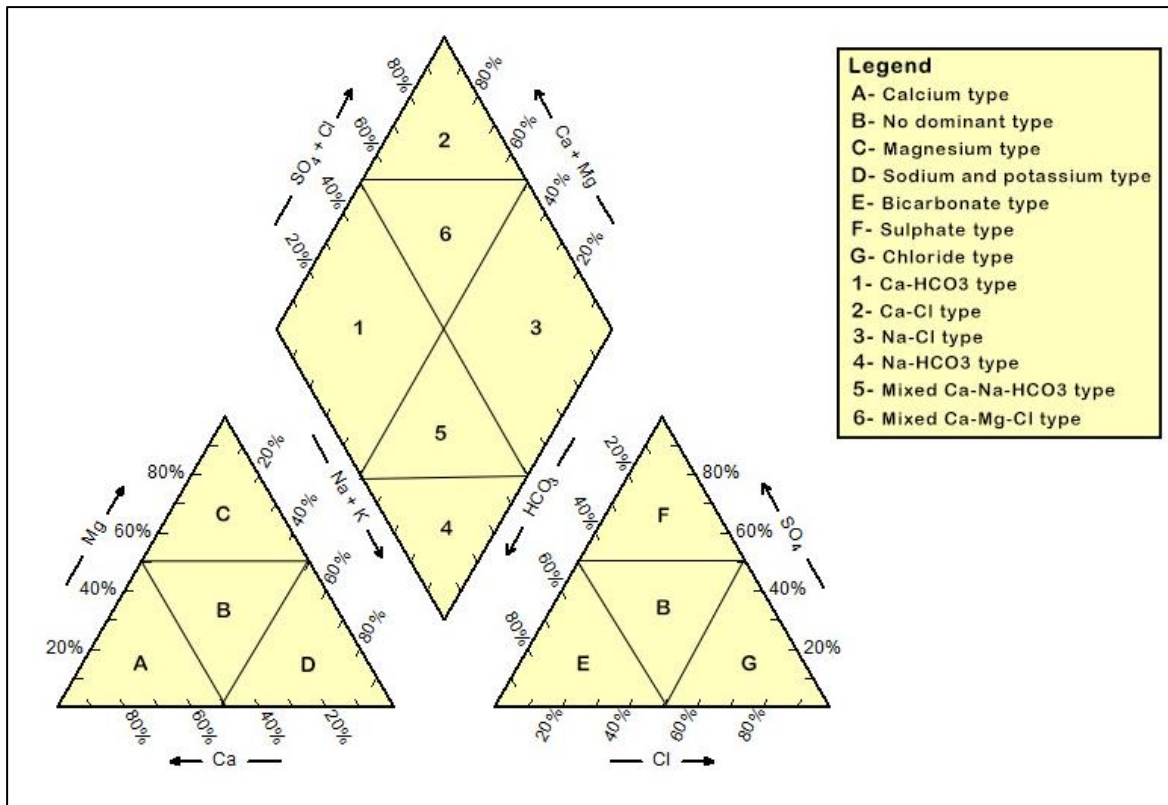


Figure 3-2: Piper Trilinear Diagram (modified from Al-Kalbani et al., 2017).

Durov Diagram

In the Durov diagram (Durov, 1948) major ions are displayed as percentages of milli-equivalents in two separate ternary graphs, the sides of the triangles are 90° apart. One graph represents cations and the other for anions (Figure 3-3). The Durov diagram is used to complement the Piper diagram as it can show geochemical processes that may affect the genesis of groundwater (Ravikumar et al., 2015).

Stiff Diagram

The stiff diagram comprises of four parallel, horizontal axes extending on each side of a vertical, zero axis. Cations and anions are plotted on the left and right of the vertical axis respectively with concentrations expressed as milli-equivalents (Hounslow, 1995). Stiff diagrams are used to identify the visual differences in the distribution of cations and anions for individual samples (Singhal and Gupta, 2010).

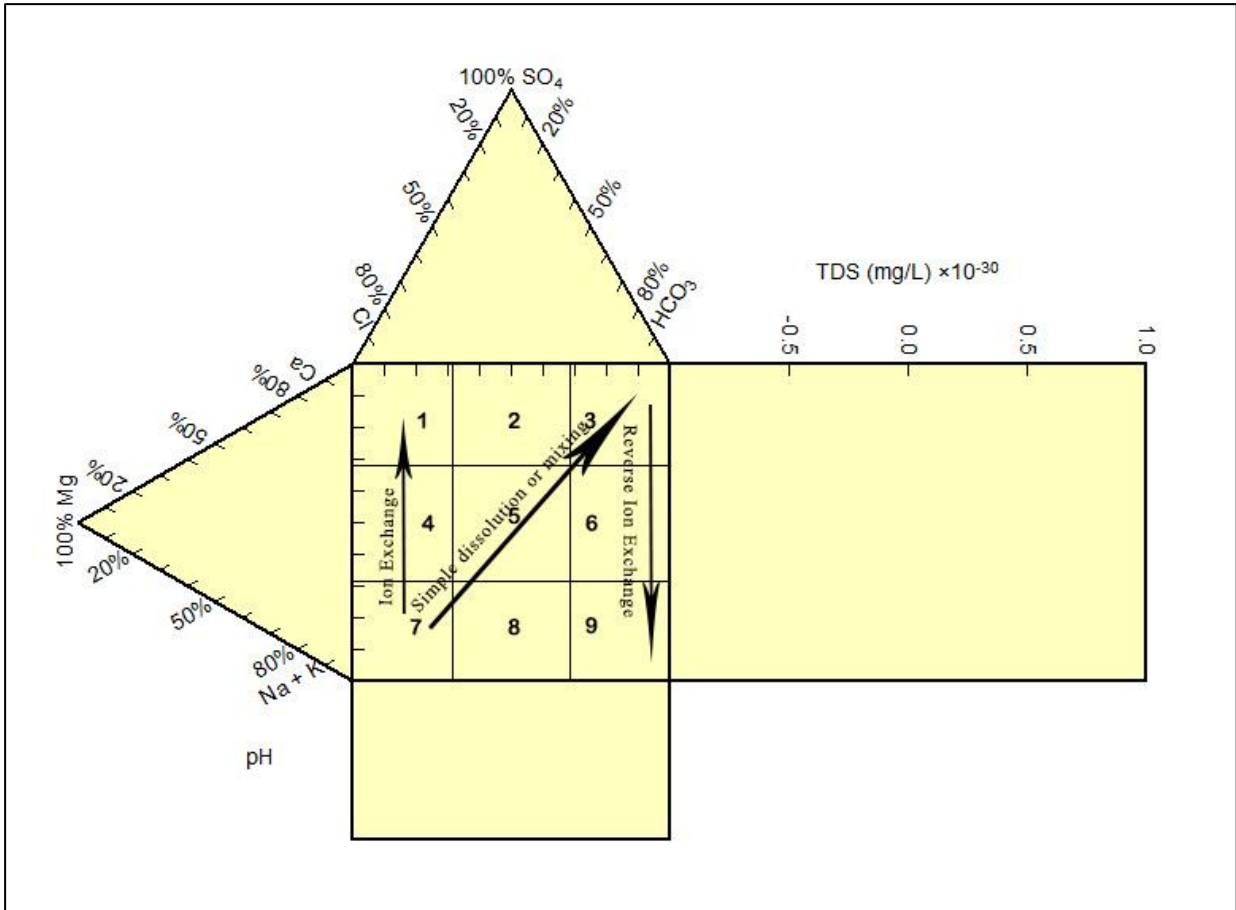


Figure 3-3: Durov diagram (Durov, 1948).

3.3.2 Univariate and Bivariate Statistical Analysis

Descriptive Statistics

Descriptive statistics is the first step in hydrochemical data analysis as it provides a way to detect patterns in the data and therefore can be used to conduct further analysis using multivariate statistics Rovai (2016). The most common descriptive statistical measures are: mean, median, mode, range, variance and standard deviation.

The sample mean is a common estimate of the centre or middle of a statistical distribution. The arithmetic mean provides the average value of all measurements. However, data outliers may considerably impact the mean and render it meaningless (Li and Migliaccio, 2011). The sample mean, \bar{X} is calculated using equation 1 based on n number of observations:

$$\bar{X} = \frac{1}{n} \sum_{i=1}^n X_i \tag{1}$$

The median is the middle value in a dataset when the data is ranked in order from highest to lowest (vice versa). The median is also used to describe the value for which half of the total observations are less than that value and half of the total observations are greater than that value. It is less sensitive to outliers and skewed distributions (Kaur et al., 2018). The median (\tilde{X}) of a sample size (n) can be expressed using the equation 2:

$$\tilde{X} = \begin{cases} \frac{1}{2} \left[X_{\left(\frac{n}{2}\right)} + X_{\left(\frac{n}{2}+1\right)} \right] & \text{if } n \text{ is even} \\ X_{\left(\frac{n+1}{2}\right)} & \text{if } n \text{ is odd} \end{cases} \quad (2)$$

Where X represents scores.

The value that occurs the most in a dataset is called the mode. Datasets that have values occurring once do not have a mode and there is a possibility that a dataset may have more than one mode (Manikandan, 2011)

The range of a dataset refers to the numeric difference between the smallest dataset value and the greatest dataset value and provides information on the variability within the dataset (Kaur et al., 2018). It is calculated using equation 3 as follows:

$$R = \max(X_i) - \min(X_i) \quad (3)$$

The variance of a dataset is a measure of the spread/dispersion (Li and Migliaccio, 2011). It is dependent on the range of the dataset and increases with an increase in the range of the dataset. It is also directly influenced by the presence of outliers. The standard deviation is the square root of the variance and indicates how much the values typically vary from the average value or mean. Variance and standard deviation are calculated using equations 4 and 5, respectively.

$$S^2 = \frac{\sum_{i=1}^n X_i^2 - \frac{1}{n} (\sum_{i=1}^n X_i)^2}{n - 1} \quad (4)$$

$$S = \sqrt{S^2} \quad (5)$$

Correlation Analysis

Correlation is a bivariate statistical data analysis method that measures the relationship between two variables. It is often represented by the Pearson's correlation coefficient (r). Studying the

correlation of water quality parameters systematically helps in assessing the overall water quality and in quantifying the relative concentration of various parameters in water (Jothivenkatachalam et al., 2010). Assuming two variables as X and Y, the Pearson's correlation coefficient (r) between these variables is calculated using equation 6.

$$r = \frac{\Sigma (x - \bar{x})(y - \bar{y})}{\sqrt{\Sigma(x - \bar{x})^2 \Sigma(y - \bar{y})^2}} \tag{6}$$

The range of r is between -1 and 1, where the greater the absolute value the stronger the relationship or correlation. A negative r value indicates an inverse relationship and a positive r indicates a direct relationship (Li and Migliaccio, 2011). The rule of thumb as given by Guildford (1973) states that the Pearson correlation coefficient (r) can construct the degree, size, magnitude and strength of the relationship (Table 3.2).

Table 3.2: Guilford's rule of thumb for interpreting correlation coefficient (adapted from Guilford, 1973).

Absolute Value of r	Degree of correlation
0 – 0.1	Slight; almost no relationship
0.10 – 0.39	Weak correlation; definite but small relationship
0.40 – 0.69	Moderate correlation; substantial relationship
0.70 – 0.89	Strong correlation; strong relationship
0.90 – 1.00	Very strong correlation; very dependable relationship

3.3.3 Multivariate Statistical Analysis

Multivariate statistical analysis involves a variety of statistical methods which may be used in several areas of empirical investigation. These include, among others, Principal Coordinates Analysis, Principal Component Analysis (PCA), Analysis of Similarity (Correlation Analysis), Analysis of Variance, Cluster Analysis, Shannon index, and Factor analysis (Rehman et al., 2016). Multivariate statistical analysis focuses on examining and comprehending data in multi-dimensions or parameters (Härdle and Simar, 2007). Multivariate statistical techniques are commonly used for studies of groundwater hydrochemistry and contamination. Interpretation of the results can be simplified by employing rotational procedures, discovering similarities among variables and therefore improving data analysis and interpretation.

Factor Analysis

Factor analysis is based on a model in which the observed vector is partitioned into an unobserved systematic part and an unobserved error part (Anderson, 2003). Factor analysis describes the independence of a set of variables in terms of the factors without regard to the observed variability. Factor analysis identifies some unique underlying factors that have completely different behaviour than the majority of all other factors (Reimanna et al., 2002).

Hierarchical Cluster Analysis (HCA)

HCA involves a group of techniques that primarily classify variables into clusters based on their characteristics (Usman et al., 2014). HCA helps to classify objects where each object is similar to the others in the cluster with respect to a predetermined selection criterion. This results in clusters of high homogeneity level within the class and high heterogeneity level between classes (Templ et al., 2006). The HCA is the most common and efficient method of recognizing groups of samples that have similar hydrochemical and physical characteristics. It can be graphically presented in an easily understood display in the form of a dendrogram. The dendrogram helps identify natural groupings for samples or variables and in turn reduces the size of the samples/variables into smaller numbers of groups (Meng and Maybard, 2001).

3.3.4 Time Series Trend Analysis

Time series data are consecutive sequence of observations of a specified variable including hydrochemical and groundwater level data (Law, 1974). Observations can be continuous over time or at discrete time intervals. Thakur and Thomas (2011) state that a time series of certain random variables display a trend that becomes evident over time. Trend analysis of hydrogeological data may be used to explain changes in climate, land use, and water use patterns. The detection of gradual trends over time uses statistical procedures. These trends can be tested to determine whether the values of the random variables are increasing or decreasing over time. Kresic (2007) identifies five components of a time series as follows:

1. Trend - a tendency to increase or decrease continuously for an extended period of time in a systematic manner.
2. Periodicity - these may be annual or seasonal and can be identified using moving average analysis, autocorrelation analysis, or spectral analysis.
3. Cycle - relating to irregular period and is hard to detect

4. Episodic variation - happens as a result of extremely rare events, supplementary information is required to identify this component
5. Random fluctuations - often a dominant source of the variations in time series information.

Machiwal and Jha (2012) recognise four steps in time series analysis. These include detection, analysis, synthesis and verification.

- Detection involves the identification of system components of the time series such as trends or periodicity.
- The analysis involves analysing the system components to identify their characteristics including magnitudes, form and their duration over which the effects exist.
- Synthesis involves the accumulation of information to develop.
- Verification evaluates the developed time series model using independent sets of data in.

A variety of statistical tools are used to detect trends in time-series environmental data. parametric tools and non-parametric mathematical methods are the two commonly used tools. The parametric tools are robust; however, they require normally distributed independent data. The non-parametric tools assume that observations are dependent (Mustapha, 2013).

The non-parametric statistical Mann-Kendal (MK) Test is one of the statistical time series trend analysis tools used widely to analyse time-series groundwater level and hydrochemical data. It is a flexible method that can handle missing values, skewed data and makes it possible to establish the existence of an increasing or decreasing trend (Vousoughi et al., 2012). The MK test relies on the null hypothesis (H_0) that data of the analysed population is independent and identically distributed, and the alternative hypothesis (H_1) affirm the existence of a monotonic trend. The Mann-Kendal test statistic is expressed as the S value defined by equation 7 (Mann, 1945; Kendall, 1955):

$$S = \sum_{k=1}^{n-1} \sum_{j=k+1}^n \text{sgn}(X_j - X_k) \quad (7)$$

Where S is the Mann-Kendal test value, X_j and X_k are the sequential data values, j, k and n are the length of the data; and $X_j - X_k = \theta$. The Signum function (Sgn) is given by equation 8.

$$\text{sgn}(\theta) = \begin{cases} 1 & \text{if } \theta > 0 \\ 0 & \text{if } \theta = 0 \\ -1 & \text{if } \theta < 0 \end{cases} \quad (8)$$

A very high positive value of S denotes an increasing trend whereas a very low negative value indicates a decreasing trend. In situations where $n \geq 10$, the MK statistics is considered nearly normally distributed with the Variance of S (Kendall, 1975), VAR(S). The variance of S is expressed as:

$$VAR(S) = \frac{1}{18} [n(n-1)(2n+5) - \sum_{p=1}^g t_p(t_p-1)(2t_p+5)] \quad (9)$$

Where n is the number of data points, g is the number of tied groups, and t_p is the number of data points in the p^{th} group. The normalised test statistics Z is denoted by:

$$Z = \begin{cases} \frac{S-1}{\sqrt{VAR(S)}} & \text{if } S > 0 \\ 0 & \text{if } S = 0 \\ \frac{S+1}{\sqrt{VAR(S)}} & \text{if } S < 0 \end{cases} \quad (10)$$

Where Z is the normalised test statistics, S is the MK test statistics, and VAR(S) is the MK test variance.

To estimate the rate of change, the Sen's slope (Sen, 1968) estimator is used. It assumes the existence of a linear trend in the data and the magnitude of the trend is estimated using equation 11.

$$Q_i = \frac{X_j - X_k}{j - k} \text{ for } 1, 2, 3, \dots, N \quad (11)$$

Where X_j and X_k are data values at times j and K ($j > K$), respectively. The median of N values of Q_i is Sen's slope estimator and is calculated using equation 12.

$$\beta = \begin{cases} Q_{[(N+1)\lfloor \frac{N}{2} \rfloor]} & \text{if } N \text{ is odd} \\ \frac{1}{2} \left(Q_{\lfloor \frac{N}{2} \rfloor} + Q_{\lfloor \frac{N}{2} \rfloor + 1} \right) & \text{if } N \text{ is even} \end{cases} \quad (12)$$

Positive β represents an increasing trend and a negative β shows a decreasing trend (Kumar et al., 2018).

3.4 Environmental Isotopes

Isotopes of a specific element differ only in the number of neutrons in the atom's nucleus and their total mass (Fitts, 2002). Most elements have various types of atoms only differing in the number of neutrons that accompany the protons (Mazor, 2004). Isotopes may be used as tracers

for the determination of the origin and age of groundwater, for understanding recharge processes, and transport processes in aquifers (Singhal and Gupta, 2010). The stable isotopes of water can be used to identify the different sources of water and the altitude at which recharge occurred. Furthermore, the recharge and flow rates of groundwater can be estimated using environmental isotope information including the groundwater's age (Plummer et al., 2004).

Natural water may contain several different isotopes of both hydrogen and oxygen. However, the most common and abundant isotopes are ^1H and ^{16}O . The most commonly used environmental isotopes in groundwater studies are those of oxygen and hydrogen, hydrogen (^2H or D, and ^3H) and oxygen (^{18}O). ^2H and ^{18}O are stable isotopes whereas ^3H is the radioactive isotope (Aggarwal et al., 2009). Stable isotopes are usually expressed as the ratio of the least abundant isotope to the most abundant isotope relative to a standard. The internationally agreed standard for water is the Vienna Standard Mean Ocean Water (VSMOW). Variations of isotopic ratios are small in nature, therefore, it is reported using the δ -notation (Appelo and Postma, 2005). The δ -notation expresses the deviation of the isotopic ratio R in the sample from the standard following equations 13 and 14 as follows:

$$\delta_{sample} = \frac{R_{sample} - R_{standard}}{R_{standard}} * 1000 \quad (13)$$

$$\delta_{sample} = \left(\frac{R_{sample}}{R_{VSMOW}} - 1 \right) * 1000 \text{‰ VSMOW} \quad (14)$$

Equation 14 is the normalised difference between the sample and reference and multiplied by 1000 to express the measurements in permil (‰) units (Clark, 2015).

The Global Meteoric Water Line (GMWL) was established from long-term studies by IAEA/WMO using measurements from the Global Network for Isotopes in Precipitation (GNIP). The GMWL describes the linear relationship between $\delta^2\text{H}$ and $\delta^{18}\text{O}$ isotopes in precipitation based on equation 15 (Craig, 1961).

$$\delta^2H = 8 * \delta^{18}O + 10 \quad (14)$$

Tritium (^3H) is widely used in determining modern recharge as it has a very short half-life of 12.43 years. Tritium is the only radioisotope is part of the water molecule that can be used to date groundwater. The activity of tritium are expressed as tritium units (TU) where one tritium unit is equivalent to 10^8 hydrogen atoms. The use of tritium to date groundwater assumes that the tritium input into the groundwater is known and that the residual tritium measured from the

groundwater is a function of natural radioactive decay only (Clark and Fritz, 1997). Groundwater ages calculated using tritium activity is given by equation 16 (Clark and Fritz, 1997):

$$t = -17.93 \ln \left(\frac{a_t^3H}{a_0^3H} \right) \quad (15)$$

Where t is mean residence time in years, a_t^3H is the residual activity of tritium remaining after decay over time and a_0^3H is the initial tritium activity. The initial tritium activity is taken as the steady natural tritium activity in modern precipitation, which is about 4 T.U. in South African precipitation (Abiye, 2013).

Clark and Fritz (1997) report the following qualitative groundwater mean residence times for continental regions based on observed tritium activity.

- < 0.8 TU: sub-modern groundwater recharged prior to 1952
- 0.8 - 4 TU: mixture of sub-modern and recent recharge
- 5 - 15 TU: modern recharge (<5 to 10 years)
- 15 - 30 TU: some bomb tritium present
- 30 TU: considerable component of recharge from 1960 or 1970s
- 50 TU: dominantly 1960s recharge.

3.5 Development of Hydrogeological Conceptual Models

Understanding of groundwater systems is best achieved through the development of conceptual models which is developed iteratively through analysis and interpretation of various hydrogeological data and information collected both in the field and laboratory. Furthermore, the conceptual hydrological model helps to construct and calibrate numerical groundwater flow and contaminant transport models (Fitts, 2002). The development of a conceptual hydrogeological model is the first and the most important step in any hydrogeological investigation. A sound conceptual model requires detailed information on the hydrogeology, hydrology, and dynamics of groundwater flow in and around the study area of interest. The conceptual models include a computerized database, basic maps and hydrogeological cross-sections.

The purpose of setting up any conceptual model is to simplify field problems and organize field data. The simplification is necessary because the field system is complex and not feasible to

reconstruct. The conceptual model should be simple enough but a valid representation of the hydrogeologic conditions (Anderson and Woessner, 2002). Since conceptual modelling is an iterative process, it evolves as new data is collected. A geographic Information system (GIS) is the most efficient tool for conceptual model development (Kresic, 2007). Generally, most conceptual hydrogeological models should include geological framework, hydrological framework, system boundaries and human-induced factors features as shown in Table 3.3 (Middlemis, 2001).

Table 3.3: Features of a conceptual Model (modified after Middlemis, 2001).

Feature	Description	Comment
1. Boundaries	Location and type of boundaries for the area to be modelled	Boundary types include specified flow, specific head, and head-dependent flow
2. Geological framework	Geological units and corresponding hydrostratigraphic units, and associated aquifer parameters. Bedrock configuration and aquifer or aquitard characteristics.	Hydrostratigraphic units comprise geological units with similar aquifer properties. Several geological formations may be combined into one hydrostratigraphic unit, or a geological formation may be subdivided into the aquifer and confining units.
3. Hydrological framework and stresses	Recharge and discharge processes and dominant aquifer flow mechanisms.	Definition of aquifer media type (porous medium, fractured rock) and surface-groundwater interaction processes.
4. Human-induced factors	Anthropogenic influences on the system.	Pumping, irrigation, drainage, weirs, floodway's, land clearing, aquifer storage and recovery, waste discharge, mining, etc.

3.6 Previous Works in the study area

Several consultants have investigated the hydrogeology around the Kusile Power Station, with different objectives. A geophysical resistivity survey based on Vertical Electrical Soundings (VES) was conducted by Golder Associates (2007) around the Kusile Power Station and the VES data interpretation indicated bedrock thickness of the Dwyka Group and Rayton Formation to be between 13 m and 33 m. The depth to dolerite bedrock sill ranges from 2 m to

17 m below ground level (bgl). JMA Consulting (2012) conducted a detailed specialist study of an environmental management programme for the New Largo Colliery. As part of the study, 28 boreholes intersecting the shallow weathered aquifers were drilled in 2006. The average depth of these boreholes is 31 m bgl. The underlying geology consisted of the Karoo Supergroup rocks represented by alternating layers of sandstone, shale and coal of the Eccca Group which is underlain by the Dwyka tillites. The Dwyka tillites were intercepted at an average depth of 18 m bgl. In some places, the Dwyka tillites are underlain by quartzites of the Pretoria Group while in other areas it is underlain by diabase. The laterally extensive shallow weathered zone is the primary aquifer in the study area and displays unconfined to semi-confined conditions. It occurs within the weathered and weathering related fractures within the Eccca Group, Dwyka Group and Pretoria Group. Fractured aquifers are localised and are limited to contact zones between the intrusive diabase and the host rock. Slug test data analysed from 15 boreholes of the shallow weathered aquifer showed an average aquifer hydraulic conductivity of 0.76 m/day and transmissivity rate of 5.06 m²/day.

GCS (2014) conducted a hydrogeological study at Kusile as part of a waste licence application requirement. During this investigation, short-duration aquifer tests were conducted on four boreholes (namely, 10490-09, 10490-10, 10490-17 and BH 27). Boreholes 10490-09 and 10490-10 were analysed to have transmissivity of 0.5 m²/day and 0.2 m²/day, respectively. The other two boreholes could not be interpreted for aquifer properties due to insufficient data gathered during the short duration tests.

JG Afrika (2016) drilled an additional three monitoring boreholes (MP14-001 to MP14-003) within the power station. The depth of these boreholes ranged between 18 and 60 m bgl, one of these boreholes was dry while the other two produced compressor yields of 0.15 and 0.22 l/s, and water strikes were encountered between 8 and 25 m bgl.

Engeolab (2019) conducted an overview of the groundwater resources in Arbour Village, south of the study area. The investigation involved the drilling of five new boreholes and yield testing of three existing boreholes. Geological logs of the drilled boreholes confirmed the rhyolites interbedded and shales of the Rooiberg Group intruded by diabase sills and dykes. Groundwater occurrence was mainly controlled by the development of secondary permeability in the seemingly impermeable lithologies, mainly due to diabase intrusions that caused fractures and joints and, to a lesser extent weathering. Borehole yields associated with the Rooiberg Group ranged between 0.1 and 1.2 l/s while those associated with diabase ranged between 0.6 to 4.2

l/s. The estimated transmissivity within the shales of the Loskop Formation of the Rooiberg Group was 4.2 m²/day, while those of the diabase ranged between 2.3 m² /day and 4 m² /day.

CHAPTER 4 : MATERIALS AND METHODS

4.1 Desktop study

All available information collected from literature relevant to the study was integrated and interpreted along with original data and incorporated into the research. These include GIS data, weather data from the South African Weather Service (SAWS), and relevant scientific work performed by several consultants.

4.2 Water quality monitoring network in the study area

Week long field visits were conducted by the author between February 2014 and June 2018 as part of the consultancy services of JG Afrika rendered to Eskom (Kusile Power Station) as part of a monthly surface water - groundwater monitoring program. The water monitoring network within the study area includes 52 sampling locations which comprise 19 surface water and 33 groundwater sampling points (25 boreholes and 8 springs) as shown in Figure 4-1. These sampling network points are part of the Kusile Power Station monthly surface water - groundwater monitoring program. These sampling points are concentrated around the Kusile Power Station as they are meant to detect changes and/or deterioration of water quality, which may result from construction and operational activities of the coal-fired power station.

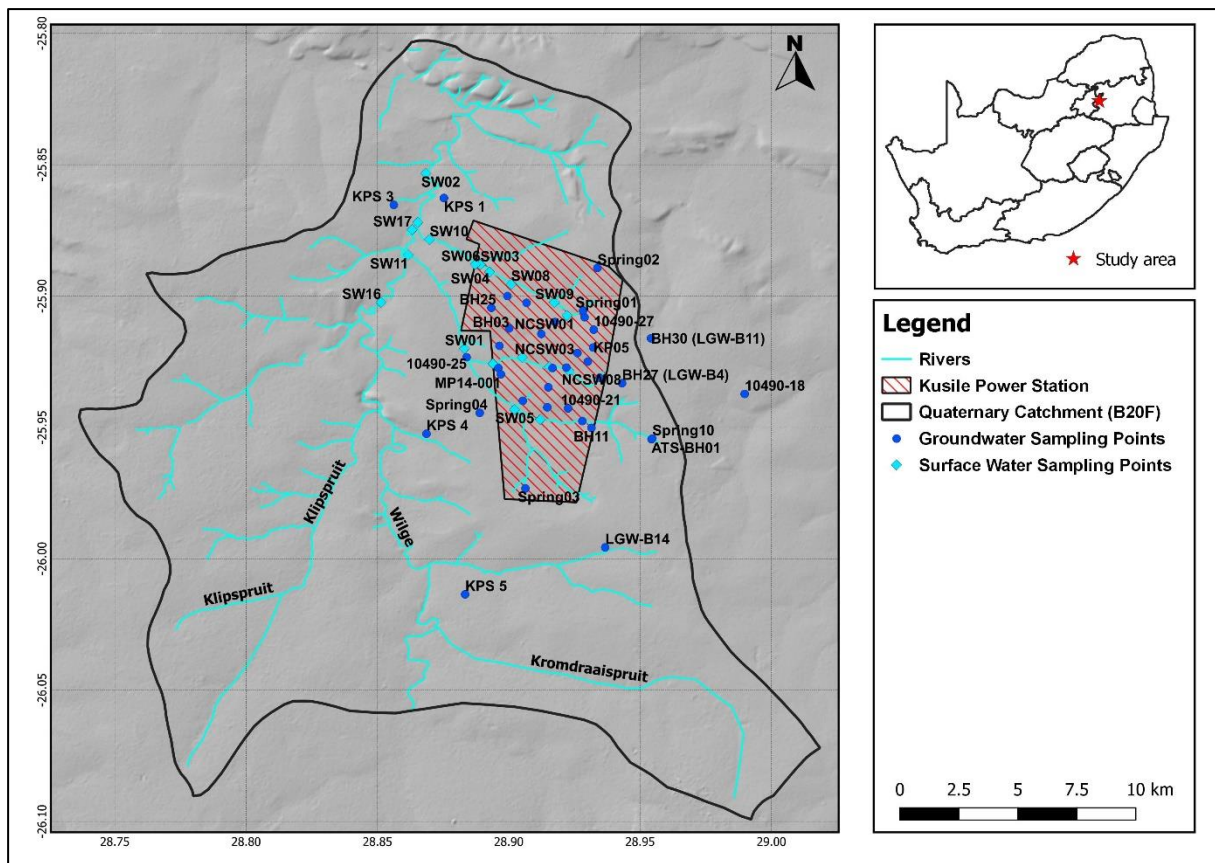


Figure 4-1: Location of data collection sites.

4.3 Fieldwork (Sampling and Hydrocensus)

A hydrocensus survey was conducted on 29 March 2018; the main aim of the hydrocensus survey was to establish the locations of groundwater resources and water use within the studied quaternary catchment. In addition to the existing monitoring stations, six boreholes were identified during the survey outside of the Power stations' monitoring system. 50 water samples were collected during two field campaigns (i.e., from 27 to 30 March 2018 and from 12 to 15 June 2018). These samples included surface and groundwater samples from the monitoring network. The sampling included 22 boreholes, 4 springs and 19 surface water points. A total of 29 water points were sampled for isotope analysis; 24 from the monitoring network (17 groundwater and 7 surface water sampling points) and 5 outside of the monitoring network and identified during the hydrocensus survey.

It should be noted that there are more groundwater users within the study area, but these are located on private properties, and access to these boreholes was not granted. Five of these

boreholes from the survey were sampled, three of the five boreholes were active (pumping wells).

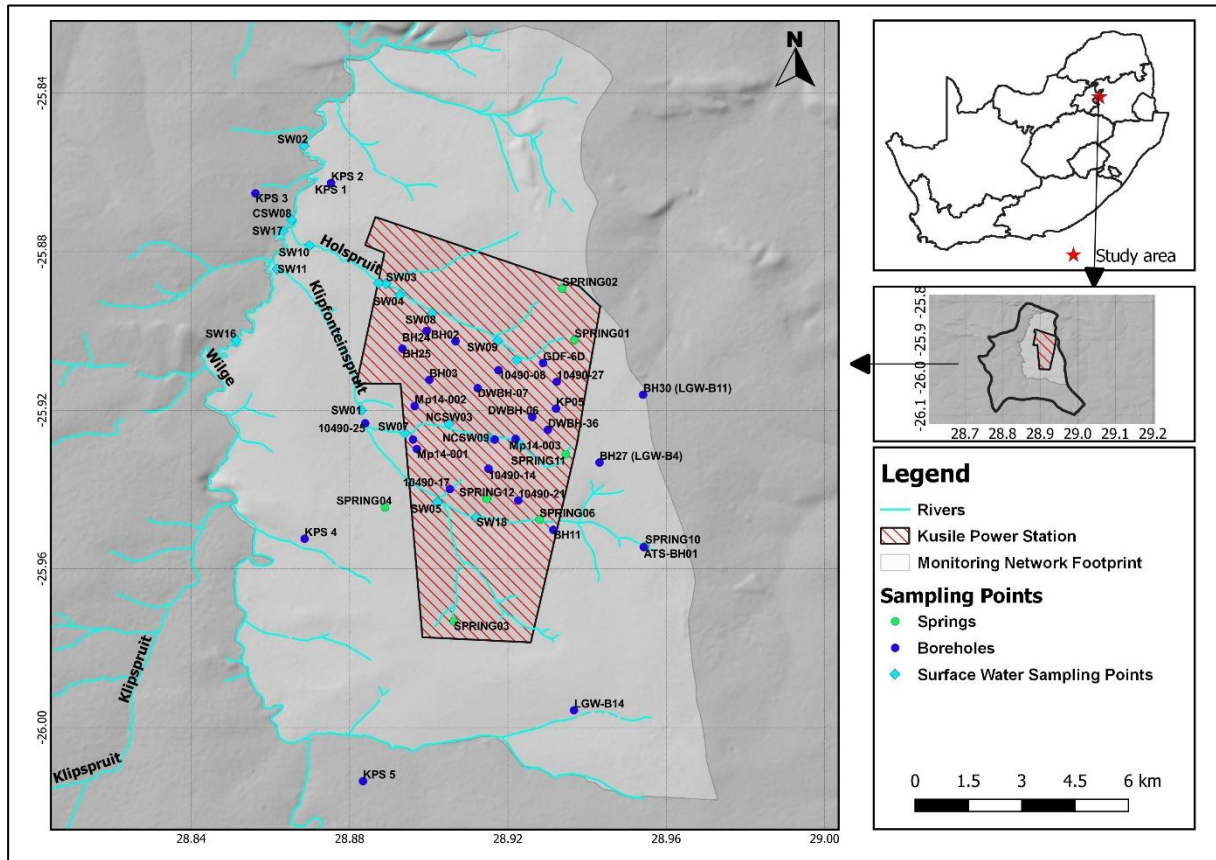


Figure 4-2: Location of groundwater and surface water sampling locations within the study area.

4.3.1 Equipment used

Equipment used for the groundwater and surface water monitoring included a Global surface water flow probe, handheld GPS receiver (Garmin Dakota 20 model), camera, 2” Submersible 12V pump, 2” Disposable bailers, handheld portable multi-meter probe (for field temperature, EC, TDS and pH measurements), dip meter for monitoring of groundwater levels, 25 Litre drum for water collection and purge monitoring, sampling bottles, cool boxes and ice bricks for the temporary storage of samples in the field, nitrile gloves, and spanners/allen keys for opening borehole covers.

4.3.2 Field measurements

Before sampling was conducted, relevant information was recorded on field sheets at each sampling location. The recorded information included location, identification number, GPS coordinates, groundwater levels; flow rates of surface water bodies; field parameters: temperature, pH, EC, and TDS. A portable multi-meter probe was used in the field after careful calibration using standard pH buffer solutions of 4, 7, and 10 each day prior to sampling. The electronic dipmeter was used to measure the depth to water for each borehole, and borehole purging was conducted using the submersible pump. Ideally, it is recommended that purging should flush three times the volume of the borehole before sample collection. However, due to the high monthly sample frequency and the restricted time constraints, a minimum representative purge volume of 100 litres was pumped from each borehole before sampling. Groundwater samples were collected from the discharge of the portable submersible pump or by using dedicated disposable bailers. The samples were placed directly into sample bottles supplied by Regen laboratory, labelled and cooled in an insulated cool box on site.

The grab method was used for surface water samples. Samples were collected from underwater to help eliminate air bubbles into sample bottles. Stream depths and flow velocities were measured and recorded at surface water sampling locations. The flow rate was measured by using the global water flow probe. The device was held in the top third of the stream (in terms of depth) for a minimum period of one minute. The minimum, maximum and average velocities were then recorded. The field measurements for June 2018 are shown in Appendix A.

4.4 Quality assurance

During sampling, disposable nitrile gloves were worn at all times throughout the sampling process to avoid contamination. Due to restricted time constraints, the samples were not filtered, and budget constraints prohibited the inclusion of blank samples. Sample bottles used for microbiological samples were preserved with sodium thiosulphate as supplied by the laboratory and sample bottles for macro-constituents were rinsed twice with sample point water before sampling. Trace element sample bottles were acidified with concentrated nitric acid by the laboratory that supplied the sampling bottles and later analysed the samples. The collected samples were immediately put in cooler boxes before analysis. All the samples were given identification codes and the sample container were labelled with the respective codes which are also recorded on the field sheet. All samples were submitted with a chain of custody (COC)

documentation, the purpose of the COC is to track the water samples from collection to laboratory analysis.

4.5 Laboratory analysis

Groundwater and surface water samples were submitted to Regen Waters, a SANAS accredited laboratory in Witbank, for chemical and microbiological analysis. The samples were delivered daily to minimise sample holding times, and this was particularly relevant for microbiological and nutrient analysis. The five samples collected during the hydrocensus survey were submitted to the University of KwaZulu-Natal for laboratory for hydrochemical analysis. All the isotope samples were analysed at the iThemba Environmental isotope Labs in Johannesburg.

4.6 Accuracy of chemical analysis

Hydrochemical data accuracy of the water samples collected was checked against the cation-anion balance or electroneutrality. The electroneutrality or charge balance error (CBE) is normally expressed in percentage as shown in equation 17. The CBE accuracy check assumes that the sum of major cation should be equal to the sum of major anions in a natural water solution of low to intermediate salinity and it is further assumed that if the CBE is not within $\pm 5\%$, the analysis is either incomplete or erroneous (Singhal and Gupta, 2010).

$$\text{Electroneutrality (\%)} = \frac{\Sigma\text{Cations} - \Sigma\text{Anions}}{\Sigma\text{Cations} + \Sigma\text{Anions}} * 100 < 5\% \quad (16)$$

If the CBE analysis is out of the $\pm 5\%$, one or more of the following is the explanation (Hounslow, 2018):

- the analysis is inaccurate,
- other constituents are present that were not used to calculate the balance,
- the water is very acidic, and the H^+ ions were not included,
- organic ions are present in significant quantities.

4.7 Groundwater recharge

By definition, groundwater recharge is an addition of water to a groundwater reservoir (Xu and Beekman, 2003). There are numerous techniques used for evaluating groundwater recharge, with each method having its own constraints regarding applicability and reliability. In Southern

Africa, the most commonly used methods include the Chloride Mass Balance (CMB), Water Table Fluctuation (WTF), Cumulative Rainfall Departure (CRD), Saturated Volume Fluctuation (SVF), and integrated approaches such as the excel spreadsheet by (Van Tonder and Xu, 2000).

Groundwater recharge in the study area was estimated using the chloride mass balance (CMB) method and the water table fluctuation (WTF) method. The groundwater spreadsheet software developed by van Tonder and Xu (2000) was used as a validation tool as it encompasses several published groundwater maps that estimate groundwater recharge.

Eriksson and Khunakasem (1969) developed the Chloride Mass Balance as a simple and cheap method that has been adopted and accepted worldwide. It relies on the measured annual rainfall and the concentration of chloride in both rainfall and groundwater. The established relationship between rainfall and recharge is expressed in equation **Error! Reference source not found.**)

$$R = P \cdot \frac{Cl_p}{Cl_{gw}} \quad (17)$$

Where R is the groundwater recharge expressed in mm/year, P is the annual precipitation in mm/year, Cl_p is the average chloride concentration in precipitation, and Cl_{gw} is the average chloride concentration in the groundwater, both expressed in mg/l.

4.8 Software used for data analysis

Data collected and collated during the research was analysed, interpreted and presented using a variety of appropriate software. All the data obtained from the laboratory analysis was captured in Microsoft Office Excel, then exported to IBM SPSS 27 for statistical analysis. The principal component and the Hierarchical Cluster Analysis were chosen as multivariate statistical analysis methods in this study. Graphical presentation of the hydrochemical data was compiled using AqQa software (Piper and the Durov diagrams). Gibb diagrams were plotted using Microsoft Office Excel. Diagrammes software was used to prepare stiff diagrams. QGIS was used for geospatial processing, viewing, editing, creating and analysing geospatial data. PHREEQC (Parkhurst and Appelo, 2013) was used to calculate saturation indices (SI) of the groundwater samples. The spreadsheet for automatic processing of water quality data was used for the MK test statistics. Surfer 11 was used to construct the groundwater contours and

determine the groundwater flow directions. Golden Software Strater 3 was used to construct the proposed conceptual hydrogeological X-section of the study area along with well-to-well logs.

CHAPTER 5 : RESULTS AND DISCUSSION

5.1 Introduction

Hydrogeochemical processes in groundwater are primarily controlled by the physical and chemical interactions that occur within the groundwater system. The spatial and temporal variations in groundwater chemistry and quality depend on the hydrogeochemical processes operating within the groundwater system. This chapter presents the results of analysis, interpretation and discussion of the original data complemented with secondary data collected during the course of the research.

5.2 Hydrogeological characteristics of the study area

5.2.1 Groundwater recharge

The CMB method of estimated groundwater recharge is presented in Table 5.1, in which the mean rainfall chloride concentration of 1 mg/l was sourced from van Wyk et al. (2011). The CMB based groundwater recharge estimation made at 24 groundwater sampling points for the studied catchment vary widely. The estimated recharge varies from a minimum of 26 mm/year (around 4% of MAP) at borehole KSP4 to a maximum of about 390 mm/year (60% of MAP) estimated based on borehole KP05 (Table 5.1). Although the CMB method captured the variability of groundwater recharge across the study catchment acceptably, the higher ranges of the CMB recharge estimate for the catchment are not acceptable. The uncertainty in the CMB recharge estimate is mainly attributed to the uncertainty of chloride concentration in precipitation taken from literature sources.

Table 5.1: Results of groundwater recharge estimated using the CMB method.

Sample Point ID	Groundwater Chloride(mg/l)	Mean chloride concentrations from precipitation (mg/l) (van Wyk et al. 2011)	Mean precipitation (mm/yr)	Recharge (mm/yr)	Recharge (% of annual rainfall)
10490-08	3.08	1	644	209.09	32.47
10490-09	3.21	1	644	200.62	31.15
10490-10	19.60	1	644	32.86	5.10
10490-14	1.98	1	644	325.25	50.51
10490-17	4.09	1	644	157.46	24.45
10490-21	5.28	1	644	121.97	18.94
10490-25	2.89	1	644	222.84	34.60
10490-27	3.19	1	644	201.88	31.35
BH11	2.71	1	644	237.64	36.90
BH25	3.71	1	644	173.58	26.95
BH27	1.69	1	644	381.07	59.17
BH30	3.41	1	644	188.86	29.33
CSW08	14.60	1	644	44.11	6.85
DWBH-06	1.72	1	644	374.42	58.14
DWBH-36	2.63	1	644	244.87	38.02
KP05	1.65	1	644	390.30	60.61
MP14-001	1.85	1	644	348.11	54.05
MP14-002	1.99	1	644	323.62	50.25
MP14-003	8.02	1	644	80.30	12.47
LGW B14	3.49	1	644	184.47	28.65
KSP 1	2.88	1	644	223.61	34.72
KSP 3	5.37	1	644	119.88	18.62
KSP 4	24.51	1	644	26.28	4.08
KSP 5	7.13	1	644	90.27	14.02
Average (Harmonic Mean)				118.2	18.3

The qualified guesses groundwater recharge estimation approach included in van Tonder and Xu (2000) that uses maps including Vegter (1995), ACRU, soil, vegetation, slope and geology is used to validate the CMB and WTF groundwater recharge estimations. The groundwater

recharge estimated through the qualified guesses approach is shown in Table 5.2 in which the average groundwater recharge is 56.6 mm/year or 8.1% of MAP, which is higher than the WTF estimate and much less than the CMB recharge estimate. The qualified guesses approach groundwater recharge estimate is comparable with the recharge rate estimated for the quaternary catchment through the Groundwater Resources Assessment II (GRA II) project (DWAF, 2006), which is 58.9 mm/year or 8.8% of MAP. Thus, groundwater recharge for the catchment ranges from the 5% MAP of the WTF estimate to 8% of MAP of the qualified guess approach.

Table 5.2: Recharge estimation using qualified guesses approach following van Tonder and Xu (2000).

Method	Recharge (mm/a)	Recharge (% of annual rainfall)
Soil information	66.3	9.5
Geology	36.3	5.3
Vegter (Vegter, 1995)	65.0	9.3
Expert's guesses	58.9	8.4
Average	56.6	8.1

Additionally, the WTF method was also used to estimate recharge in the study to complement the CMB method. The WTF method of groundwater recharge is given by equation 18.

$$R = Sy \frac{\Delta h}{\Delta t} \quad (18)$$

Where R is groundwater recharge, Δt is observation time related to the seasonal groundwater level variation Δh and Sy is the specific yield of the aquifer under consideration.

Monthly groundwater level records between 2014 and 2017 were used in this study. The Sy values estimated by Groundwater Square (2018) for the various aquifer in the study area were adopted, where the Dwyka Group's estimated Sy was about 0.01 and for that of the Pretoria and Ecca Groups were 0.04. Consequently, the calculated groundwater recharge ranges from a minimum of 0.63 mm/year to a maximum of 143 mm/year, with an overall average value of 31.6 mm/year or 5% of MAP (Table 5.3). The rate and spatial variability of groundwater recharge estimated by the WTF method for the study area is much reasonable compared to the recharge estimated using the CMB method. The groundwater recharge variability across the

studied quaternary catchment is attributed to variation in geology which translates into variation in the rate of infiltration and precipitation.

Table 5.3: Estimation of groundwater recharge using the WTF method for the period of 2014 to 2017.

Sample Point ID	Specific Yield	Annual Rise of water Table (m)				Annual Groundwater Recharge (mm)				Average Annual Groundwater Recharge (mm)	Recharge (% of annual rainfall)
		2014	2015	2016	2017	2014	2015	2016	2017		
BH30(LGW-B11)	0.04	0.01	1.59		0.19	0.4	63.6		7.6	23.87	3.71
BH03	0.01	0.85	4.48		1.12	8.5	44.8		11.2	21.50	3.34
10490-25	0.01		0.52	0.02	0.05		5.2	0.2	0.5	1.97	0.31
BH25	0.01	1.02	4.21	0.68	13.93	10.2	42.1	6.8	139.3	49.60	7.70
BH02	0.01	0.88	2.13		1.56	8.8	21.3		15.6	15.23	2.37
BH24	0.01		1.24	0.55	0.33		12.4	5.5	3.3	7.07	1.10
BH27(LGW-B4)	0.04		3.88		0.88		155.2		35.2	95.20	14.78
DWBH-06	0.04	0.55	0.81		0.18	22	32.4		7.2	20.53	3.19
KP05	0.01		1.38	0.15	0.44		13.8	1.5	4.4	6.57	1.02
10490-27	0.04		3.57				142.8			142.80	22.17
DWBH-36	0.04	0.44	0.27	0.75	0.08	17.6	10.8	30	3.2	15.40	2.39
10490-09	0.01	0.06		0.08	0.14	0.6		0.8	1.4	0.93	0.14
10490-10	0.01	0.11		0.01	0.07	1.1		0.1	0.7	0.63	0.10
10490-08	0.01	1.56	2.67		1.05	15.6	26.7		10.5	17.60	2.73
10490-21	0.04		4.02	1.63	0.07		160.8	65.2	2.8	76.27	11.84
10490-17	0.01		0.3	0.2	2.55		3	2	25.5	10.17	1.58
Average										31.58	4.90

5.2.2 Groundwater levels and groundwater flow direction

A total of 109 boreholes with groundwater level measurements were used to understand the depth to groundwater and construct a groundwater contour map for the studied quaternary catchment. The depth to groundwater ranges from near-surface to 88 m bgl (Figure 5-1). The southwestern parts of the study area close to Intibane Colliery shows the greatest water depth most probably attributed to some mine related dewatering.

The Advanced Spaceborne Thermal Emission and Reflection Radiometer (ASTER) Digital Elevation Model (DEM) data was acquired from the National Aeronautic and Space Administration (NASA). The DEM was imported into QGIS for the generation of topographic characteristics of the study area. The topography map together with the depth to groundwater data was used to calculate the hydraulic heads of the boreholes. There is a good correlation between the surface topography and the measured water levels, where approximately 94% of observed water level variations can be explained by variations in surface elevation. This strong linear relationship ($R^2 = 0.94$) between groundwater elevations and topography is shown in Figure 5-2. Based on the observed relationship, interpolation using the Bayesian method was done to indicate the groundwater elevations together with inferred groundwater flow directions Figure 5-3. Groundwater flow direction is towards the north, controlled mainly by the local topographic gradients in the area.

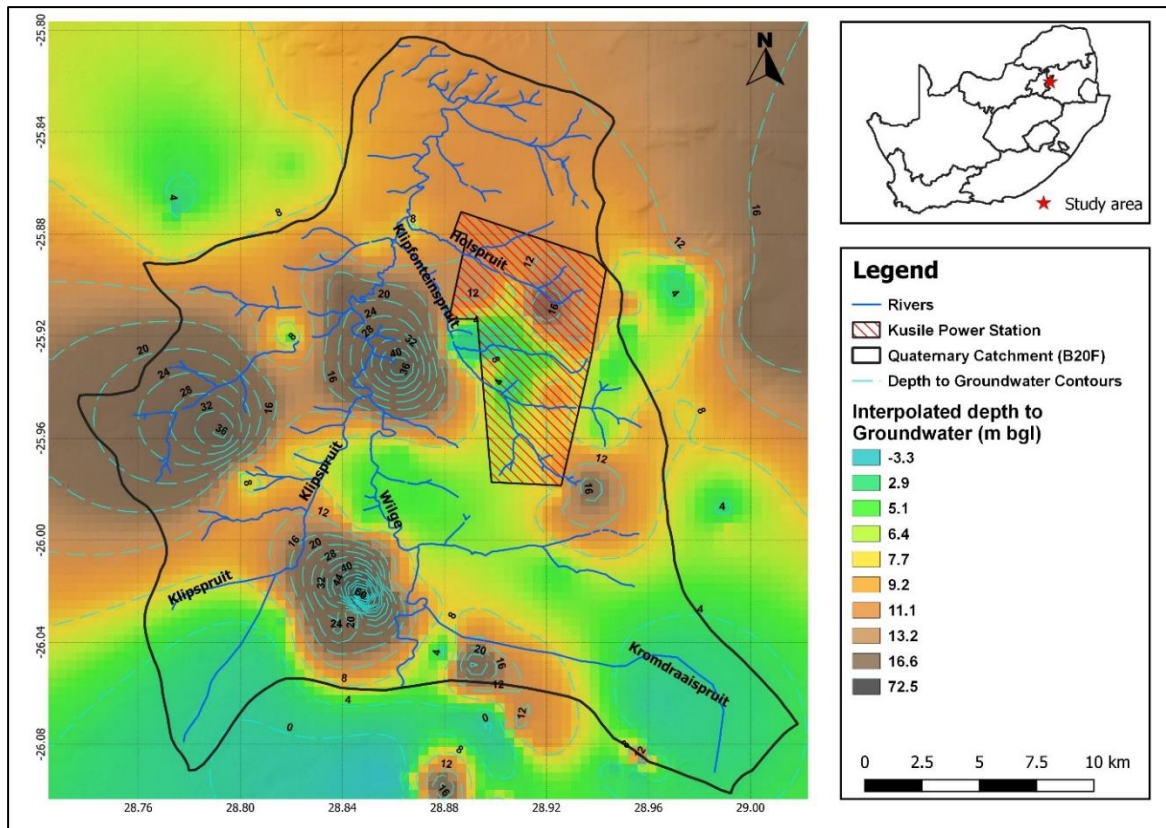


Figure 5-1: Interpolated depth to groundwater levels of the study area.

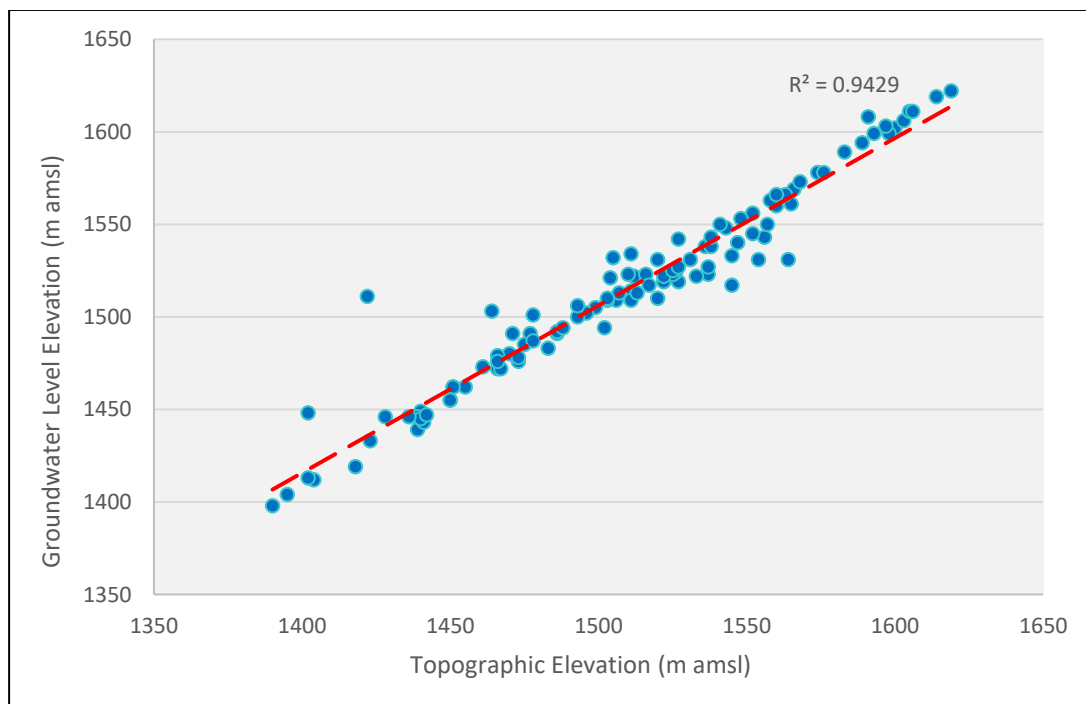


Figure 5-2: Correlation between surface topography and potentiometric heads. (Compiled from all available recorded water level data).

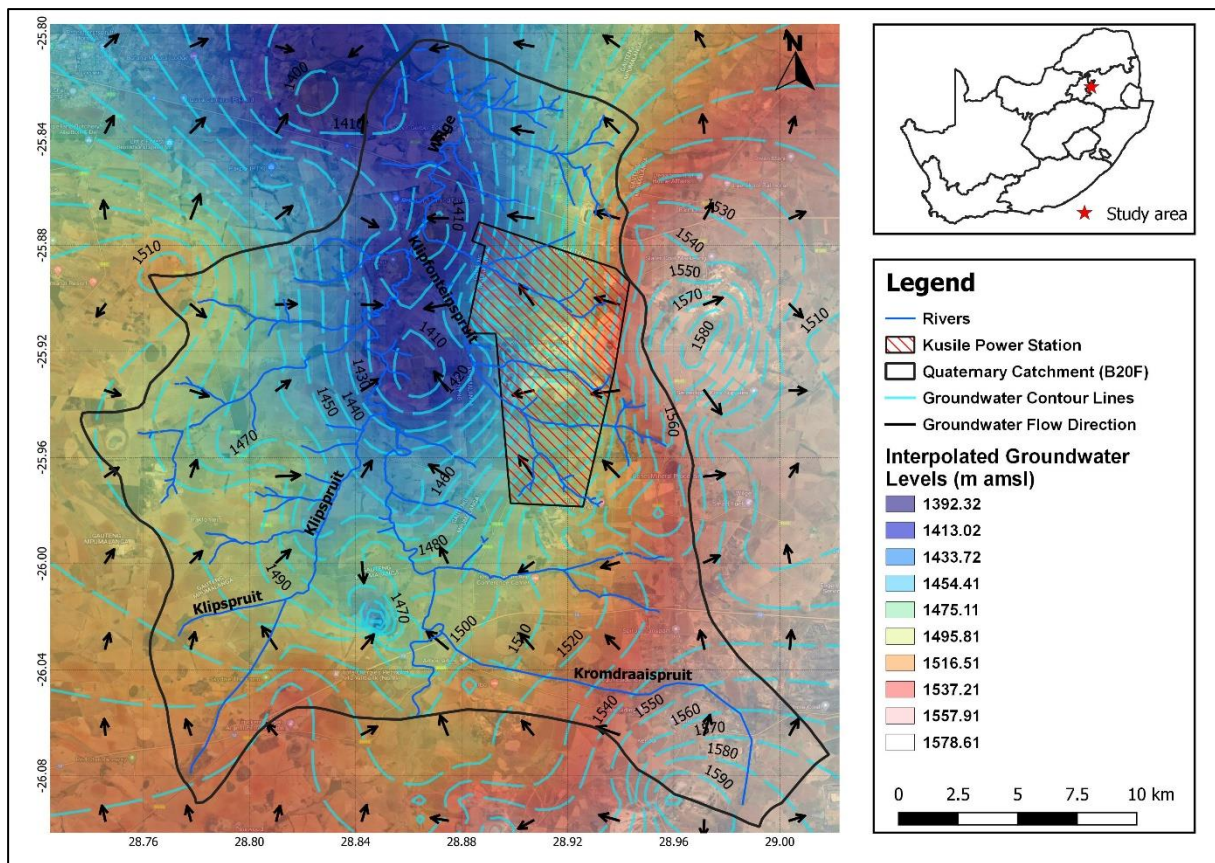


Figure 5-3: Map showing the hydraulic head pattern, groundwater flow direction, groundwater depth within the study area.

5.3 Hydrogeochemical Characteristics

Assessing the groundwater chemistry is vital to understanding the region's groundwater resource quality and its evolution. Conventional geochemical methods were used to assess the hydrogeochemical regime of the groundwater system in the study area. Descriptive statistics, graphical visualizations (box plots), together with correlation matrices were used to describe the distribution and characteristics of hydrochemical data. Furthermore, the spatial distribution of important physicochemical parameters (pH and EC) was assessed. Geochemical signatures and their origin were interpreted using graphical methods such as the Piper, Durov and Stiff diagrams. The dominant hydrogeochemical processes in the study area were explored using different bivariate plots. To complement the conventional geochemical methods, multivariate statistical methods in the form of hierarchical cluster analysis (HCA) and principal component analysis (PCA) were used to analyse the hydrochemical data.

5.3.1 Descriptive Statistics and Correlation Matrices of hydrochemical data

The descriptive statistics of the most important hydrochemical parameters analysed in the study area is given in Table 5.4. The corresponding Box plot that provides a useful and concise graphical display for summarising the distribution of the data is shown in Figure 5-4, while groundwater-surface water comparison statistics for the concentration of physicochemical parameters in the study area is shown in Table 5.5. The various physicochemical parameter values and measured groundwater and surface water trace elements concentration within the study area are presented in Appendix B and C, respectively.

The pH of groundwater in the study area ranges from 6 to 8, which is the range commonly encountered in natural groundwaters (Hiscock, 2005). However, two outliers of an acidic pH of 5.21 and an alkaline pH of 9.59 were measured at a spring and borehole, respectively (Appendix B). The EC values range from 3.27 to 67.20 mS/m indicating very fresh to fresh groundwater with low salinity. Both groundwater and surface water samples have low variations in dissolved oxygen (DO) and it ranges from 4.07 to 5.87 mg/L in groundwater and from 2.79 to 6.30 mg/L in surface waters. The turbidity varies from 0.31 to 275 NTU with a mean of 43.56 NTU. The highest value of groundwater turbidity measured is 275 NTU from borehole MP14-003 and the minimum value is 0.31 from Spring04. Poor borehole development during drilling could account for the high turbidity from the borehole and/or unprotected boreholes with shallow groundwater indicates high turbidity as well due to impact from the surface. For the surface water samples, the highest and lowest turbidity values are 1.99 and 89.40 NTU obtained from sample locations SW18 and NCSW01 respectively. Sample point NCSW01 is collected from a surface runoff sediment dam hence the high turbidity while the sample location for sample point SW18 is along the Klipfonteinspruit which gets filtered by bamboo upstream.

The Ca^{2+} concentrations of groundwater and surface water samples vary from 0.60 to 56.90 and 4.66 to 94.70 mg/L, with mean concentrations of 8.17 and 30.67 mg/L respectively. Concentrations of Mg^{2+} , Na^+ , HCO_3^- , and Cl^- in groundwater vary from 0.53-26.30 mg/L, 1.53-62.60 mg/L, 5.49-248.90 mg/L, and 1.25-24.50 mg/L, respectively. In surface water samples concentrations of Mg^{2+} , Na^+ , HCO_3^- , and Cl^- vary from 3.00-19.10 mg/L, 4.6-68.7 mg/L, 43.92-119.56 mg/L, and 3.620-14.90 mg/L, respectively. Surface water samples have elevated SO_4 concentrations with a mean value of 97.22 mg/L while for groundwater samples is 52.76 mg/L. For all the water samples, SO_4 has the highest standard deviation (81.25 mg/L), compared with

other parameters. The sources of SO_4 may be attributed to the oxidation and dissolution of pyrite contained in the coal mined and used in the study area. It is clear that mining activities, predominantly coal, have a greater impact on the surface water chemistry within the study area. Trace metals that are typically associated with coal-fired power stations are As, Cd, Co, Cr, Cu, Hg, Mn, Ni, Pb, and Zn (Dalton et al., 2018). Based on the results of trace element analysis undertaken in the study area as presented in Appendix C, the majority of samples have concentrations of As, Cd, Co, Cr, Hg, Pb and Sb that are below the laboratory detection limits. Iron concentrations in groundwater samples is relatively high, with a mean concentration of 7.57 mg/L compared to a mean concentration of 1.19 mg/L in surface water samples. The mean concentrations of Mn in both groundwater and surface water are 0.16 and 0.06 mg/L, respectively. Borehole 10490-10 ($37.2 \text{ mg}^{-1} \text{ L}$) and NCSW01 ($3.84 \text{ mg}^{-1} \text{ L}$) has the highest concentration of iron for groundwater and surface water, respectively. These elevated iron and manganese concentrations could be related to the oxidation of pyrite which in turn leads to the precipitation of iron.

Table 5.4: Descriptive statistics of the hydrochemical variables measured within the study area (all values are reported in mg/L unless and otherwise stated).

Variables	No. of samples	Min	Max	Mean (μ)	Median	Variance (σ^2)	Standard deviation (σ)	Coefficient of variation (σ/μ)	Standard error of the mean
pH	50	5.21	9.59	7.23	7.16	0.48	0.69	0.10	0.10
EC (mS/m)	50	3.27	67.20	13.65	22.72	353.70	18.81	0.83	2.69
Turbidity as N.T.U.	50	0.31	275.00	15.30	43.56	3872.95	62.23	1.43	9.38
Ca ²⁺	50	0.60	94.70	6.04	16.72	499.61	22.35	1.34	3.19
Mg ²⁺	50	0.53	26.30	3.67	6.33	33.20	5.76	0.91	0.82
Na ⁺	50	1.53	68.70	8.20	14.84	290.55	17.05	1.15	2.46
HCO ₃ ⁻	50	5.49	248.88	54.90	62.12	1847.30	42.98	0.69	6.14
Cl ⁻	50	1.25	24.51	5.08	6.60	26.37	5.14	0.78	0.73
SO ₄ ²⁻	50	0.09	271.00	5.88	48.84	6601.51	81.25	1.66	11.85
DO	50	2.79	6.30	5.55	5.27	0.48	0.69	0.13	0.10
Al	50	0.01	5.55	0.11	0.29	0.65	0.81	2.80	0.12
Fe	50	0.02	37.20	1.40	5.15	71.32	8.45	1.64	1.21
Mn	50	0.01	1.26	0.06	0.12	0.04	0.21	1.70	0.03

Table 5.5: Comparison of a statistical summary of physicochemical data of groundwater and surface water in the study area.

Variables	Groundwater					Surface water				
	No. of samples	Min	Max	Mean (μ)	Standard deviation (σ)	No. of samples	Min	Max	Mean (μ)	Standard deviation (σ)
pH	31	5.21	9.59	6.86	0.74	19	7.27	8.10	7.64	0.19
EC (mS/m)	31	3.27	67.20	16.20	13.64	19	10.30	62.90	33.34	21.91
Turbidity as N.T.U.	31	0.31	275.00	63.26	75.06	19	1.99	89.40	16.61	23.00
Ca ²⁺	31	0.60	56.90	8.17	13.50	19	4.66	94.70	30.67	27.44
Mg ²⁺	31	0.53	26.30	4.43	4.85	19	3.00	19.10	9.43	6.05
Na ⁺	31	1.53	62.60	11.04	14.04	19	4.60	68.70	20.84	20.28
HCO ₃ ⁻	31	5.49	248.88	54.79	50.15	19	43.92	119.56	74.10	26.36
Cl ⁻	31	1.25	24.51	5.23	5.45	19	3.62	14.90	8.83	3.90
SO ₄ ²⁻	31	0.09	250.00	17.14	52.76	19	5.36	271.00	97.22	95.83
DO	31	4.07	5.87	5.04	0.60	19	2.79	6.30	5.59	0.72
Al	31	0.01	5.55	0.32	1.05	19	0.05	0.54	0.25	0.17
Fe	31	0.02	37.20	7.57	10.11	19	0.32	3.84	1.19	1.02
Mn	31	0.01	1.26	0.16	0.26	19	0.02	0.24	0.06	0.05

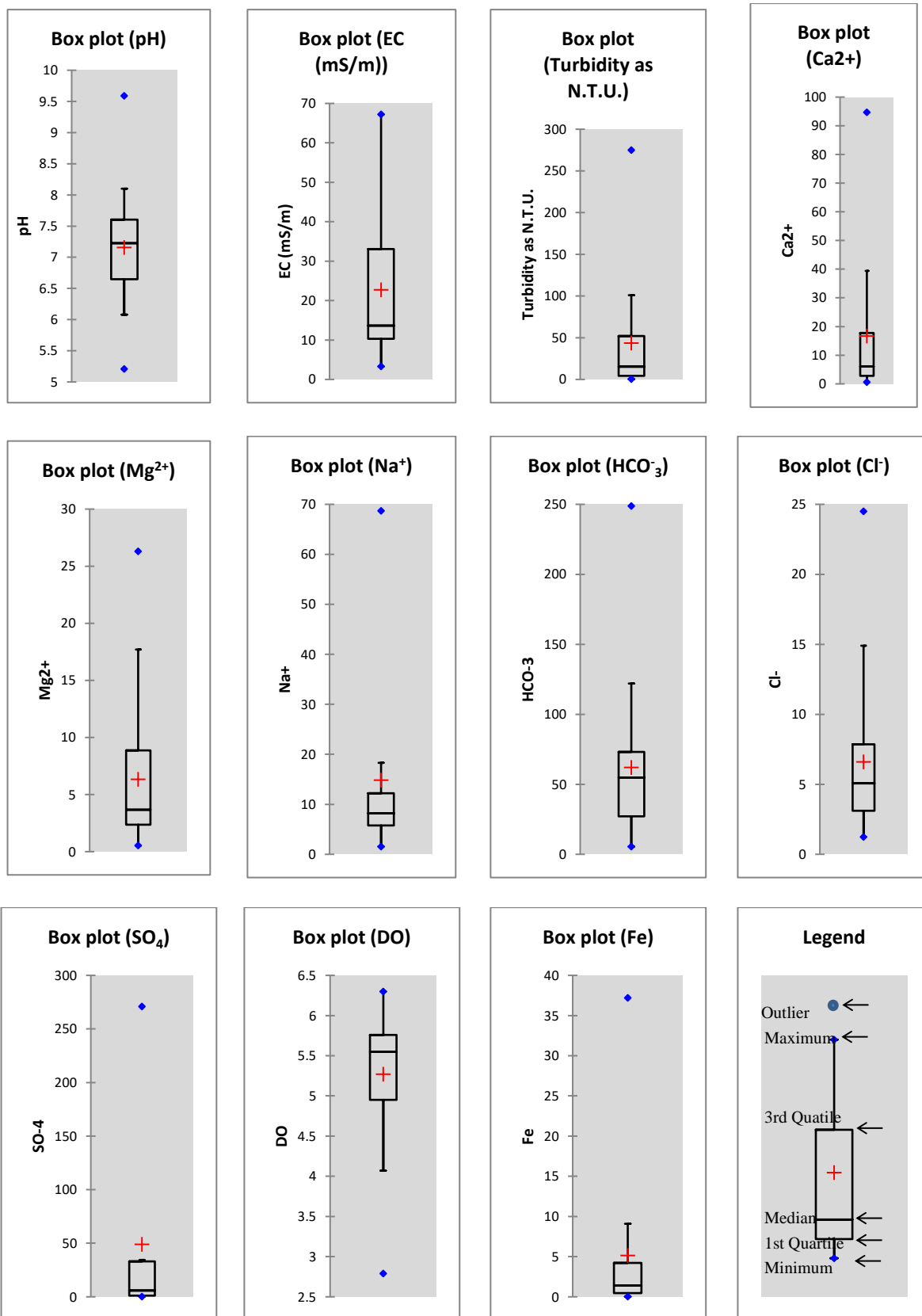


Figure 5-4: Box plots of chemical parameters used in descriptive statistics of all the water samples. Plots of Al and Mn were excluded due to their low concentrations.

Pearson's Correlation Matrix

Major hydrogeochemical processes that control chemical characteristics can be understood as correlations between the water quality variables. The relationship of the dissolved ions was assessed to identify the main hydrogeochemical processes responsible for the chemical composition of the water within the study area. The results of Pearson's correlation matrix presented in Table 5.6 illustrate that the electrical conductivity has high correlations with Na ($r = 0.72$), Ca ($r = 0.89$), Mg ($r = 0.94$), SO₄ ($r = 0.94$) and moderate correlation with Cl ($r = 0.67$), indicating the contribution of major ions to the salinity of groundwater in the area. Sulphate has high correlation with calcium ($r = 0.94$) indicating possible buffering of acid mine affected groundwater by carbonate minerals. The moderate negative correlation of dissolved oxygen with iron ($r = -0.51$) suggests reducing conditions occurring in the system. Turbidity and iron are highly correlated ($r = 0.80$), indicating possible aeration of a reduced groundwater during pumping.

Table 5.6: Pearson's correlation matrix of hydrochemical variables analysed in the study area.

	pH	EC	Turbidity	Ca ²⁺	Mg ²⁺	Na ⁺	HCO ₃ ⁻	Cl ⁻	SO ₄ ²⁻	DO	Fe
pH	1.00										
EC	0.48	1.00									
Turbidity	-0.21	-0.20	1.00								
Ca ²⁺	0.33	0.89	-0.20	1.00							
Mg ²⁺	0.32	0.94	-0.10	0.82	1.00						
Na ⁺	0.59	0.72	-0.15	0.33	0.64	1.00					
HCO ₃ ⁻	0.66	0.54	0.04	0.29	0.48	0.73	1.00				
Cl ⁻	0.12	0.67	-0.16	0.48	0.71	0.57	0.23	1.00			
SO ₄ ²⁻	0.31	0.94	-0.24	0.94	0.90	0.51	0.26	0.63	1.00		
DO	0.20	0.18	-0.46	0.24	0.12	0.06	-0.02	0.12	0.23	1.00	
Fe	-0.27	-0.03	0.80	-0.07	0.13	-0.03	0.04	0.04	-0.06	-0.51	1.00

5.3.2 Spatial distribution of pH and EC

The degree of dissociation of weak acids and bases is affected by variations in pH, which in turn affect the composition of the dissolved constituents. The measured groundwater pH in the study area ranges from 6 to 8, which is within the normal range commonly encountered in groundwaters (Figure 5-5), with an average of 7.23. Borehole MP14-002 and Spring04 seem to be outliers with an acidic pH of 5.21 and an alkaline pH of 9.59 measured, respectively. The

alkaline pH of borehole MP14-002 is related to the buffering effect of carbonate minerals related to the underlying geology (shale). The acidic pH of Spring04 could be linked to animal waste as the spring is used as a water drinking point for the cattle, this results in biogenic carbon dioxide and methane hence the reduction in pH. The pH of the surface water samples is between 7 and 8. The pH of the groundwater samples appears to tend towards alkalinity in the direction of groundwater flow as observed in boreholes DWBH-36, BH02, BH24, 10490-25, and KSP 1, indicating possible buffering reactions.

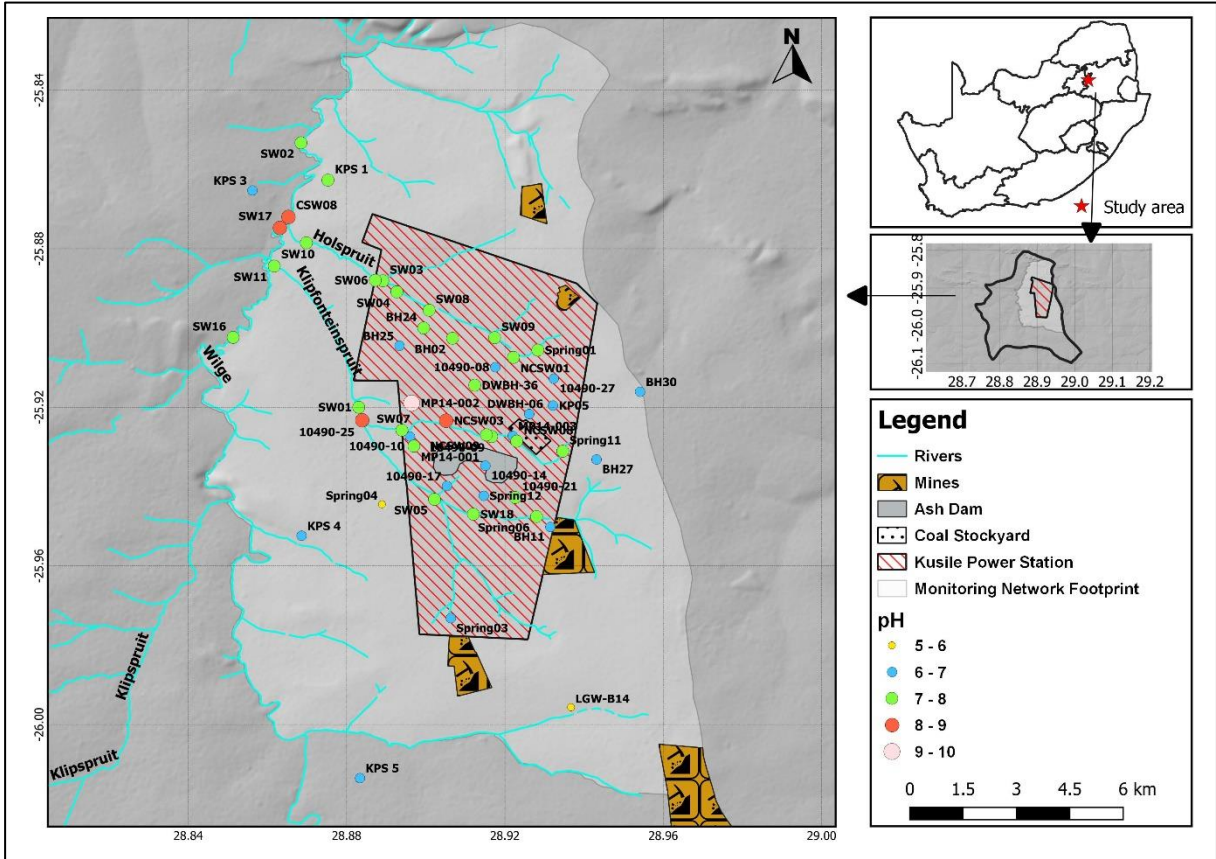


Figure 5-5: Spatial distribution of pH in the study area.

The electrical conductivity (EC) values of EC in the study area vary from 3.27 to 67.20 mS/m (Figure 5-6). All the groundwater samples have low EC that ranges between 3.27 mS/m and 40 mS/m except borehole 10490-10 (67.20 mS/m). This borehole is located in a wetland area where it is hydraulically connected to surface water bodies that are affected by activities from the ash dam as the surface waters flow through the footprint of the power station.

The EC of the groundwater system increases from upstream to downstream. The ‘dilution effect’ due to different tributaries of ‘better quality headwaters is witnessed in the surface water

samples along the Wilge River. Sample SW16 (62.90 mS/m) is located on the Wilge River before the confluence of the streams that drain the Kusile power station, it has the highest EC content, signifying that the surface water is already polluted upstream of the power station. Surface water samples SW17, CSW08 and SW2 are taken just after the confluence of the Klipfonteinspruit and Holspruit streams and have EC values of 58.5 mS/m, 57.6 mS/m, and 58.2 mS/m, respectively. This indicates that the tributary streams have diluted the Wilge River. A similar dilution effect is noted on the Klipfonteinspruit between sample SW18 and SW01 (46.50 mS/m), where sample SW18 has a high EC of 62.8 mS/m affected by the coal mining at Malachite Mining. A drop in EC is noticed in Sample SW05 (54.3 mS/m) which is located just after a confluence of the two streams. The Holspruit tributary generally has low EC (10 - 20 mS/m) as there is minimum mining activity along this drainage line.

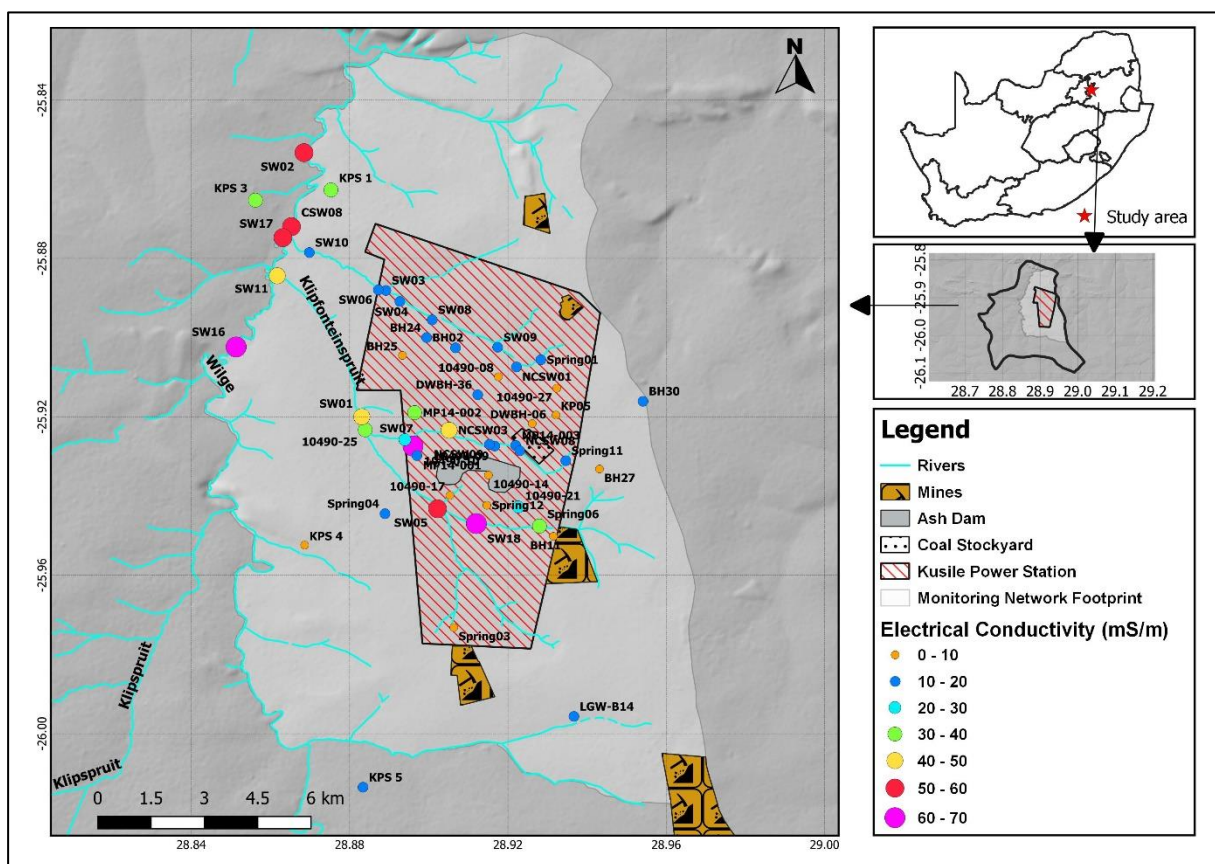


Figure 5-6: Spatial distribution of EC in the study area.

5.3.3 Hydrochemical Facies

The origins and distributions of groundwater that display different geochemical signatures can be compared using graphical charts such as Stiff diagrams, Piper plots and Durov diagrams.

Chemical proportions for individual samples may be represented using Stiff diagrams, while the Piper and Durov diagram show water quality classifications for groups of samples. The Durov diagram complements the Piper plot as it can reveal geochemical processes that may affect groundwater hydrochemical genesis.

The Piper trilinear diagram (Figure 5-7) shows that the majority of the groundwater and surface water samples are dominated by alkali earth metals (Ca^{2+} and Mg^{2+}) over alkalis (Na^+ and K^+). The alkali earth metals account for 78% over 22% by the alkalis while the weak acids account for 64% compared to 36% by the strong acids. The groundwater samples are dominated by weak acid (HCO_3^-) compared to strong acids (SO_4^{2-} and Cl^-), while the surface water samples show strong variability. The most frequent water type for the groundwater samples is Ca- HCO_3 , followed by mixed Ca-Na- HCO_3 type. The most frequent surface water hydrochemical facies is Ca- HCO_3 , followed by mixed Ca-Mg-Cl type. Overall, 50% of the groundwater and surface water samples are of Ca- HCO_3 type, 12% Ca-Cl type, 8% of Na-Cl type, 2% of Na- HCO_3 type, and the remaining 28% are constituted by mixed water types (Ca-Na- HCO_3 and Ca-Mg-Cl type) (Table 5.7).

Based on the dominance of the Ca- HCO_3 water type, it is evident that the groundwater in the study area is associated with contemporary recharge originating from direct precipitation to the surface and subsequent percolation through the unsaturated zone into the aquifer. Spring 04 and Spring 01 are classified as Na-Cl water type, the water quality of these springs is influenced by livestock that uses these springs as drinking points. The spatial distribution of the hydrochemical facies is shown in Figure 5-8. The Ca-Cl water type is related to surface water samples draining along the Klipfonteinspruit, and one of the boreholes (10490-10) that is hydraulically connected to the stream also exhibits the same water type. The Ca-Cl water type is linked to the impacts of coal mines and coal stockpiles from the Kusile power plant. Furthermore, the Malachite open cast mine is located in the headwaters of this stream and could have affected the water chemistry. Fly ash from the ash dump within the power station is another contributing factor to the water quality in the area. Surface water samples from the Holspruit are dominated by Ca- HCO_3 water type, unaffected by pollution as there is limited mining activity on the northern parts of the site. Sample points within the Wilge River, which is the main river in the study area, all have a mixed water type which is a result of intermixing of waters from the different streams.

Table 5.7: Classification of the water types in the study area based on the Piper diagram (Figure 5.7).

Water Types	Number of samples (GW=31; SW=19)	Percentage of samples in this category
Calcium Bicarbonate type	25 (17 Groundwater; 8 Surface water)	50
Calcium Chloride type	6 (2 Groundwater; 4 Surface water)	12
Sodium Chloride type	4 (4 Groundwater; 0 Surface water)	8
Sodium Bicarbonate type	1 (1 Groundwater; 0 Surface water)	2
Mixed type	14 (7 Groundwater; 7 Surface water)	28
Total Percentage		100
Alkaline earths exceeding alkalis	39 (21 Groundwater; 18 Surface water)	78
Alkalis exceeding alkaline earths	11 (10 Groundwater; 1 Surface water)	22
Total Percentage		100
Weak acids exceeding ding strong acids	32 (23 Groundwater; 9 Surface water)	64
Strong acids exceeding weak acids	18 (8 Groundwater; 10 Surface water)	36
Total Percentage		100

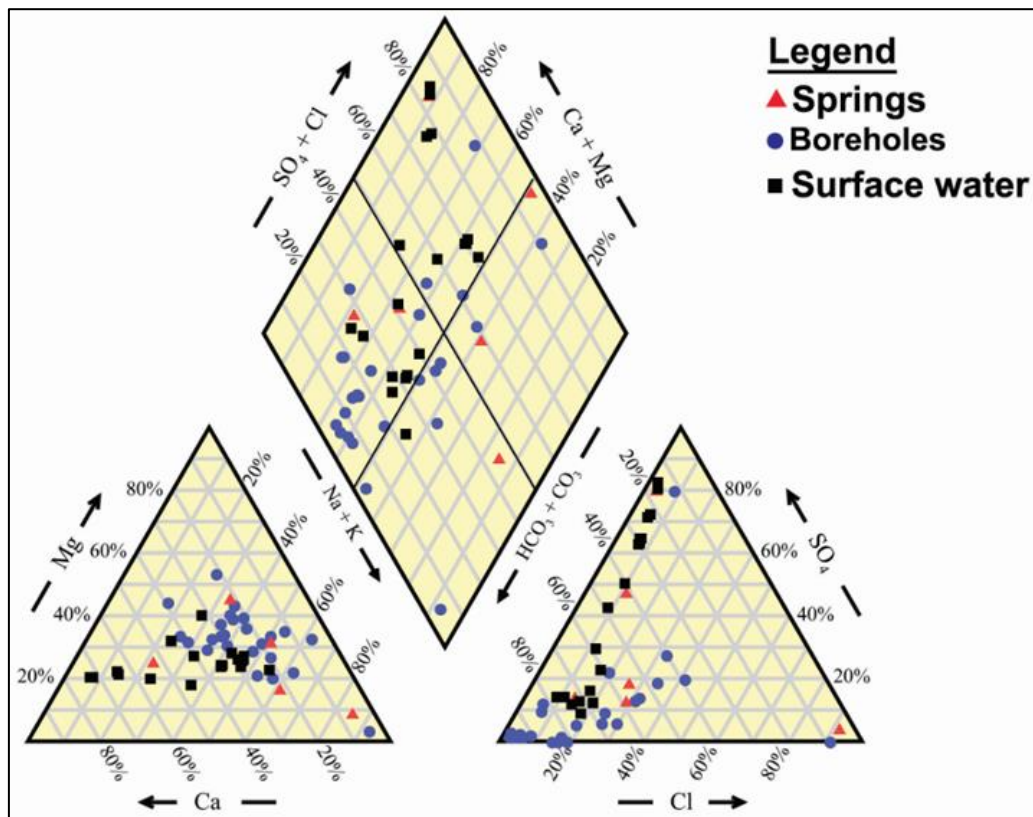


Figure 5-7: Piper Plot reflecting major hydrochemical water types.

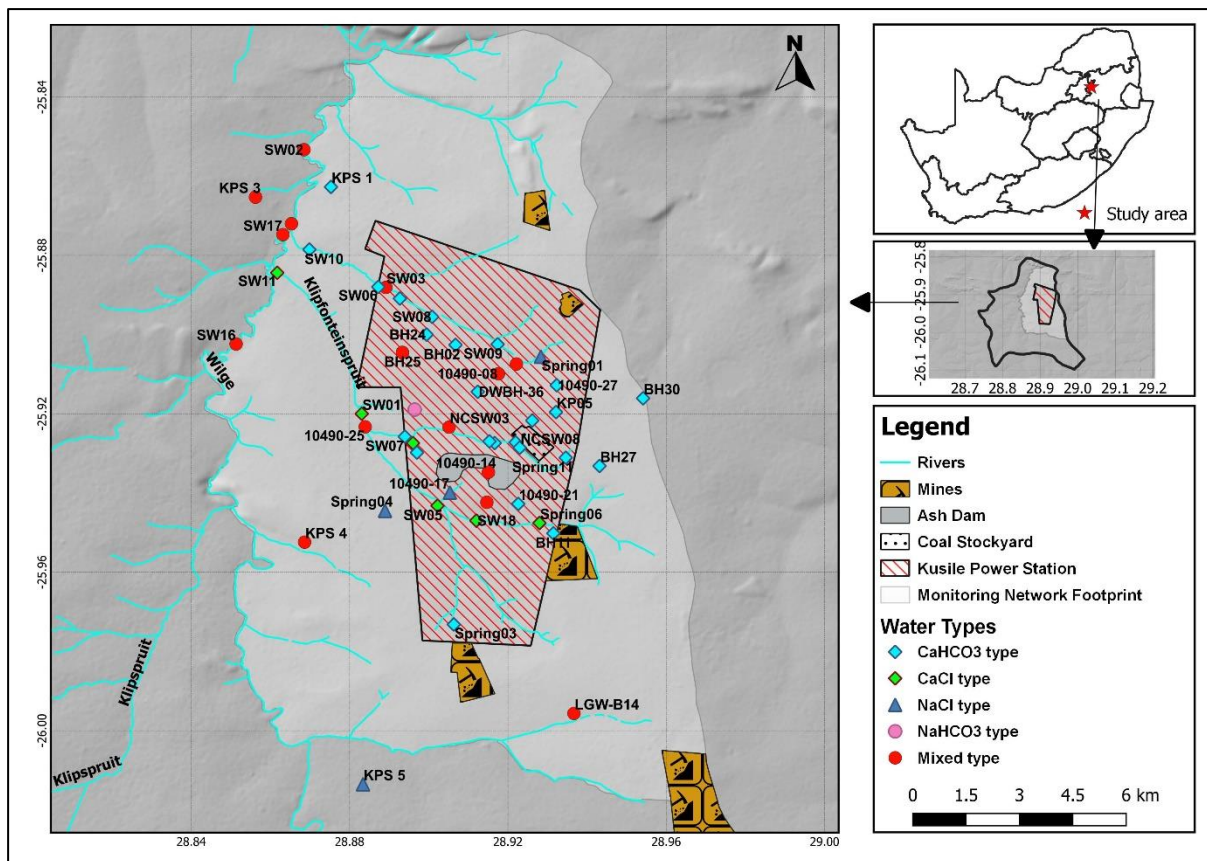


Figure 5-8: Spatial distribution of the hydrochemical water types in the study area.

The shape of the stiff diagram is used to emphasize the dominant cation and anion components, whereas the width of the plot is proportional to the concentration in milliequivalents. From the stiff diagrams of Figure 5-9 and Figure 5-10, it is evident that the boreholes do not show a dominant cation, however, they are dominated with HCO_3 anion. Water samples that are dominated with SO_4 are more prevalent in the surface water samples, even though HCO_3 is still the dominant anion. Similarly, the surface water samples do not have a dominant cation but combined the alkali earth metals appear to be dominating the alkalis.

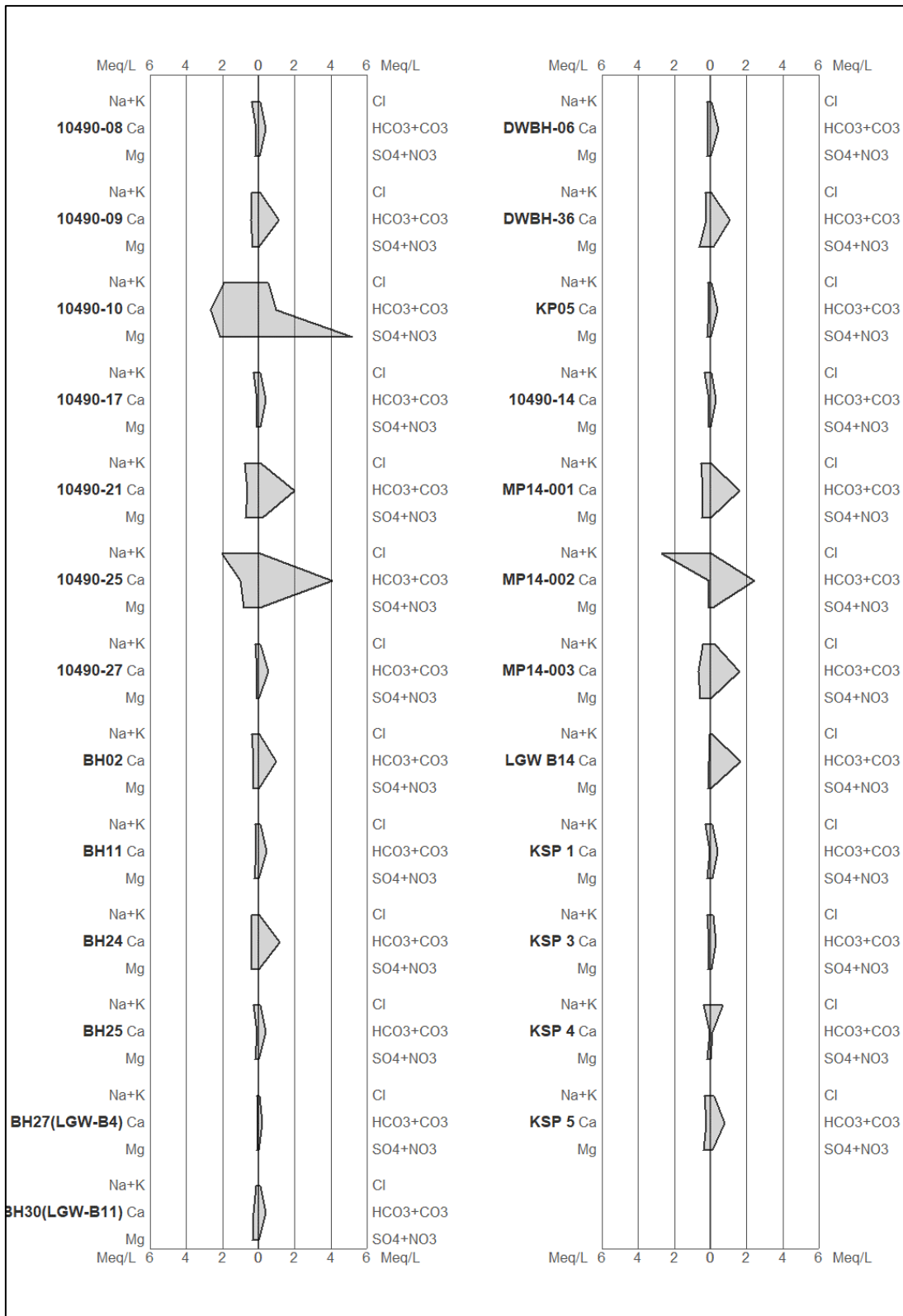


Figure 5-9: Stiff diagrams showing the various distinct shapes for the samples in the study area for borehole samples.

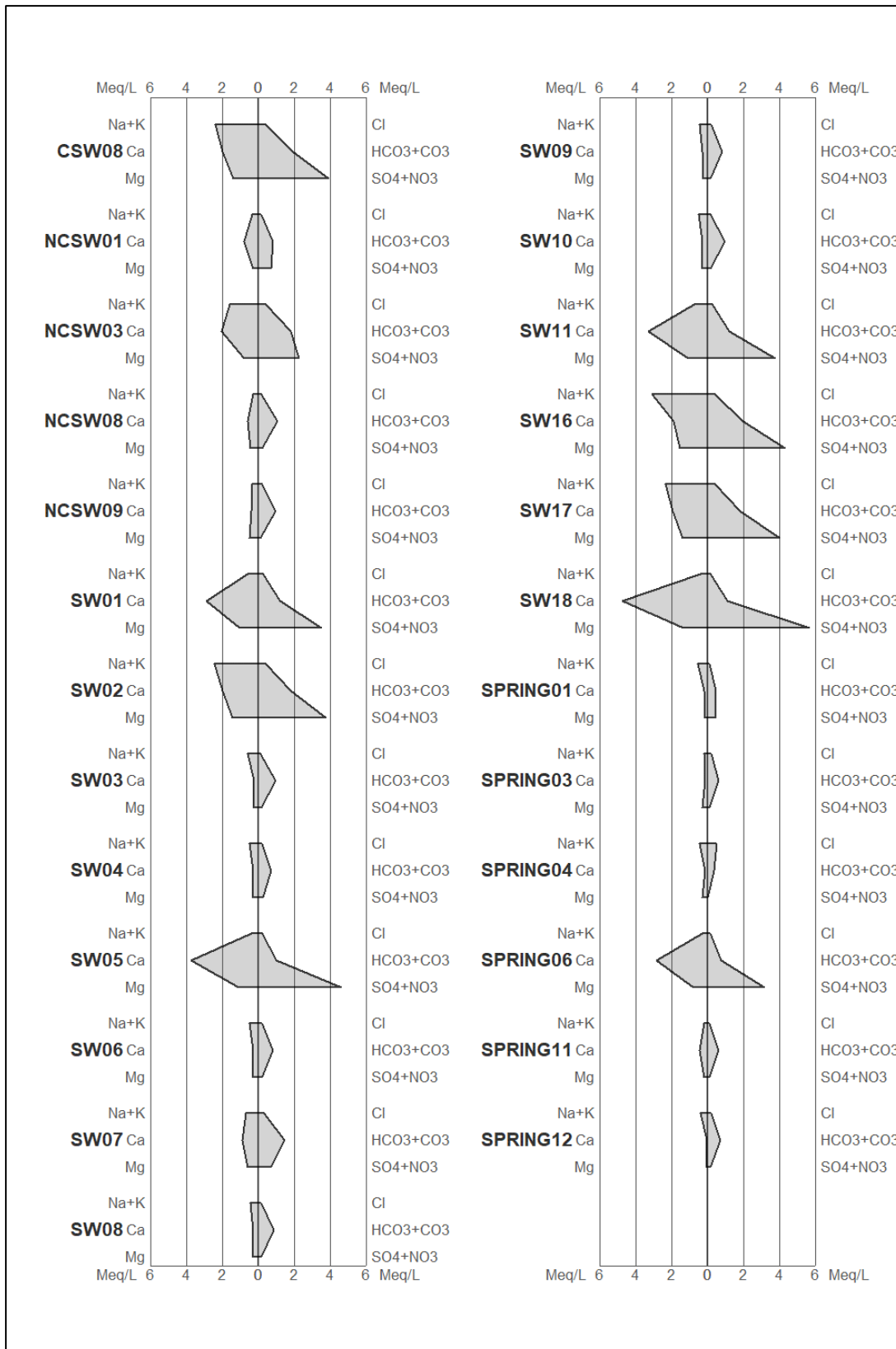


Figure 5-10: Stiff diagrams showing the various distinct shapes for the samples in the study area for surface water samples and springs.

The Durov plot of Figure 5-11 indicates possible hydrogeochemical processes that control the genesis of the hydrochemical composition of waters in the study area (Durov, 1948). According to the classification of Lloyd and Heathcoat (1985) (Table 5.8), water samples of the area plot according to the order in fields 8, 5, 6, 7, 4 and 1. The majority of the water samples plot mainly in field 6 indicating reverse ion exchange process driving the hydrochemical composition followed by field 5 where relatively fresh recent recharge water driving simple mineral dissolution controlling the hydrochemical composition. About 50% of samples plotted in field 6 indicate SO_4^{2-} as the dominant ion as a result of the impact of coal mines and coal stockpiles from the Kusile power plant. Similarly, the few samples plotted in fields 7, 4 and 1 are controlled by ion exchange, pyrite oxidation from the coal mining operations and recharge area Ca-HCO_3 water types, respectively. The Durov diagram evidently indicates that most of the water samples have total dissolved solids (TDS) clustering between 20 mg/L and 150 mg/L while the pH is between 7 and 8.

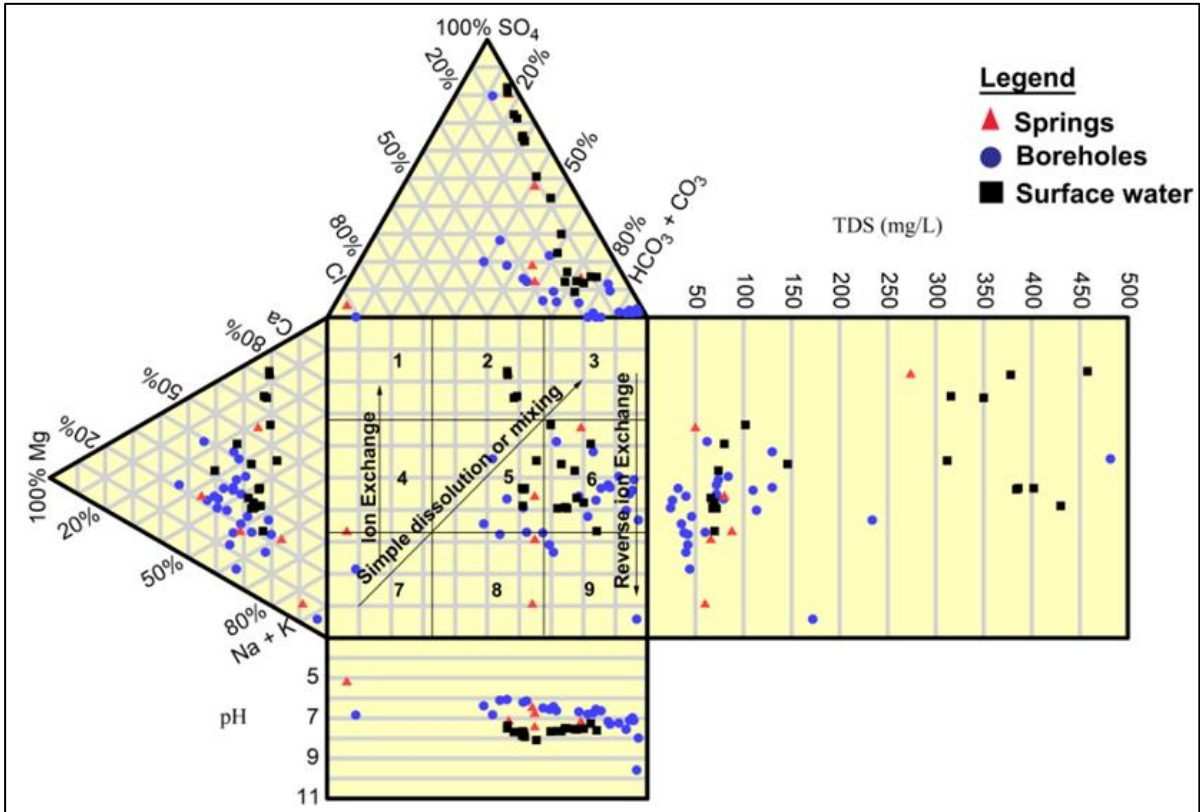


Figure 5-11: Durov diagram showing mixing and reverse ion exchange as hydrochemical processes involved .

Table 5.8: Classification of water based on the Durov diagram (after Lloyd and Heathcoat, 1985).

SI. No.	Water Types	Number of samples (Groundwater =31; SW=19)	% Of samples in this category
1	Cl dominant anion and Na dominant cation, indicate that the groundwaters be related to reverse ion exchange of Na-Cl waters.	0	0
2	Cl dominant anion and Na dominant cation, indicate that the groundwaters be related to reverse ion exchange of Na-Cl waters.	5 (1 Groundwater; 4 Surface water)	10
3	Cl and Na dominant is frequently encountered unless cement pollution is present. Otherwise, the water may result from reverse ion exchange of Na-Cl waters.	0	0
4	SO ₄ dominant or anion discriminate and Na dominant; is a water type that is not frequently encountered and indicates probable mixing or uncommon dissolution influences.	0	0
5	No dominant anion or cation, indicates water exhibiting simple dissolution or mixing.	13 (8 Groundwater; 5 Surface water)	26
6	SO ₄ dominates, or anion discriminant and Ca dominant, Ca and SO ₄ dominant, frequently indicates recharge water in lava and gypsiferous deposits, otherwise mixed water or water exhibiting simple dissolution may be indicated.	25 (15 Groundwater; 10 Surface water)	50
7	HCO ₃ and Ca dominant frequently indicate recharging waters in limestone, sandstone, and many other aquifers	2 (1 Groundwater; 1 Surface water)	4
8	This water type is dominated by Ca and HCO ₃ ions. Association with dolomite is presumed if Mg is significant. However, in those samples in which Na is significant, important ion exchange is presumed	3 (3 Groundwater; 0 Surface water)	6
9	HCO ₃ and Na are dominant, normally indicates ion-exchanged water, although the generation of CO ₂ at depth can produce HCO ₃ where Na is dominant under certain circumstances	2 (2 Groundwater; 0 Surface water)	4

5.3.4 Hydrogeochemical Processes Controlling Major Solute Compositions

Groundwater chemical composition indicates the rock-water interaction and chemical processes. Rock-water interactions processes are analysed using scatter plots as proposed by Gibb (1970). These diagrams use $\text{Na}/(\text{Na} + \text{Ca})$ ratio for cation, and $\text{Cl}/(\text{Cl} + \text{HCO}_3)$ for anion of the water samples data plotted against the respective values of total dissolved solids. The Gibbs diagrams show four distinct fields, namely evaporation dominance, evaporation-precipitation dominance, rock dominance, and precipitation dominance. Samples that fall in the centre of these areas originate from rock–water interaction. The Gibbs diagrams for the water samples analysed in this study indicate that the hydrochemical composition in the study area is controlled mainly by rock-water interaction processes (Figure 5-12).

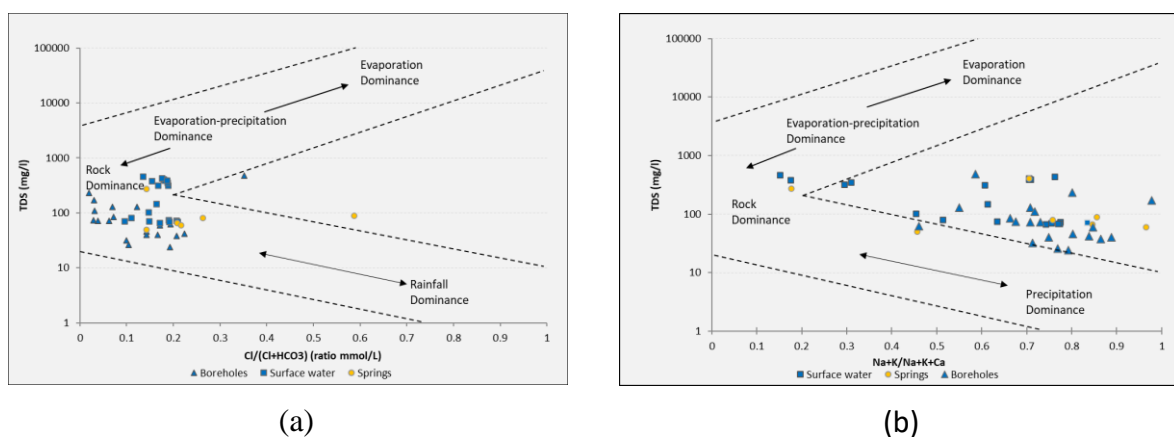


Figure 5-12: Gibb’s diagrams depicting the mechanism of controlling groundwater quality in the study area (a) TDS versus $\text{Cl}^-/(\text{Cl}^- + \text{HCO}_3^-)$. and (b) TDS versus $(\text{Na}^+ + \text{K}^+)/(\text{Na}^+ + \text{K}^+ + \text{Ca}^{2+})$.

Since the alkali earth metals (Ca and Mg) are the dominant cations in the groundwater of the study area, it is attributed to the dissolution of carbonate minerals. As water infiltrates into the subsurface and moves along the flow path, CaCO_3 and $\text{CaMg}(\text{CO})_2$ present in the host rocks may dissolve to increase the concentration of calcium and magnesium ions. The ratio between $\text{Ca}^{2+}/\text{Mg}^{2+}$ is utilised to investigate the source of ions from the weathering of minerals. Dissolution of calcite as the major controlling factor is indicated by a value of $\text{Ca}^{2+}/\text{Mg}^{2+}$ greater than 1, however, a ratio less than 1 signify the dissolution of dolomite (Singh et al., 2017). The majority of the groundwater samples (62%) have a $\text{Ca}^{2+}/\text{Mg}^{2+}$ value < 1 indicating the dissolution of dolomite as the dominant process (Figure 5-13). Only two springs show the dissolution of silicate minerals controlling their chemical composition. Thus, carbonate

weathering is the most likely process responsible for the buffering reactions and the observed hydrochemical composition of groundwater in the study area.

The scatter diagram of $(Ca + Mg)$ vs. $(HCO_3 + SO_4)$ identifies ion exchange processes and it is used to explain carbonate dissolution and silicate weathering (Datta and Tyagi, 1996). If dissolution of gypsum, dolomite and calcite dominate in an aquifer system, then the scatter plot of $(Ca^{2+} + Mg^{2+})$ versus $(HCO_3^- + SO_4^{2-})$ will be close to the 1:1 line. The dominance of ion exchange processes will tend to move the ratios towards the right and the dominance of reverse ion exchange will move the ratios to the left. In Figure 5-14, all the samples plot on or above the equiline, towards the $HCO_3 + SO_4$ field signifying silicate weathering as the main source for bicarbonate.

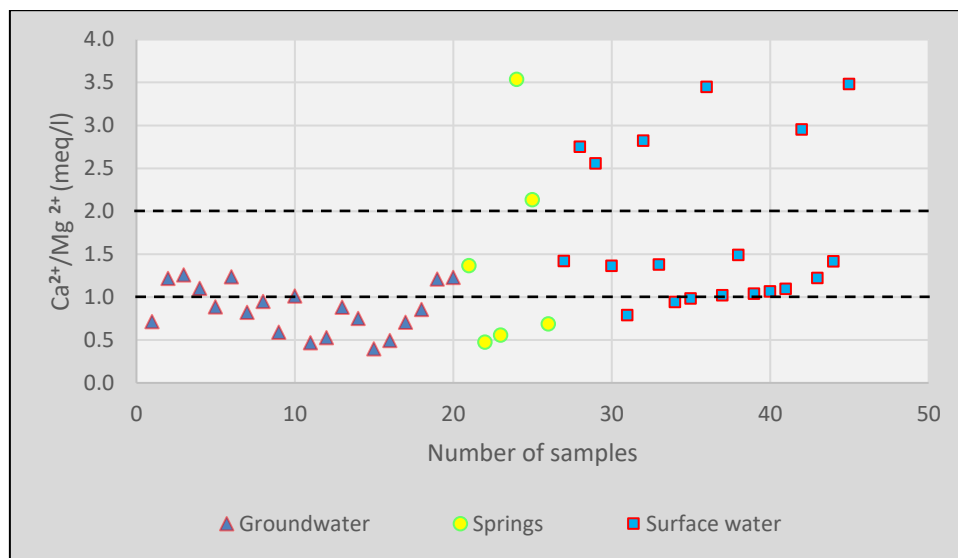


Figure 5-13: Scatter plot of Ca^{2+}/Mg^{2+} .

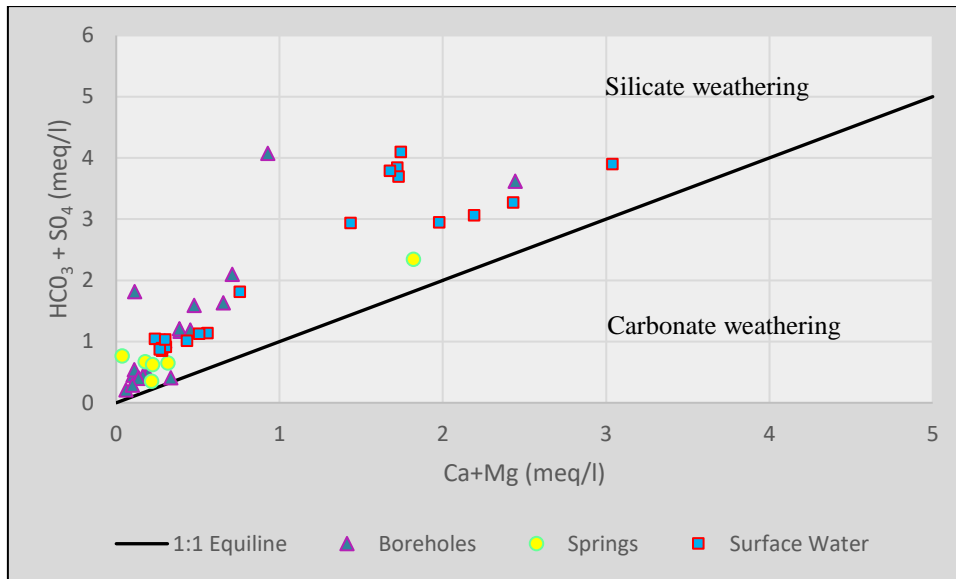


Figure 5-14: Relationship between (Ca + Mg) vs. (HCO₃+SO₄)

Furthermore, the relationship between Na and Cl ions is often used to recognise the processes responsible for the salinity of groundwater in semi-arid regions. Dissolution of halite in water releases equal concentrations of Na and Cl, hence a 1:1 relationship. If concentrations of Na are increased more than those of Cl, it can be typically interpreted as Na is being released from silicate weathering (Dehnavi et al., 2011). The majority of the groundwater samples (88%) have a Na/Cl ratio greater than 1, indicative of sodium released from weathering of silicate minerals. Therefore, the Na vs. Cl scatter plot (Figure 5-15) of the water samples shows that most plots above the equiline, indicative of Na⁺ and Cl⁻ ion sources from weathering of Na-bearing silicates and cation exchange processes as indicated by the Durov diagram.

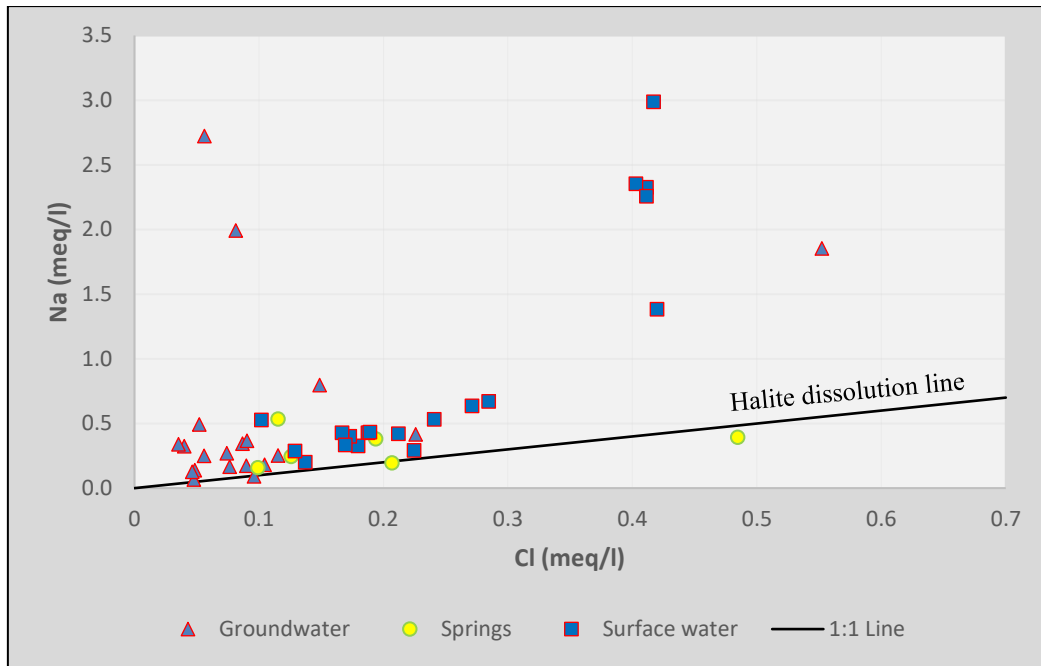


Figure 5-15: Na vs. Cl scatter diagram suggesting that Na may be derived from silicate weathering

The influence of anthropogenic activities on the hydrochemical characteristics of water resources can be identified by the correlation of various ions with TDS (Marghade et al., 2010). The Ca^{2+} , Mg^{2+} and SO_4^{2-} concentrations show a good correlation with TDS, with R^2 of 0.82, 0.89, 0.89, respectively suggesting that the salinity of the groundwater samples is influenced by these major ions (Figure 5-16). The possible source of the SO_4^{2-} in the study area are attributed to pyrite oxidation from the coal mining activity and leaching from storage of coal from the Kusile Coal-fired Power plant. Based on the relationship of TDS and the major ions, dissolution of minerals containing Ca^{2+} , Na^+ and HCO_3^- contribute to the major ions' composition of groundwater, indicating once again rock-water interaction processes controlling the hydrochemical composition.

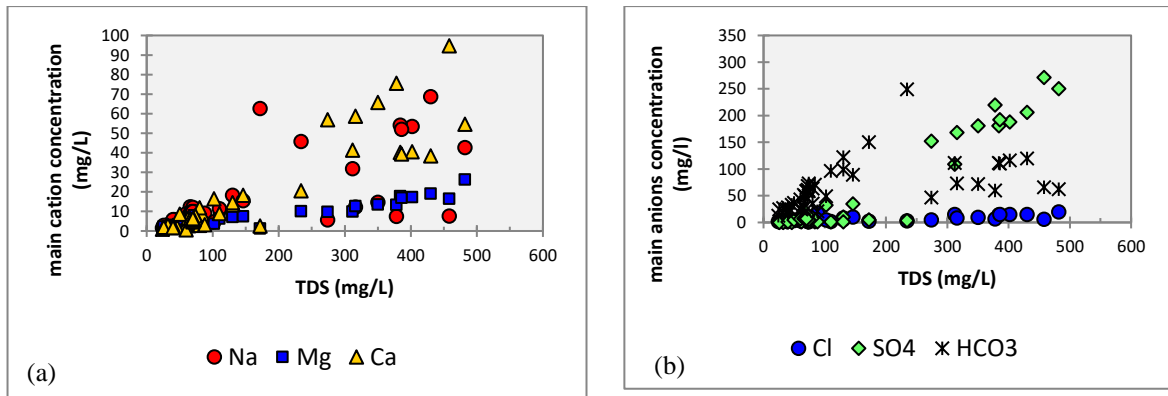


Figure 5-16: Scatter plots of main cations (a) and main anions (b) vs TDS of groundwater analysed in the study area (the regression coefficient for Na⁺, Ca²⁺, Mg²⁺, Cl⁻, SO₄²⁻ and HCO₃⁻ against TDS are 0.46, 0.82, 0.89, 0.46, 0.92 and 0.25, respectively).

5.3.5 Multivariate Statistical Analysis

Multivariate statistical methods have been frequently used to extract useful information from hydrochemical data. The advantage of these methods is that they are unbiased compared to the graphical techniques. Two well-proven multivariate statistical methods, hierarchical cluster analysis (HCA) and principal component analysis (PCA) were used to analyse the hydrochemical data.

Factor Analysis

To understand the hydrogeochemical processes responsible for the observed hydrochemical composition of the water samples, factor analysis on eleven selected hydrochemical variables (i.e., EC, pH, Turbidity, Ca, Mg, Na, Cl, HCO₃, SO₄, DO, and Fe) was undertaken. Several hydrochemical parameters were initially computed following a trial-and-error approach with a couple of iterations being explored. The final hydrochemical parameters were chosen based on their communalities, which correspond to the proportion of the variance in the original variables that is accounted for by the factor. Communality values of 0.5 or higher were chosen as they explain at least half of each original parameter's variance (Brebba, 2011). The Kaiser criterion of keeping components with eigenvalues greater than 1 was applied as shown on the Scree plot of Figure 5-17 (Hayton et al., 2004). Eigenvalues assess the degree of the variance extracted by a given component, while the Cattell scree test is a graphical method used to identify the suitable number of principal components to use in the statistical analysis.

Table 5.9 shows the Principal Component Factor Analysis results of the hydrochemical data using the varimax rotation method to maximise the variance between each of the principal components as it produces extreme positive or negative, or near-zero values. To improve interpretations, a 'strong' loading was defined as > 0.75 , a 'moderate' loading from 0.50 to 0.75 and loadings < 0.5 were considered 'weak' and were ignored from reporting and interpretation (Odat, 2015). The three extracted components, with eigenvalues greater than 1, account for 81.5% of the total variance in the hydrochemical data. The first principal component Factor 1 explains the greatest variance, accounting for 47% of the variance, followed by Factor 2 with 23%, then Factor 3 which accounts for 13.8% of the variance. Factor 1 is primarily composed of strong positive loadings of EC (0.98), Ca^{2+} (0.83), Mg^{2+} (0.92), Na^+ (0.77), and SO_4^{2-} (0.90) which explains the contribution of major ions to the salinity of groundwater as indicated by the Pearson's correlation (Table 5.6). Among the cations, Mg^{2+} has the highest loading followed by Ca^{2+} , while among anions, the highest loadings are for SO_4^{2-} followed by Cl^- . The second factor (Factor 2) has strong positive loadings of Fe, turbidity, and a moderate negative loading of dissolved oxygen indicating reducing conditions. Factor three shows moderate positive loadings of HCO_3^- , pH, and Na^+ , where the positive correlation of HCO_3^- and pH shows carbonate buffering on the pH of the system. The three dominant components are shown in a rotated space in Figure 5-18.

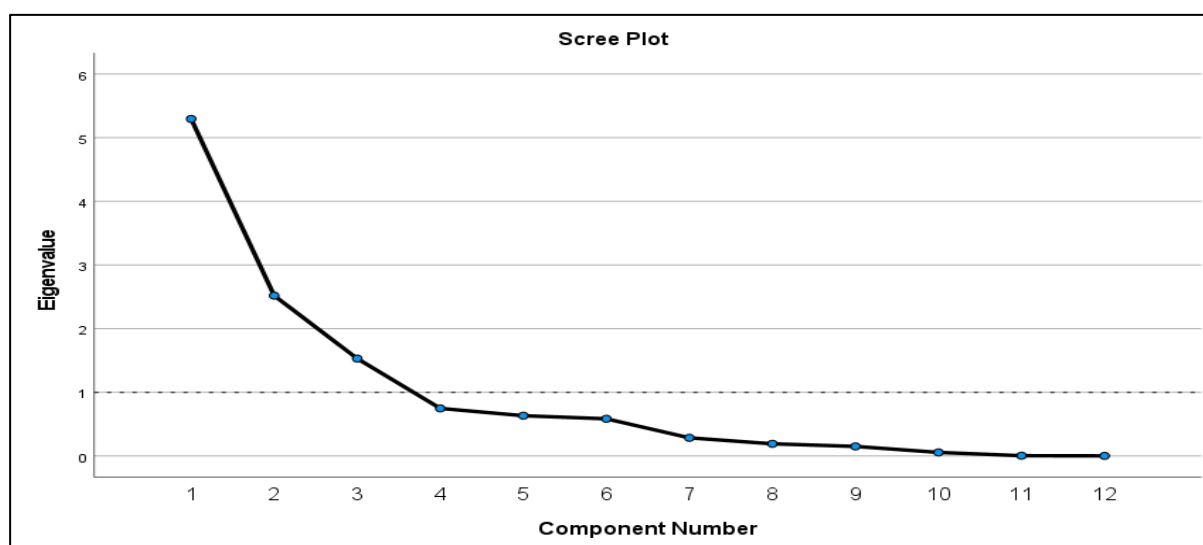


Figure 5-17: Scree plot used to identify the three factors with eigenvalues greater than 1. The dashed line indicates eigenvalues equal to 1, and represents the 'factorial scree' line used in this study.

Table 5.9: Results of principal component factor analysis of the hydrochemical data.

Variable	Communalities	Factor 1	Factor 2	Factor 3
EC mS/m	0.99	0.98		
pH	0.78	0.56		0.66
Turbidity	0.79		0.84	
Ca ²⁺	0.82	0.83		
Mg ²⁺	0.94	0.92		
Na ⁺	0.80	0.77		
Cl ⁻	0.59	0.71		
HCO ₃ ⁻	0.87	0.59		0.69
SO ₄ ⁻	0.95	0.90		
DO	0.56		-0.69	
Fe	0.88		0.92	
Eigenvalues		5.25	2.20	1.52
Explained variance (%)		47.69	20.03	13.80
Cumulative variance (%)		47.69	67.72	81.52

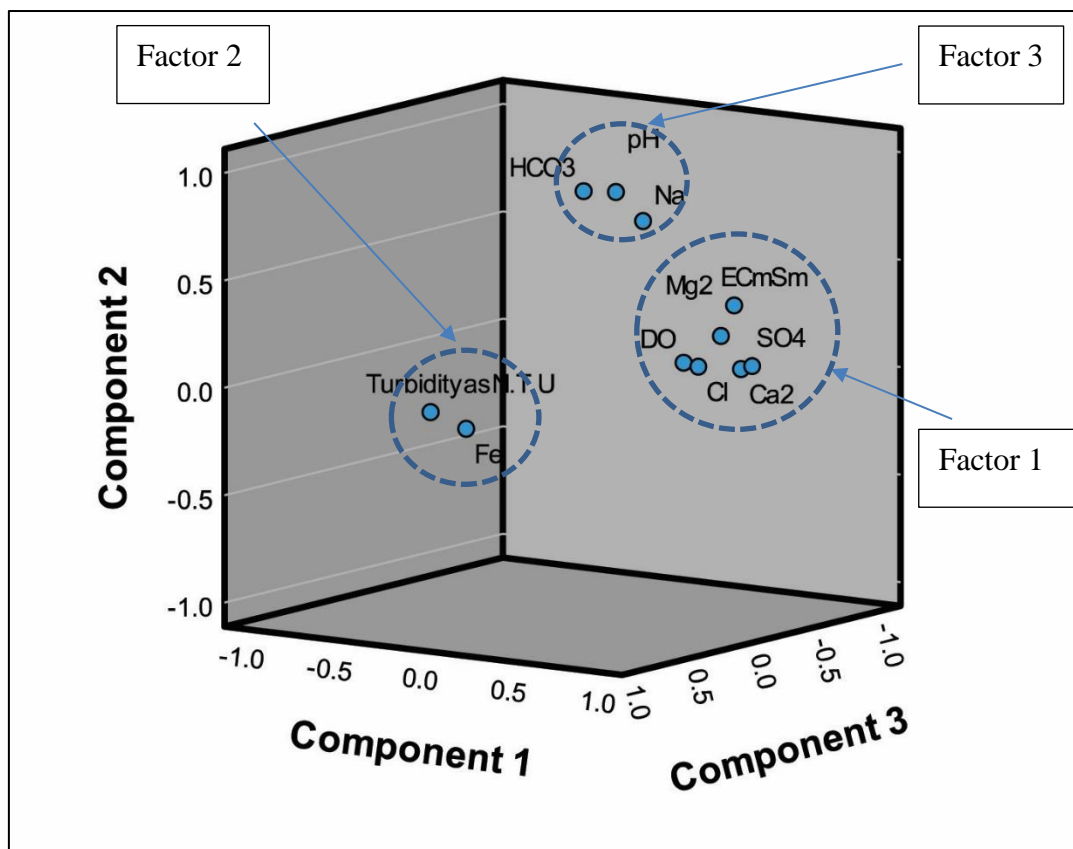


Figure 5-18: Principal component analyses plot of the variables in rotated space.

Hierarchical Cluster Analysis (HCA)

In addition to the Principal Component Facto analysis, HCA was applied on eleven hydrochemical variables (i.e., EC, pH, Turbidity, Ca^{2+} , Mg^{2+} , Na^+ , Cl^- , HCO_3^- , SO_4^{2-} , DO, and Fe) using Ward's linkage method (Ward, 1963) with squared Euclidean distance. The Euclidean distance measure the groups observation sites with the largest similarity first, and Ward's method links similar samples together using analysis of variance to assess the distances between cluster groups (Abu-Khalaf et al., 2013).

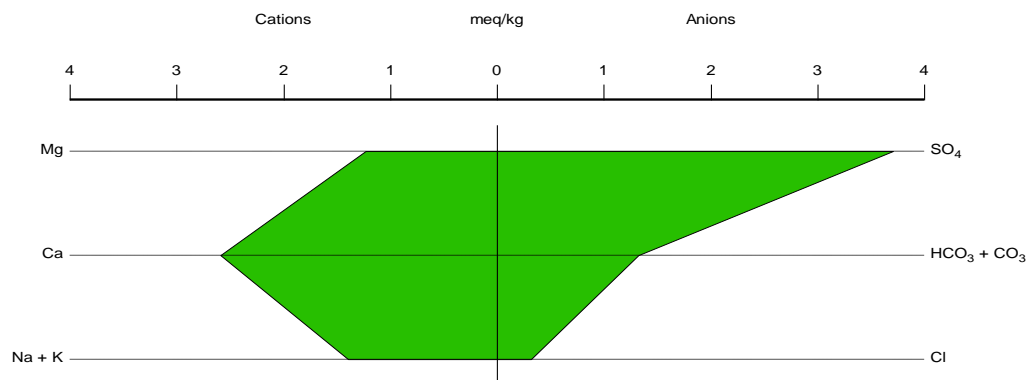
In the current HCA analysis, a phenon line was drawn at a linkage distance of 11 and samples with a linkage distance lower than 11 are thus grouped into the same cluster. This enables the dendrogram to be categorised into two major cluster groups (C1 and C2) as can be observed in the resulting dendrogram shown in Figure 5-20, where the second cluster is further classified into two distinct sub-clusters. Cluster 1 is dominated by surface water samples that are located along the same drainage path. One borehole sample (10490-10) located in a wetland area along the same drainage line as the surface water samples is grouped into C-1, indicating that the borehole is in direct hydraulic link with the surface waters (wetland and stream). Samples classified as C-1 are characterised by elevated concentration of HCO_3^- , turbidity, and SO_4^{2-} . The second cluster (C- 2) has two sub-clusters. Cluster C-2-1 is characterised by groundwater samples that have low Cl^- and K^+ concentrations and are located in the recharge area or upgradient, while cluster C-2-2 represents groundwater samples located in the middle and downstream section of the study area and are characterised by a relatively higher major ion concentration and EC values indicating some degree of hydrochemical evolution from C-2-1 including anthropogenic impacts.

Mean concentrations of major ions for each cluster were calculated to explain the hydrochemical associations portrayed in each cluster (Table 5.10). Cluster 1 which represents surface water samples is characterised by high sulphate and EC values, indicating anthropogenic impacts on surface water systems including mining and the operations of the power plant. The dominant water type in this cluster is Ca-Cl. Cluster C-2-1 has moderate concentrations of major ions indicating no or very limited anthropogenic impact. Cluster C-2-2 is characterised by high turbidity and iron content, indicating a reducing environment. The dominant water type in cluster-2 is Ca- HCO_3 . The Stiff diagrams of Figure 5-19 confirms these dominant water types.

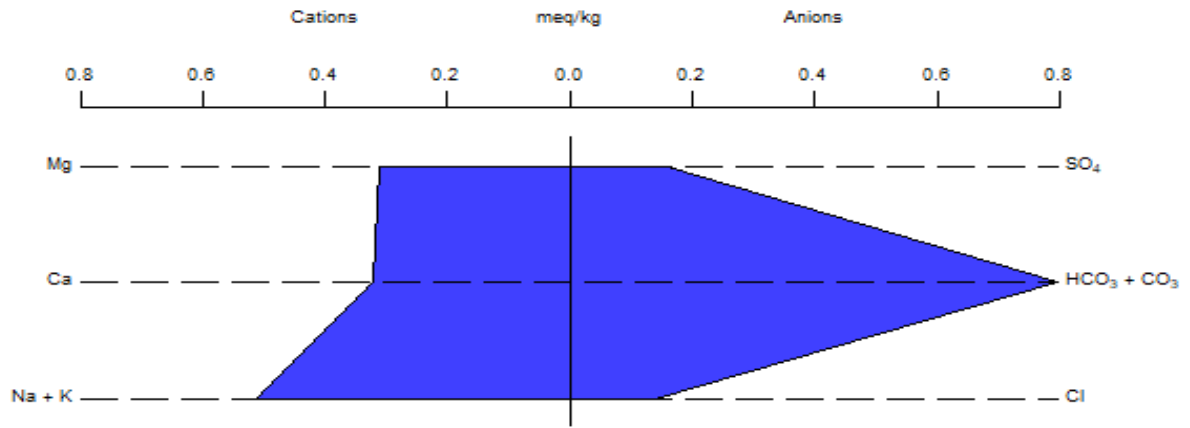
Table 5.10: Mean concentrations of the major chemical parameters for the different clusters.

All values in mg/l unless otherwise stated.

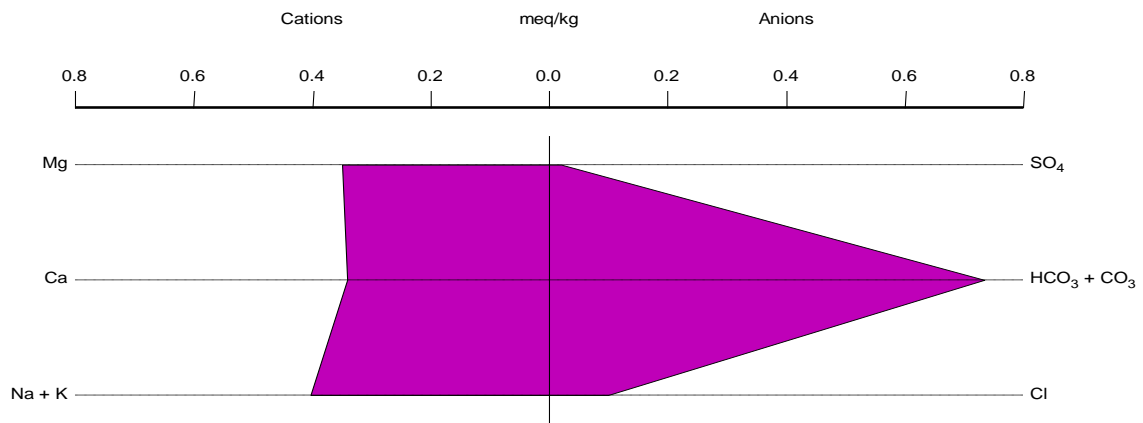
Parameter	Cluster-1	Cluster C-2-1	Cluster C-2-2
pH	7.57	7.16	6.76
EC (mS/m)	51.83	15.26	11.57
Turbidity as N.T.U.	18.53	26.30	197.20
Ca²⁺	51.91	9.10	6.83
Mg²⁺	14.98	4.41	4.24
Na⁺	29.91	12.05	8.03
HCO₃⁻	85.40	57.99	62.95
Cl⁻	11.37	5.18	3.51
SO₄²⁻	177.94	18.22	0.99
DO	5.55	5.30	4.53
Fe	4.55	3.64	20.33
Water types	Ca-Cl	Ca-HCO₃	Ca-HCO₃



(a)



(b)



(c)

Figure 5-19: Stiff diagrams showing the average compositions of each cluster (a) Cluster 1, (b) Cluster C-2-1 and (c) Cluster C-2-2.

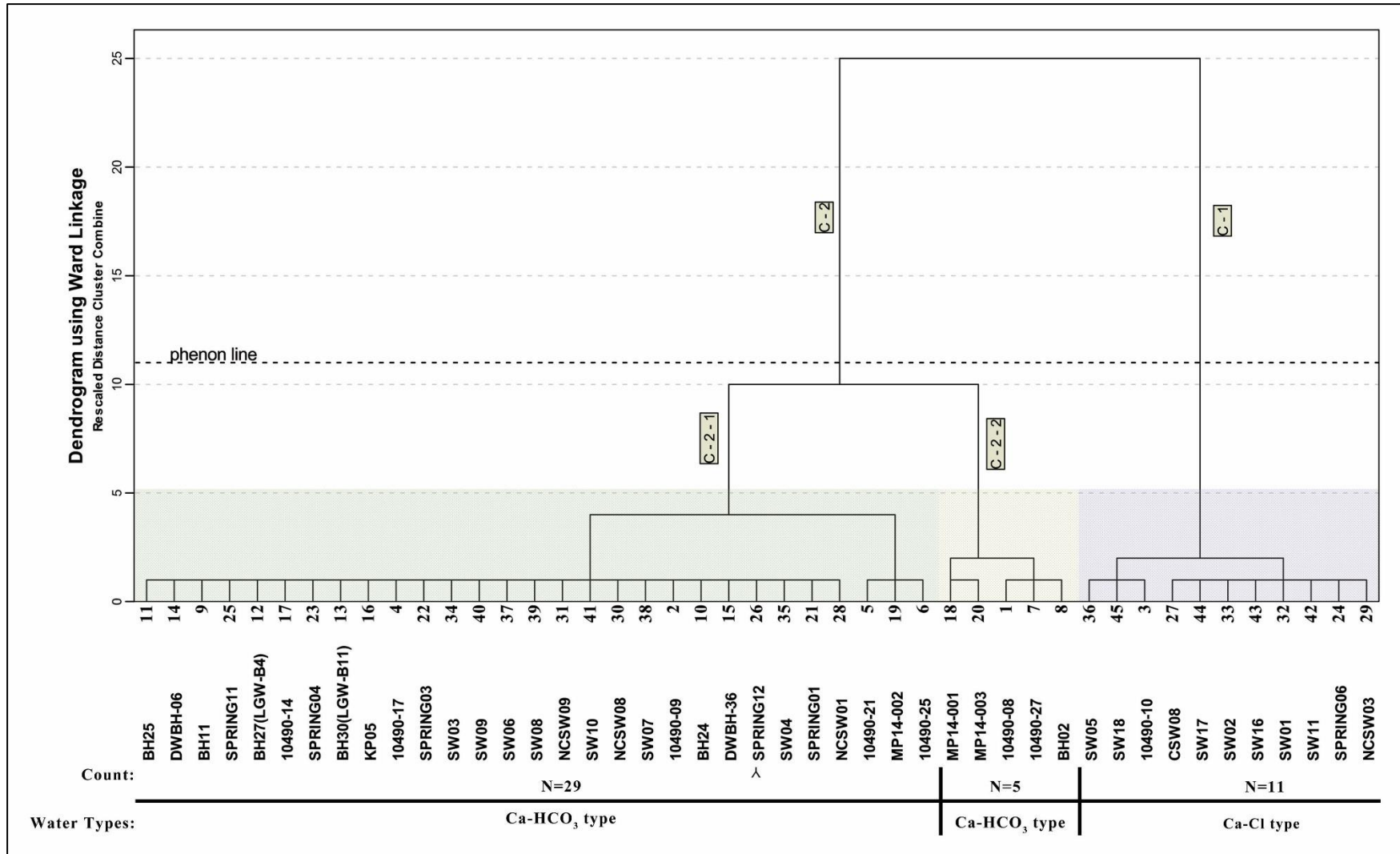


Figure 5-20: HCA Dendrogram of the hydrochemical samples for the study area

5.4 Saturation Index

The geochemical modelling code, PHREEQC (Parkhurst and Appelo,1999) was used to calculate the saturation indices (SI) of the groundwater samples in the study area to explore further the impact of rock-water interaction on the hydrochemical composition. The chemical equilibrium for anhydrite, aragonite, calcite, dolomite, gypsum and halite were examined from the calculated SI. Saturation indices of these minerals are calculated using equation 19 (Lloyd and Heathcote, 1985).

$$SI = \log \frac{IAP}{K_s} \quad (19)$$

Where, IAP is an ion activity product and K_s is the solubility product of the mineral. A positive SI suggests that the groundwater is oversaturated and precipitation will occur while a negative SI is indicative of undersaturation and mineral dissolution is an ongoing process. When the groundwater is at equilibrium with some minerals, SI will have a value of about zero (Appelo and Postma, 1994). The calculated saturated index values are presented in Table 5.11. The Si values indicate that nearly all the groundwater samples are almost undersaturated with respect to most reactive minerals, indicating either young recharge area waters with short residence time or the absence of most of the minerals along the flow path. This is in line with the observations from the Piper and Durov diagrams where groundwater in the study area is young less evolved in nature. Halite is the most undersaturated mineral.

Table 5.11: Phreeqc saturation indices for minerals present within the study area: anhydrite, aragonite, calcite, dolomite, gypsum, and halite.

Sample ID	Anhydrite	Aragonite	Calcite	Dolomite	Gypsum	Halite
10490-08	-4.73	-3.44	-3.29	-6.31	-4.43	-9.13
10490-09	-4.56	-1.45	-1.31	-2.57	-4.25	-9.09
10490-10	-1.67	-1.32	-1.18	-2.34	-1.37	-7.65
10490-17	-4.41	-3.6	-3.46	-6.83	-4.11	-9.13
10490-21	-3.45	-1.01	-0.87	-1.56	-3.15	-8.55
10490-25	-3.79	0.12	0.26	0.57	-3.49	-8.43
10490-27		-2.82	-2.68	-5.14		-9.4
BH02	-4.67	-1.81	-1.66	-3.17	-4.36	-9.49
BH11	-4.98	-2.87	-2.72	-5.09	-4.67	-9.49
BH24	-4.6	-1.61	-1.47	-2.8	-4.3	-9.53
BH25	-5.18	-3.33	-3.18	-5.9	-4.88	-9.32
BH27 (LGW-B4)	-5.46	-4.2	-4.06	-7.7	-5.15	-10.09
BH30 (LGW-B11)	-4.66	-2.65	-2.5	-4.82	-4.35	-9.66

Sample ID	Anhydrite	Aragonite	Calcite	Dolomite	Gypsum	Halite
DWBH-06		-2.93	-2.78	-5.31		-9.77
DWBH-36	-3.96	-1.78	-1.63	-2.73	-3.66	-9.31
KP05	-	-3.24	-3.09	-5.75		-9.82
10490-14	-5.19	-3.56	-3.42	-6.55	-4.89	-9.45
MP14-001	-4.57	-1.59	-1.44	-2.69	-4.27	-9.21
MP14-002	-4.64	0.33	0.47	1.04	-4.33	-8.44
MP14-003	-4.35	-1.6	-1.46	-2.87	-4.05	-8.65
SPRING01	-3.51	-1.97	-1.83	-3.67	-3.21	-8.82
SPRING03	-4.36	-2.67	-2.53	-4.6	-4.05	-8.99
SPRING04	-4.96	-4.44	-4.29	-8.2	-4.66	-8.32
SPRING06	-1.78	-1.03	-0.89	-2.21	-1.47	-9.16
SPRING11	-3.84	-1.77	-1.63	-3.45	-3.54	-9.41
SPRING12	-4.85	-3.56	-3.42	-6.54	-4.55	-8.73
Minimum	-5.46	-4.44	-4.29	-8.20	-5.15	-10.09
Maximum	-1.67	0.33	0.47	1.04	-1.37	-7.65
Mean	-4.27	-2.30	-2.16	-4.12	-3.96	-9.12

5.5 Environmental Isotopes (^2H , ^{18}O , ^3H) analyses

The stable isotopes of oxygen and hydrogen in water are used to trace the origin and recharge sources of groundwater (Krishnaraj et al., 2011). As such, a total of 29 water samples (19 boreholes, 3 springs and 7 surface water samples) were analysed for $\delta^{18}\text{O}$, $\delta^2\text{H}$ and tritium in this study. The results of the environmental isotope analyses are presented in Table 5.12. The stable isotope data were plotted along with the local meteoric water line (LMWL) and the global meteoric water line (GMWL) (Craig, 1961) (Figure 5-21). All groundwater samples show a depleted heavy isotope signature, where the $\delta^{18}\text{O}$ and $\delta^2\text{H}$ values range between -4.78 ‰ and -3.62 ‰, and -24.29 ‰ and -14.4 ‰, respectively (Figure 5-21 and Table 17), indicating that groundwater was recharged from local rainfall with little or no evaporation prior to or during infiltration. One groundwater (DWBH 36) sample plots relatively away from the LMWL and GMWL compared to the rest of the groundwater samples, indicating perhaps shallow circulating groundwater subjected to either evaporation or recharged by surface water sources that have undergone some evaporation. According to Gibrilla et al. (2010), the effect of evaporation in groundwater can be studied by analysing the relationship of $\delta^{18}\text{O}$ and EC measurements, where a positive correlation between the two suggests the occurrence of evaporation. Figure 5-22 show a negative relationship between EC and $\delta^{18}\text{O}$ of groundwater samples confirming no major evaporation prior or during recharge.

Four surface water samples that are located along the Holspruit stream show a similar isotopic signature as the groundwater samples (Figure 5-21), indicating the interaction between groundwater and surface water, where groundwater flows into the streams contributing to the baseflow of the stream. Three other surface water samples have a relatively enriched heavy isotope signal and plot below the LMWL and GMWL, clearly showing a relatively strong evaporation signal (Figure 5-21).

The mean residence time and recharge processes of the groundwater system in the study area were evaluated using tritium data (Table 5.12). These tritium activities in the groundwater of the study area range from 0.5 to 2.6 T.U. The estimated residence time of groundwater in the study area ranges from 7.7 years to 37 years. Sample 10490-25 taken from a relatively deep borehole has the lowest tritium activity (0.5 T.U.) and hence relatively the longest residence time of about 36 years. According to the qualitative tritium activity classification of Clark and Fritz (1997), most of the groundwater samples in the study area exhibit a mixture between sub-modern and recent recharge. The measured tritium activity and the calculated residence time indicates that the aquifers of the area are receiving active recharge and by extension vulnerable to pollution.

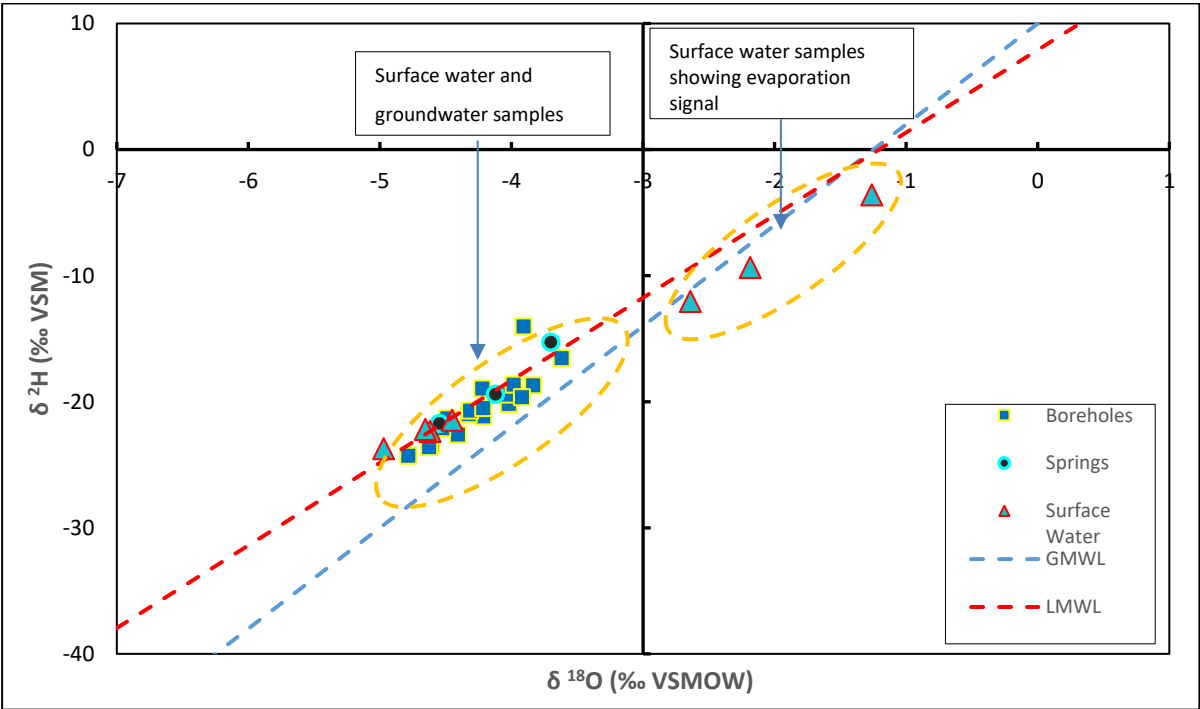


Figure 5-21: Stable environmental isotope ($\delta^{18}\text{O}$ and $\delta^2\text{H}$) plot of water samples for the study area along with GMWL and the Pretoria LMWL.

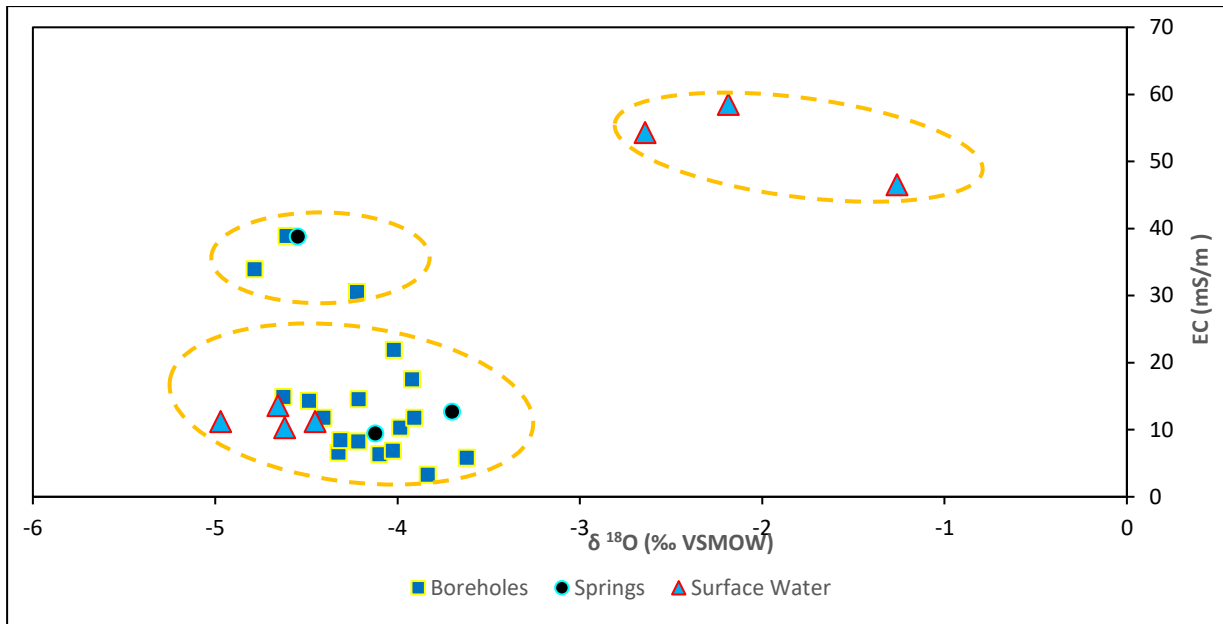


Figure 5-22: Plot of $\delta^{18}\text{O}$ versus EC values of the water samples within the study area.

Table 5.12: Environmental isotope (^2H , ^{18}O , ^3H) analysis results of surface and groundwater samples.

Sample ID	Sample Type	Sampling Date	Altitude (m amsl)	Depth to Water (m bgl)	Field Measurements			$\delta^{18}\text{O}$ (‰)	δD (‰)	Tritium (T.U.)	Estimated residence time (year)
					pH	EC (mS/m)	T (°C)				
10490-14	Borehole	29/03/2018	1502	1496.3	5.55	6.70	20.4	-4.22	-21.2	1.1 ± 0.3	23.15
10490-21		29/03/2018	1480	1469.6	7.00	20.70	18.8	-4.02	-20.2	1.4 ± 0.3	18.82
10490-25		27/03/2018	1419	1417.8	7.50	33.90	18.6	-4.61	-23.4	0.5 ± 0.2	37.28
10490-27		29/03/2018	1531	1520.4	7.05	7.12	20.5	-4.10	-19.4	1.7 ± 0.3	15.34
BH 11		28/03/2018	1498	-	6.37	6.10	21.9	-4.03	-19.4	1.0 ± 0.3	24.86
BH 24		27/03/2018	1462	1450.8	6.59	11.74	19.7	-4.41	-22.6	1.0 ± 0.3	24.86
BH 27		28/03/2018	1548	1542.9	6.28	3.24	24.4	-3.83	-18.7	2.6 ± 0.3	7.72
BH 3		27/03/2018	1475	1470.7	6.03	40.00	18.6	-4.53	-22.1	1.3 ± 0.3	20.15
BH 30		28/03/2018	1569	1566.5	5.74	9.64	20.8	-3.98	-18.7	2.1 ± 0.3	11.55
DWBH 06		28/03/2018	1522	1511.1	6.34	6.14	20.9	-3.62	-16.5	1.3 ± 0.3	20.15
DWBH 36		29/03/2018	1505	1498.6	6.31	11.91	20.7	-3.91	-14.0	1.7 ± 0.3	15.34
KP05		29/03/2018	1542	1527.5	5.58	5.71	22.1	-4.32	-21.0	0.6 ± 0.2	34.02
KPS 1		30/03/2018	1416	1407.0	5.90	12.69	21.6	-4.22	-19.0	1.8 ± 0.3	14.32
KPS 3		30/03/2018	1505	-	6.20	10.73	20.5	-4.31	-20.7	0.8 ± 0.2	28.86
KPS 4		30/03/2018	1459	1448.0	5.70	15.07	22.6	-4.49	-21.3	2.5 ± 0.3	8.43
KPS 5		30/03/2018	1531	1512.2	6.20	21.70	20.5	-4.21	-20.5	1.1 ± 0.3	23.15
LGW-B14		30/03/2018	1534	1511.3	7.30	34.90	22.1	-4.78	-24.3	-	-
MP14-001	29/03/2018	1449	1440.0	6.40	15.72	20.5	-4.63	-23.6	1.0 ± 0.3	24.86	

Sample ID	Sample Type	Sampling Date	Altitude (m amsl)	Depth to Water (m bgl)	Field Measurements			$\delta^{18}\text{O}$ (‰)	δD (‰)	Tritium (T.U.)	Estimated residence time (year)
					pH	EC (mS/m)	T (°C)				
MP14-003		29/03/2018	1457	1473.4	6.81	25.20	20.5	-3.92	-19.6	1.1 ± 0.3	23.15
Spring 01	Springs	27/03/2018	1491	-	6.26	12.56	20.0	-3.70	-15.3	2.0 ± 0.3	12.43
Spring 03		27/03/2018	1501	-	7.84	11.23	19.4	-4.12	-19.4	2.6 ± 0.3	7.72
Spring 06		28/03/2018	1474	-	6.36	53.40	19.7	-4.55	-21.7	2.0 ± 0.3	12.43
SW 01	Surface Water	27/03/2018	-	-	7.67	42.80	21.5	-1.26	-3.6	-	-
SW 08		27/03/2018	-	-	6.80	7.80	16.9	-4.97	-23.7	-	-
SW 09		27/03/2018	-	-	6.97	9.47	19.4	-4.62	-22.4	-	-
SW 10		28/03/2018	-	-	6.78	9.19	19.8	-4.45	-21.5	-	-
SW 17		28/03/2018	-	-	6.98	35.10	19.3	-2.19	-9.4	-	-
SW 5		27/03/2018	-	-	7.55	50.30	19.5	-2.64	-12.1	-	-
SW06		27/03/2018	-	-	6.88	8.80	22.2	-4.66	-22.2	-	-

5.6 Groundwater levels and hydrochemical data trend analysis

Assessing the long-term trends in groundwater levels and hydrochemical data is important to understand the changes occurring in the groundwater system. As such the MK test statistics was applied on groundwater levels and groundwater quality data following equation 7 so as to identify trends in these data sets. A spreadsheet for automatic processing of water quality data developed by Daughney (2007) was used for this analysis. In this study, the MK test was applied on monthly groundwater levels measured between 2008 and 2018 across 21 boreholes and on the major hydrochemical data within the same period for all the monitoring sites within the study area. All the boreholes are exclusively for monitoring purposes, none of them have pumping equipment installed.

5.6.1 Groundwater level trend analysis

The results of the MK trend analysis and Sen's slope estimator of groundwater levels are presented in Figure 5-24 and Table 5.13. Positive Z values identify long-term increasing trends while negative ones represent long-term decreasing trends. Five boreholes did not have a statistically significant trend at a 95% significance level, therefore the H_0 was accepted. All the other boreholes exhibit long term trends.

Most of the boreholes displayed negative trends, indicating a decline in groundwater levels in the study area for the entire record period. About 81% (13 boreholes) of the statistically significant data witnessed decreasing trends, on the other hand, only three boreholes show positive or increasing trends (19%). The Sen's slope which measures the magnitude of the trend varies from -2.28 to 0.16 m/year. The average estimated rate of groundwater level decline is -0.45 m/year (Table 5.13). The highest decreasing trend is observed at borehole BH27 (-6.58 m) and the highest increasing trend is observed at borehole DWBH-06 (with a net groundwater increase of 5.63 m over the monitoring period). The increase and decrease in groundwater levels are presented in Appendix E.

One of the effects of climate change is recurring droughts and South Africa has been not been spared from such droughts. The effect of droughts on groundwater is the lack of recharge as precipitation seasonality is altered leading to a failure of previously wet seasons. Decreasing rainfall patterns over the study area are confirmed by a study conducted by Mafamadi (2017), this study analysed rainfall data collected over a 91-year period (1925 – 2016) in the Witbank area and it concludes that rainfall over this period shows decreasing trends at a rate of -0.091

and -0.081 mm/month. Similar decreasing observations were made by Mackeller et.al., (2014) who noted a considerable decline in precipitation and the number of rain days in the wet season. Opencast mining alters drainage systems and lowers the water table as pumping is an integral part of operations. Two active coal mines (Figure 5-23) are located within the vicinity of the monitoring network, these are the Malachite Mining and Klipfontein Mine. The problems with open cast mining are related to the increased cone of depression and decreased regional groundwater levels as a result of dewatering during the operational phase of the mine (Peplinski and Czubak, 2021). Both the changes in climatic conditions and mining activities may be the major driving force in the overall declining trends in groundwater within the study area. The short-term seasonal variations contribute to the negative trends as well, however, its impacts are considered minimum. Figure 5-24 shows selected time-series graphs of groundwater levels, in Figure 5-25 (a), borehole DWBH 06 shows an increasing trend while Figure 5-25 (b) borehole 10490-21 displays a decreasing trend.

DWBH-06 and DWBH-36 are located approximately 520 m apart, and both are displaying increasing trends in groundwater. No specific reason can be found to explain the increasing trends observed in these boreholes. The increasing trend observed from borehole 10490-10 situated at riverine wetland system can be explained by increased aquifer recharge induced by the wetland, which is corroborated by the hydrochemical and isotope signatures.

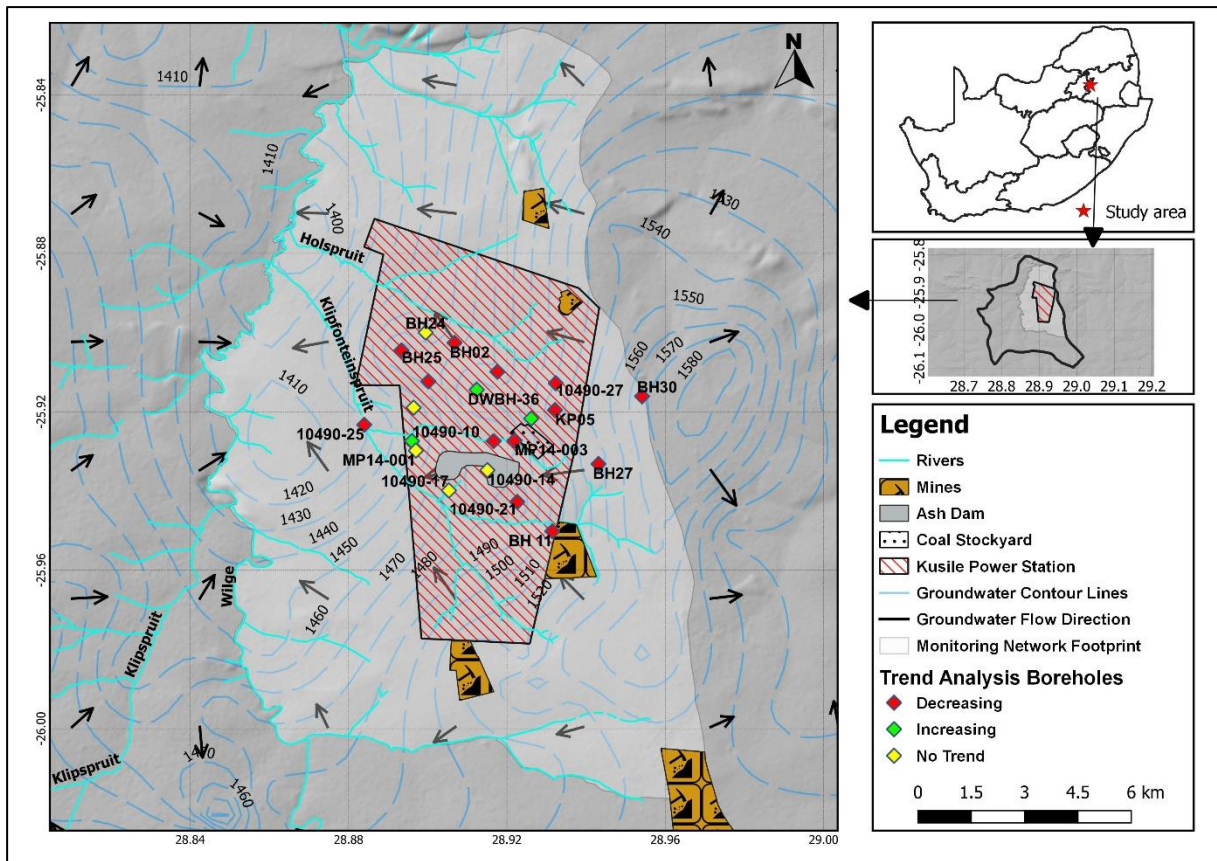
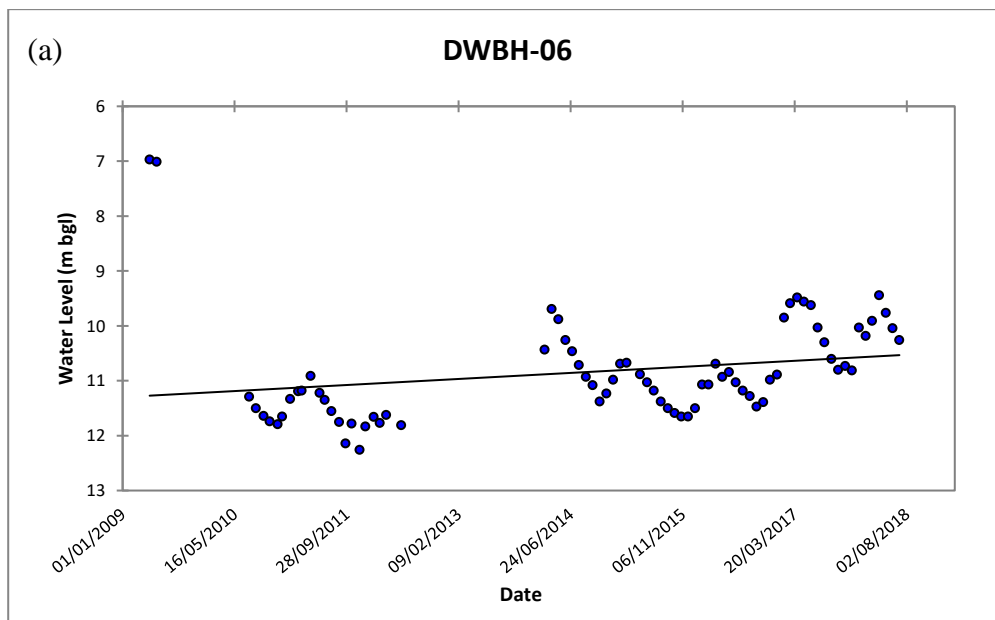


Figure 5-23: Boreholes considered for trend analysis within the monitoring network.



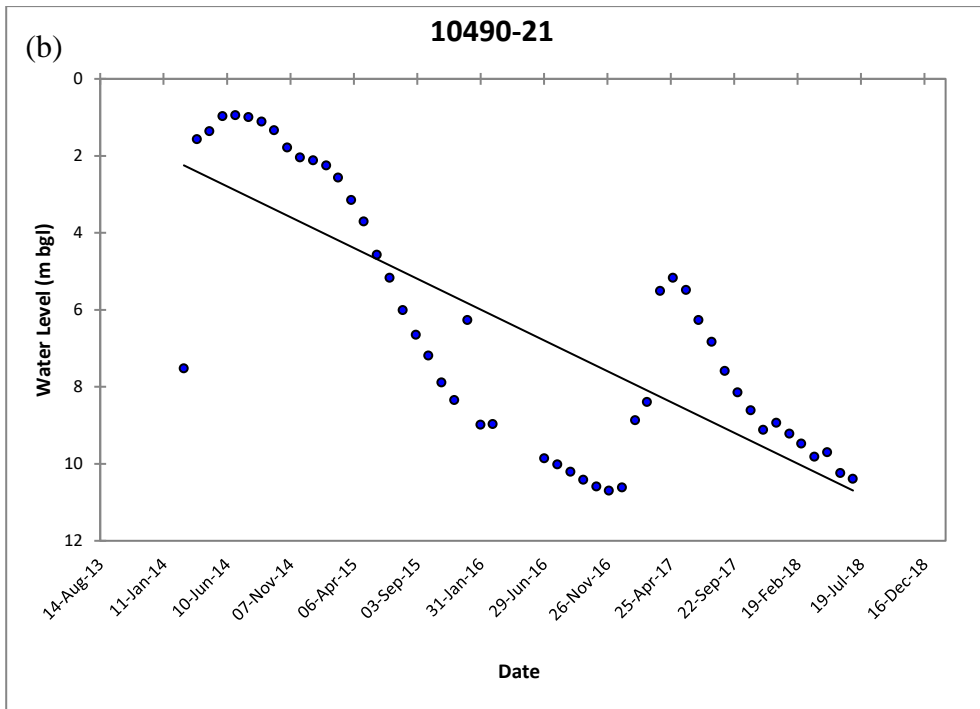


Figure 5-24: Selected time-series graphs of groundwater levels. An increasing trend in groundwater levels for (a) Borehole DWBH-06 and (b) decreasing trend in groundwater levels for Borehole 10490-21.

Table 5.13: Results of the MK test and Sen's Slope Estimator for groundwater levels within the study area. Bold sample points are not statistically significant at 95%

Count	Sample Point ID	First Year	Last Year	N	Trend (At 95% level of significance)	p value	Z value	Sen's Slope (m/year)
1	10490-08	01/05/2009	30/06/2018	85	Decreasing	0.03461	-2.113	-0.102
2	10490-09	01/05/2009	30/06/2018	71	Decreasing	0.00026	-3.651	-0.037
3	10490-10	01/05/2009	30/06/2018	83	Increasing	0.00001	4.374	0.080
4	10490-14	31/10/2016	30/06/2018	20	No Trend	0.21000	-1.254	-0.219
5	10490-17	20/07/2010	30/06/2018	71	No Trend	0.06217	1.865	0.052
6	10490-21	28/02/2014	30/06/2018	50	Decreasing	0.00000	-6.313	-2.279
7	10490-25	01/05/2009	30/06/2018	84	Decreasing	0.00000	-5.425	-0.040
8	10490-27	01/05/2009	30/06/2018	81	Decreasing	0.02018	-2.323	-0.110
9	BH 11	01/12/2009	29/05/2012	25	Decreasing	0.00967	-2.587	-1.533
10	BH02	20/07/2010	30/06/2018	74	Decreasing	0.00032	-3.600	-0.220
11	BH03	01/07/2009	31/05/2018	86	Decreasing	0.00000	-4.579	-0.267
12	BH24	28/02/2014	30/06/2018	48	No Trend	0.05601	-1.911	-0.187
13	BH25	01/05/2009	30/06/2018	87	Decreasing	0.00000	-6.410	-0.795
14	BH27	01/05/2009	30/06/2018	80	Decreasing	0.00000	-6.577	-0.233
15	BH30	01/05/2009	30/06/2018	82	Decreasing	0.03223	-2.142	-0.050
16	DWBH-06	01/05/2009	30/06/2018	74	Increasing	0.00000	5.635	0.162
17	DWBH-36	01/05/2009	30/06/2018	85	Increasing	0.00004	4.086	0.138
18	KP05	01/05/2009	30/06/2018	79	Decreasing	0.00107	-3.273	-0.127
19	MP14-001	31/10/2016	30/06/2018	21	No Trend	0.26946	-1.104	-0.491
20	MP14-002	31/10/2016	30/06/2018	17	No Trend	0.09218	-1.684	-0.163
21	MP14-003	31/10/2016	30/06/2018	19	Decreasing	0.00408	-2.872	-0.107
Average							-2.36	-0.35

5.6.2 Hydrochemical data trend analysis

Ten hydrochemical parameters across all sampling points in the study area were evaluated for trends for the period from 2008 to 2018. These parameters include pH, EC, Turbidity, Total Alkalinity, Ca, Cl, Mg, K, Na, and SO₄. The results of the MK test applied at each sampling point to each water quality variable at a significance level of 95% is presented in Table 5.14. The Sen's slope estimator results are presented in Table 5.15, while p-values are presented in Appendix F.

The MK test revealed that 17 sampling points statistically significant trend for pH, 32 for EC, 24 for both turbidity and alkalinity, 29 for Ca, 34 for Cl, 19 for Mg, 25 for K, 28 for both Na and SO₄. The following observations are made for each of the hydrochemical parameters considered in the trend analyses:

- 82% and 18% of the sampling points show decreasing and increasing trend for pH, suggesting that the system is becoming more acidic. The most decline in pH is observed at Spring04 and the most increase is observed at borehole KP05. Surface water samples are the most affected by the decreasing pH as they account for 56% of the increase, indicating an anthropogenic impact. The degree of increase and decrease estimated using Sen's slope estimator varies from -0.12 to 0.06 (pH units/ year).
- 72% of the samples indicate an increasing EC trend, among which surface water samples account for 56% of the increase in the EC trend. The MK test revealed that the magnitude of the EC increase and decrease estimated using Sen's slope estimator varies from -0.993 to 7.6 (mS m⁻¹/year). Most of EC decreasing trend is observed from groundwater samples (accounting 77% of the total decrease). Mining activities, dust from the coal stockyard and fly ash from the Kusile power station may be the main contributors to the increase in EC, especially in the surface water samples.
- 63% and 56% of sampling show an increasing trend for total alkalinity and potassium (K), respectively with the Sen's slope ranging from -6.47 to 69.72 mg L⁻¹/year for alkalinity and -0.95 to 0.28 mg L⁻¹/year for K.
- 55%, 58% and 64% of the water samples show decreasing trends for Ca, Mg and Na, respectively, with Sen's slopes varying from -2.01 to 9.01 mg L⁻¹/year, -2.31 to 1.67 mg L⁻¹/year, and -1.54 to 8.16 mg L⁻¹/year, respectively.

- 94% and 79% of the samples show increasing trends for Cl and SO₄ sulphate, respectively. The recorded decreasing trends in Cl are all from groundwater sampling points. Sen's slope for Cl varies from -0.42 to 1.11 mg L⁻¹/year while SO₄ Sen's slope varies from -2.45 to 32.08 mg L⁻¹/year. The oxidation of pyrite from the open cast mining, fly ash from Kusile Power Station could be attributed to the increases in chloride and sulphate.

Examples of graphical displays of the increase and decrease in the hydrochemical data is shown in Figure 5-25. Borehole KP05 shows increasing pH in Figure 5-25 (a) while borehole 10490-27 displays increasing turbidity in Figure 5-25 (b).

The general long-term hydrochemical time-series data reveals a general decrease in the water quality of the study area.

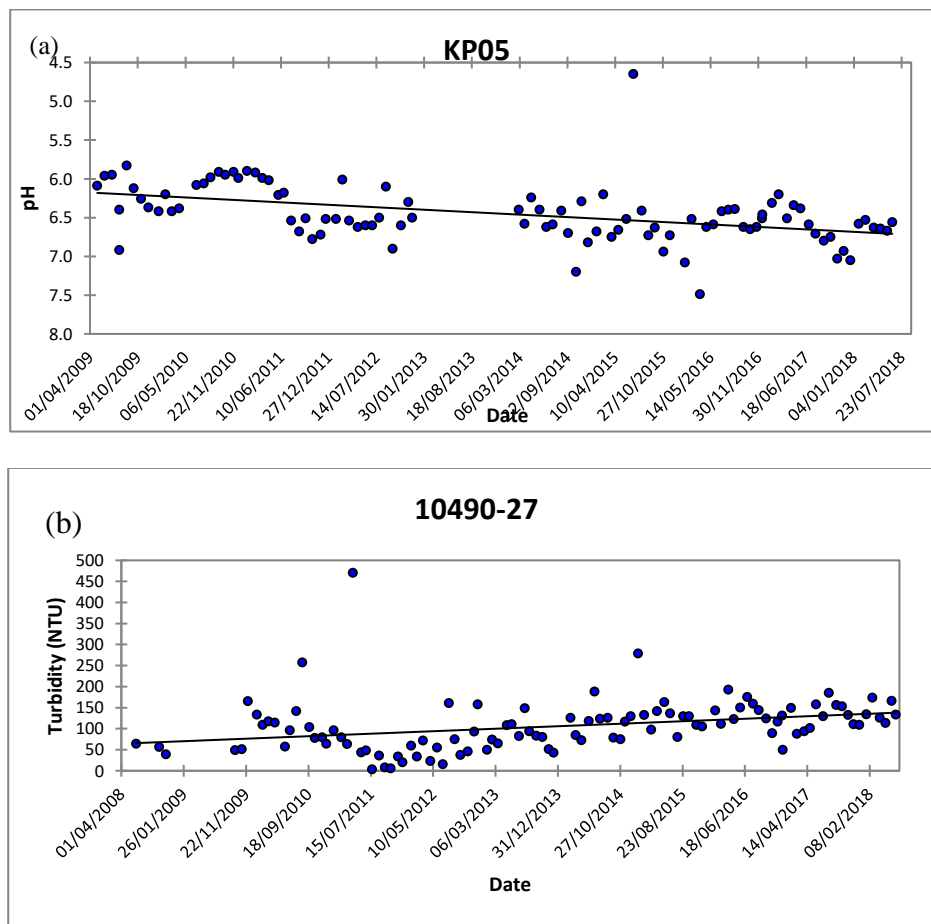


Figure 5-25: Selected time-series graphs displaying trends of the hydrochemical data. (a) an increasing trend of pH in borehole KP05 and (b) an increasing trend of turbidity in borehole 10490-27.

Table 5.14: Mann-Kendal Z statistics for hydrochemical data. All results in mg/L unless indicated. Bold numbers indicate significance at 95%.

Count	Sample Point ID	pH	EC (mS/m)	Turbidity (NTU)	Total Alkalinity	Ca	Cl (Mg	K	Na	SO ₄
1	10490-08	-4.50	-2.06	0.77	-2.98	-4.46	6.91	-3.66	2.09	-6.00	4.39
2	10490-09	0.58	0.00	-3.92	-0.20	-2.26	7.23	-1.27	-1.84	-2.56	2.76
3	10490-10	1.83	-0.69	-0.98	2.04	-2.29	-1.35	-1.10	2.98	0.79	3.09
4	10490-14	0.30	1.37	-2.43	-0.53	0.00	0.00	-1.50	-3.72	0.00	-1.72
5	10490-17	-1.30	-4.62	1.09	-3.19	-6.48	4.62	-4.28	-0.93	-5.94	-0.47
6	10490-21	-2.31	-2.66	1.23	-3.49	-3.33	3.95	-3.73	-2.69	-3.66	1.78
7	10490-25	0.25	2.86	2.12	3.57	2.61	7.67	1.17	1.85	1.76	-3.10
8	10490-27	-0.46	-0.71	5.64	-3.60	-3.32	5.48	-4.12	-3.30	-3.61	3.58
9	BH02	2.09	3.64	3.98	2.68	0.39	2.61	1.79	2.44	-5.93	-1.83
10	BH03	-0.02	-3.30	-2.30	-0.64	-3.95	-2.89	-3.57	-3.36	-4.58	3.20
11	BH11	-0.68	-3.07	1.42	0.88	-2.92	0.72	-3.28	-1.06	-5.24	3.03
13	BH24	-2.08	2.41	1.16	0.67	0.90	4.00	-3.83	0.61	-6.28	0.65
14	BH25	1.10	-3.62	-3.14	4.53	-1.28	-2.23	1.41	-0.99	-4.61	-1.90
15	BH27	-3.70	2.49	-4.12	-3.89	-1.27	6.80	1.51	-1.56	-1.21	4.02
16	BH30	-4.07	6.74	-2.28	-4.24	3.39	7.80	4.81	4.08	1.30	4.43
17	CSW08	-0.29	3.71	-1.79	-1.65	3.63	3.16	0.63	1.60	-0.07	5.59
18	DWBH-06	1.37	2.58	-2.20	-1.49	0.90	5.11	1.00	-1.60	0.14	2.56
19	DWBH-07	0.00	2.44	1.21	2.63	0.18	1.03	2.50	1.34	-2.80	2.04
20	DWBH-36	-2.59	-1.41	-4.52	-2.46	-2.37	4.71	-1.91	-0.18	-4.01	1.50
21	KP05	5.24	6.03	-4.24	4.48	1.37	7.50	4.21	-0.74	-4.62	0.55
22	MP14-001	0.13	1.49	2.14	0.91	-1.92	-1.01	-1.72	-3.65	-3.28	-2.10
23	MP14-002	1.38	3.56	-1.98	2.14	-2.74	-0.72	-3.19	-3.29	2.02	0.00
24	MP14-003	0.64	0.00	-0.23	-0.32	-0.96	0.42	-1.32	0.23	-1.81	-2.02
25	NCSW01	-1.12	1.28	0.73	0.84	1.42	1.50	-0.84	0.95	-1.67	1.40
26	NCSW03	-2.87	1.45	-0.61	0.56	2.33	1.09	0.05	-3.61	-0.56	0.85

Count	Sample Point ID	pH	EC (mS/m)	Turbidity (NTU)	Total Alkalinity	Ca	Cl (Mg	K	Na	SO ₄
27	NCSW08	-0.95	4.95	-1.83	4.02	5.52	1.89	1.44	-0.07	1.16	1.64
28	NCSW09	-2.76	1.35	-3.90	0.83	0.24	0.65	0.00	-2.17	-2.15	-3.58
29	Spring01	0.13	0.31	-0.03	-1.41	-0.18	2.37	-0.89	1.51	-0.46	2.31
30	Spring02	-3.66	3.04	-0.90	2.69	3.75	3.18	3.20	0.33	-0.79	1.63
31	Spring03	-2.04	1.89	1.14	-0.49	-2.87	2.19	-0.12	-0.05	0.82	-3.84
32	Spring04	-4.69	7.08	1.99	0.11	4.90	4.83	8.63	3.45	-0.32	1.40
33	Spring06	0.35	2.60	-0.89	3.19	2.02	5.22	2.38	2.26	3.96	2.22
34	Spring11	1.72	5.91	0.50	4.33	5.63	4.60	-1.37	1.57	-2.81	2.88
35	Spring12	-3.62	-5.76	3.86	-4.94	-5.36	4.49	-5.02	-4.63	-4.96	2.86
36	SW01	1.53	2.67	-3.12	5.22	1.64	6.34	1.94	5.01	5.74	1.96
37	SW02	0.00	2.72	-2.37	-1.94	1.80	3.80	0.33	3.34	2.65	4.43
38	SW03	-0.90	-3.80	2.67	-3.82	-4.77	1.00	-5.69	3.70	-3.06	1.39
39	SW04	0.59	-3.32	-2.38	-0.98	-3.21	-0.30	-4.64	-0.17	-3.80	2.48
40	SW05	-3.54	3.28	1.31	1.19	3.23	5.26	3.18	3.48	3.08	3.58
41	SW06	0.02	1.91	-1.22	0.65	-0.45	3.40	-0.28	-1.18	0.39	-1.27
42	SW07	-0.47	4.40	-1.67	3.37	5.41	4.66	0.55	2.32	4.83	3.84
43	SW08	-1.18	2.09	-2.76	2.08	-0.73	2.79	0.50	-2.03	1.44	-3.34
44	SW09	-3.20	1.35	1.49	0.36	-2.02	3.05	-0.49	-3.46	1.02	-1.72
45	SW10	-0.59	0.27	0.52	0.06	-3.32	1.82	-1.67	-0.66	0.44	-1.52
46	SW11	3.09	6.43	-2.15	3.74	5.65	6.55	5.32	3.79	5.85	5.64
47	SW16	-1.74	3.18	-0.76	-1.90	4.03	3.00	1.34	3.44	2.88	5.43
48	SW17	-0.19	3.78	-2.42	-1.74	1.94	3.41	1.03	3.65	2.76	4.74
49	SW18	0.81	-0.08	-0.81	1.61	0.68	-1.01	0.19	-0.92	-1.65	-0.98

Table 5.15: Sen's slope values for hydrochemical data. All results in mg/L unless indicated.

Count	Sample Point ID	pH	EC (mS/m)	Turbidity (NTU)	Total Alkalinity	Ca	Cl	Mg	K	Na	SO4
1	10490-08	-0.053	-0.080	1.094	-1.501	-0.340	0.419	-0.211	0.034	-0.533	0.227
2	10490-09	0.008	0.000	-8.602	-0.010	-0.153	0.351	-0.051	-0.021	-0.093	0.113
3	10490-10	0.024	-0.055	-1.750	0.597	-0.239	-0.120	-0.062	0.044	0.076	0.241
4	10490-14	0.065	0.735	-50.864	-0.959	-0.017	-0.024	-0.224	-0.952	-0.050	-0.885
5	10490-17	-0.011	-0.614	2.287	-2.968	-0.603	0.258	-0.251	-0.027	-0.619	-0.063
6	10490-21	-0.054	-0.423	7.365	-6.465	-0.821	0.905	-0.464	-0.050	-0.890	0.783
7	10490-25	0.000	0.167	1.195	1.109	0.143	0.329	0.038	0.025	0.197	-0.213
8	10490-27	-0.004	-0.010	10.132	-0.420	-0.081	0.228	-0.048	-0.022	-0.152	0.153
9	BH02	0.044	0.317	11.572	2.936	0.054	0.154	0.124	0.100	-0.598	-0.140
10	BH03	0.000	-0.276	-1.005	-0.062	-0.238	-0.425	-0.097	-0.102	-0.534	0.176
11	BH11	-0.007	-0.130	0.027	0.068	-0.095	0.026	-0.069	-0.008	-0.431	0.145
13	BH24	-0.030	0.100	0.188	0.396	0.083	0.177	-0.196	0.018	-0.670	0.032
14	BH25	0.011	-0.134	-0.624	1.104	-0.037	-0.156	0.033	-0.016	-0.416	-0.090
15	BH27	-0.039	0.063	-6.385	-0.390	-0.019	0.269	0.006	-0.005	-0.023	0.166
16	BH30	-0.060	0.328	-1.207	-1.357	0.140	0.334	0.109	0.035	0.027	0.176
17	CSW08	-0.003	3.682	-0.511	-2.362	3.629	0.541	0.214	0.128	-0.129	20.050
18	DWBH-06	0.010	0.100	-0.226	-0.234	0.028	0.296	0.024	-0.019	0.001	0.167
19	DWBH-07	0.000	0.262	10.828	2.502	0.048	0.038	0.311	0.034	-1.026	0.319
20	DWBH-36	-0.024	-0.149	-8.357	-1.420	-0.174	0.240	-0.166	-0.002	-0.406	0.114
21	KP05	0.059	0.214	-212.487	1.048	0.045	0.344	0.160	-0.007	-0.454	0.057
22	MP14-001	0.044	0.761	69.718	4.870	-0.654	-0.620	-0.399	-0.706	-1.543	-1.153
23	MP14-002	0.186	4.628	-25.841	12.812	-2.007	-0.729	-2.306	-0.611	8.163	0.042
24	MP14-003	0.125	-0.109	-9.099	-1.594	-1.384	0.267	-0.955	0.020	-3.395	-2.446
25	NCSW01	-0.056	0.456	18.657	0.673	0.477	0.350	-0.056	0.146	-0.320	1.068
26	NCSW03	-0.122	0.931	-7.349	1.760	1.887	0.557	0.037	-0.940	-0.448	1.998
27	NCSW08	-0.027	1.172	-3.956	4.014	1.365	0.324	0.123	-0.018	0.281	0.481

Count	Sample Point ID	pH	EC (mS/m)	Turbidity (NTU)	Total Alkalinity	Ca	Cl	Mg	K	Na	SO4
28	NCSW09	-0.057	0.149	-4.560	0.842	0.050	0.087	0.000	-0.161	-0.423	-1.213
29	Spring01	0.003	0.028	-0.028	-1.289	-0.008	0.167	-0.046	0.032	-0.114	0.939
30	Spring02	-0.062	0.209	-0.057	0.657	0.311	0.286	0.118	0.004	-0.145	0.199
31	Spring03	-0.034	0.109	1.111	-0.194	-0.122	0.265	-0.002	-0.002	0.050	-0.445
32	Spring04	-0.082	0.434	0.022	0.000	0.175	0.471	0.311	0.062	-0.031	0.066
33	Spring06	0.003	2.889	-0.072	2.293	3.902	0.269	0.780	0.100	0.265	12.135
34	Spring11	0.024	0.288	0.045	1.325	0.424	0.254	-0.023	0.046	-0.192	0.343
35	Spring12	-0.054	-0.993	8.857	-5.089	-0.631	0.203	-0.523	-0.316	-0.892	0.186
36	SW01	0.013	2.147	-1.003	2.993	1.684	0.530	0.399	0.199	0.585	6.449
37	SW02	0.000	1.059	-0.503	-1.393	0.700	0.346	0.034	0.085	0.628	6.308
38	SW03	-0.008	-0.721	2.354	-3.653	-0.675	0.125	-0.448	0.117	-0.554	0.303
39	SW04	0.006	-0.288	-3.070	-0.645	-0.155	-0.032	-0.179	-0.008	-0.465	0.433
40	SW05	-0.035	3.442	0.196	0.831	5.264	0.304	0.891	0.143	0.249	18.078
41	SW06	0.000	0.260	-3.306	0.701	-0.060	0.351	-0.019	-0.063	0.062	-0.379
42	SW07	-0.003	1.403	-0.981	2.323	1.394	0.921	0.071	0.192	1.258	2.076
43	SW08	-0.019	0.165	-8.609	1.618	-0.056	0.359	0.030	-0.143	0.281	-1.241
44	SW09	-0.048	0.138	3.290	0.177	-0.226	0.494	-0.033	-0.147	0.172	-0.328
45	SW10	-0.010	0.010	0.512	0.000	-0.321	0.313	-0.101	-0.032	0.097	-0.555
46	SW11	0.037	7.555	-0.694	4.440	9.012	1.111	1.672	0.283	1.257	32.084
47	SW16	-0.017	1.112	-0.110	-1.295	0.988	0.402	0.152	0.102	1.124	7.336
48	SW17	0.000	1.663	-0.359	-1.577	0.964	0.377	0.102	0.122	0.816	11.755
49	SW18	0.044	-0.096	-0.104	5.040	5.131	-0.286	0.050	-0.102	-0.384	-13.922

5.7 Hydrogeological conceptual model for the study area

The results of the various data analyses including geological, hydrogeological, hydrochemical and environmental isotope data and their interpretations are systematically integrated into a hydrogeological conceptual model proposed for the study area (Figure 5-27). A Hydrogeological conceptual model depicts a simplified version of the hydrogeologic system under investigation, and the proposed model must be considered as such. The various borehole log data helped to understand the subsurface geological units, aquifers and groundwater flow conditions. The various analyses results reported in the preceding sections are supported with the well-to-well geological logs shown in Figure 5-26 to develop the proposed conceptual model. The information from the lithologic logs shows that the Vyheid Formation of the Eccca Group consists of alternating layers of sandstone, shale and coal. These are underlain by tillites of the Dywka Group and are typically present at depths greater than 30 m below ground level. The Dywka tillites are either underlain by quartzites of the Daspoort Formation of the Pretoria Group or dolerite intrusions.

The mean annual groundwater recharge of the area ranges from 5% of Map to 9% of MAP. Borehole yields from both secondary aquifer systems range from 0.1 to 2 L/s. The intergranular and fractured aquifer of the Eccca Group has median hydraulic conductivity (K) of 0.04 m/day. Fractured aquifers of the Dwyka Group and the Pretoria Group are characterised by low K values that range from 0.002 to 0.01 m/day and 0.03 to 0.06 m/day, respectively. The depth to groundwater level in the study area ranges from near ground surface to as deep as 23 m bgl. Groundwater in the catchment occurs mainly in secondary weathered and fractured, and fractured aquifers mainly in unconfined conditions. The general groundwater flow direction follows the topographic gradient.

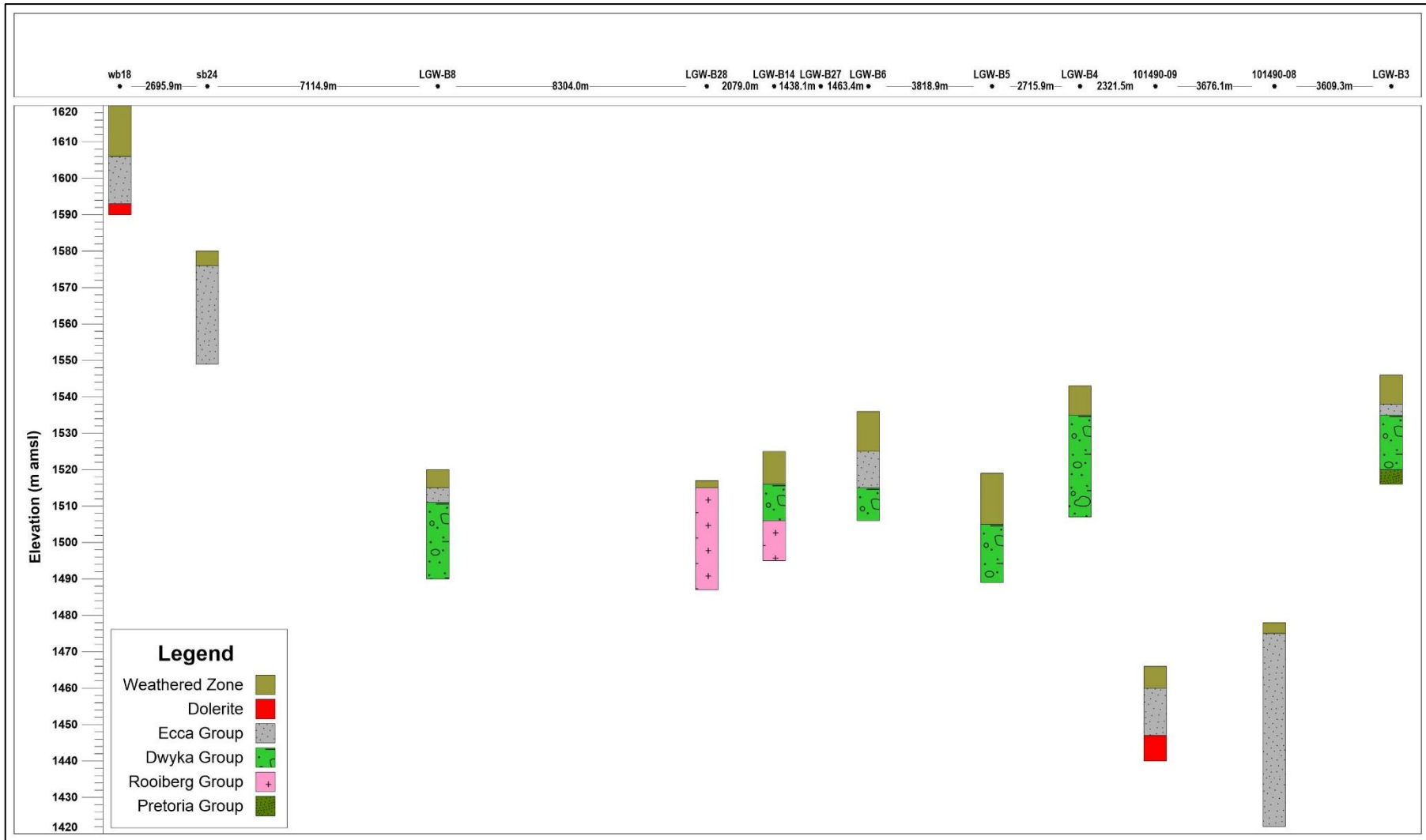


Figure 5-26: Well to well log geological cross-section from A-A.

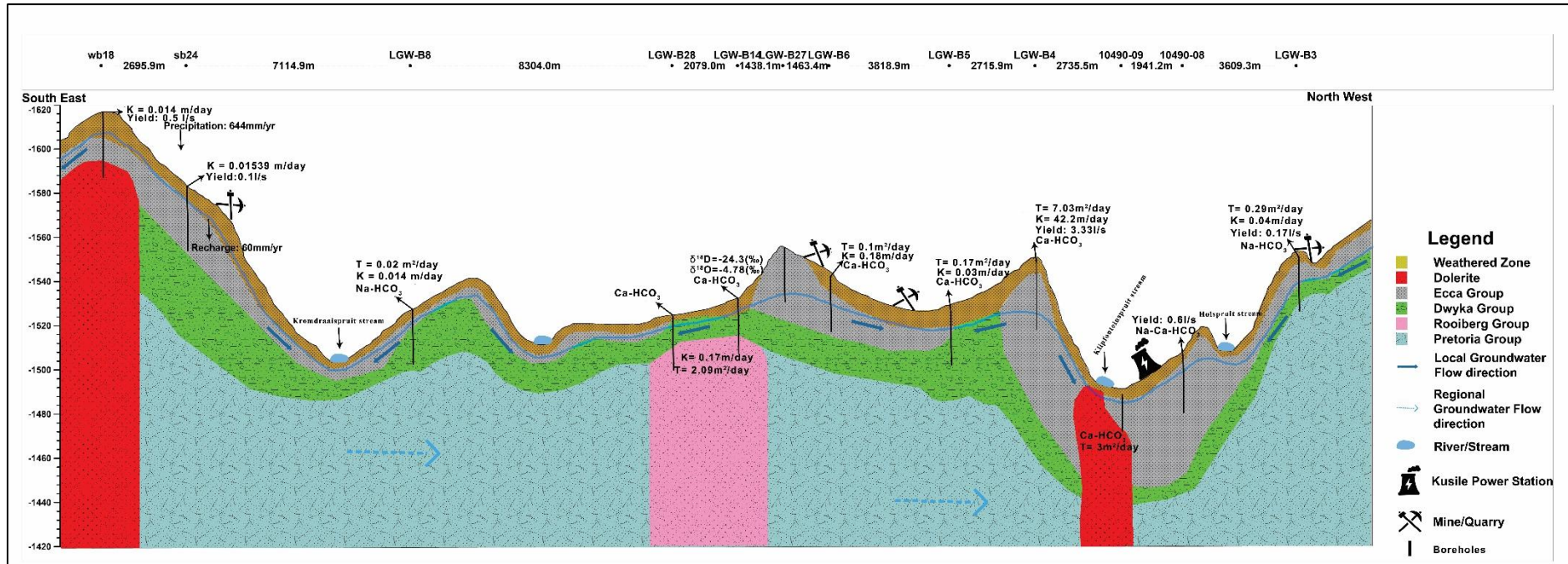


Figure 5-27: Conceptual hydrogeological model of the study catchment based on a southeast-northwest cross-section line.

CHAPTER 6 : CONCLUSIONS AND RECOMMENDATIONS

6.1 Conclusion

The groundwater in the studied catchment occurs within the laterally extensive shallow weathered and fractured aquifers of the Eccra Group and fractured aquifers of the Dwyka Group and Pretoria Group mainly unconfined to semi-confined conditions. The fractures in the various aquifers are prevalent along the contact zones with the diabase intrusions. Generally, the transmissivity of the weathered zone averages about 5.06 m²/day while its average permeability is in the order of 0.76 m/day. Groundwater flow direction is towards the north and is controlled by the topographic gradient.

The area receives approximately 644 mm/year of rainfall. Groundwater recharge is primarily from precipitation and estimated using CMB, WTF and qualified guesses approaches. The CMB method returned annual recharge rates that vary from 26 to 390 mm/year with a harmonic mean of 118 mm/year or 18.3% of MAP, which is very high. While the WTF method gave a recharge rate between 0.63 and 143 mm/year, averaging 31.6 mm/year or 5% of MAP. The qualified guesses gave an average recharge rate of 56.6 mm/year or 8.1 % of the MAP, which is more comparable with the 58.9 mm/year or 8.8% of MAP that was determined in the GRAII project. Thus, the recharge rate for the region lies between the 5% of MAP estimated using the WTF method and the 8% estimated following the qualified guesses approach.

The groundwater in the study area is characterised by less evolved young waters recharged from local rainfall as demonstrated by the tritium activities in the groundwater. Its hydrochemistry mainly controlled by rock-water interactions, this is supported by the dominance of Ca-HCO₃ water type, Durov and Gibbs plots. The high concentrations of Ca²⁺, Mg²⁺, and SO₄²⁻ are attributed to the oxidation of pyrite facilitated by the mining activities operating within the study area, coal stockpiles related to the operational activities of the Kusile Power Station and later buffering with carbonate minerals along the flow path. The stable isotope composition shows that all the groundwater samples are characterised by a lighter isotopic signal indicating recharge from local rainfall with little or no evaporation. The overall hydrochemistry of the study area is controlled by natural geochemical processes of rock-water interaction including dissolution, ion exchange and limited anthropogenic impact such as coal mining and to a lesser extent the coal-fired power plant operation.

Historical groundwater level time series observed in 23 boreholes shows that the majority (81%) of the boreholes exhibit decreasing groundwater level trends with an average value rate of decline of - 0.35 m/year. Changes in recharge dynamics as a result of climate change and anthropogenic activities such as mining are attributed to be the primary drivers of the decline in groundwater levels. Results of trend analysis of the hydrochemical data showed both increasing and decreasing trends. However, the general long-term hydrochemical time-series data reveals a statically significant general decrease in the water quality of the study area.

6.2 Recommendations

Based on the conclusions and findings drawn from the study, the following recommendations are made:

- Continued monitoring of both groundwater levels and hydrochemical data as both have shown significant decreasing and increasing temporal variations.
- In a catchment where many water resources impacting land use activities are operating, a catchment-wide monitoring network system should be considered as the current monitoring is concentrated in the foot-print area of the power station.
- The NGA needs to be updated to reflect the adequate number of boreholes within the study area. Currently, there are fewer boreholes registered on the NGA database than found during hydrocensus surveys conducted by several consultants.
- Further research focussing on groundwater-surface water interactions and a numerical model should be conducted for the catchment so as to broaden knowledge of the groundwater flow regimes. Since the power station is now in full operation, environmental pollution risk assessment is recommended.

REFERENCES

- Abiye, T. (2013). *The Use of Isotope Hydrology to characterize and assess water resources in Southern Africa*. Pretoria: Water Research Commission.
- Abu-Khalaf, N., Khayat, S., and Natsheh, B. (2013). Multivariate Data Analysis to Identify the Groundwater Pollution Sources in Tulkarm Area / Palestine. *Science and Technology*, 99-104.
- Ailun, Y., Kang, R., Xingmin, Z., Xu, H., Hanhua, Z., Miaohan, S., and Fei, L. (2010). *The True Cost of Coal-An Investigation into Coal Ash in China*. Greenpeace.
- Aggarwal, P. K., Froehlich, K., and Kulkarni, K. M. (2009). Environmental Isotopes in Groundwater Studies. *Groundwater*, 2(69).
- Al-Kalbani, M. S., Price, M. F., Ahmed, M., Abahussain, A., and O'Higgins, T. (2017). Environmental quality assessment of groundwater resources in Al Jabal Al Akhdar, Sultanate of Oman. *Applied Water Science*, 7, 3539–3552.
- Amfo-Otu, R., Agyenim, J. B., and Nimba-Bumah, G. B. (2014). Correlation Analysis of Groundwater Colouration from Mountainous Areas, Ghana. *Environmental Research, Engineering and Management*, 1(67), 16-24.
- Anderson, T. W. (2003). *An Introduction to Multivariate Statistical Analysis* (3rd ed.). Hoboken: John Wiley & Sons.
- Anderson, M. P., and Woessner, W. W. (2002). *Groundwater Modeling: Simulation of Flow and Advective Transport*. London: Academic Press.
- Appelo, C. A., and Postma, D. (2005). *Geochemistry, Groundwater and Pollution*. Amsterdam: A.A. Balkema Publishers.
- Banks, V. J., Palumbo-Roe, B., van Tonder, D., Davies, J., Fleming, C., and Chevrel, S. (2011). *Conceptual models of Witbank coalfield, South Africa*. Pretoria: EO-MINERS.
- Barnard, H. C. (2000). *An Explanation of the 1:500 000 General Hydrogeological Map - Johannesburg 2526* (1st ed.). Pretoria: Department of Water Affairs and Forestry.

- Barnes, M., and Vermeulen, P. D. (2012). Guide to groundwater monitoring for the coal industry. *Water SA* (38), 831-836.
- Brebbia, C. A. (2011). *River Basin Management VI*. Southampton: WIT Press.
- Chadha, D. (1999). A proposed new diagram for geochemical classification of natural waters and interpretation of chemical data. *Hydrogeology Journal*, 7(5), 431-439.
- Clark, I. D., and Fritz, P. (1997). *Environmental Isotopes in Hydrogeology* (2nd ed.). Florida: CRC Press LLC.
- Clark, I. (2015). *Groundwater Geochemistry and Isotopes* (1st ed.). Florida: Taylor & Francis Group.
- Craig, H. (1961). Isotopic variations in meteoric waters. *Science*, 1702-1703.
- Dai, Z., Samper, J., and Ritzi, R. (2006). Identifying geochemical processes by inverse modeling of multicomponent reactive transport in the Aquia aquifer. *Geosphere*, 2(4), 210-219.
- Dalton, A., Feig, T. G., and Barber, K. (2018). Trace metal enrichment observed in soils around a coal fired power plant in South Africa. *Clean Air Journal*, Volume 28 (No 2), 1-9.
- Datta, P. S., and Tyagi, S. K. (1996). Major ion chemistry of groundwater in Delhi area: Chemical weathering processes and groundwater flow regime. *Journal of Geological Society of India*, 47(2), 179–188.
- Daughney, C. (2007). *Spreadsheet for automatic processing of water quality data: 2007 Update*. GNS Science.
- De Vivo, B., Belkin, H. E., and Lima, A. (2008). *Environmental Geochemistry: Site Characterization, Data Analysis and Case Histories* (First edition ed.). Amsterdam: Elsevier.
- Dehnavi, A. G., Sarikhani, R., and Nagaraju, D. (2011). Hydro geochemical and rock water interaction studies in East of Kurdistan, N-W of Iran. *International Journal of Environmental Sciences and Research*, 1(1), 16-22.
- Department of Mineral and Energy Affairs. (1986). 1:250000 Geological Map Series 2628 of East Rand. Pretoria, Gauteng, South Africa.

- Department of Mines. (1978). 1:250000 Geological Map Series 2528 of Pretoria. Pretoria, Gauteng, South Africa.
- Department of Water and Sanitation. (2017, November 13). Retrieved from <http://www.dwa.gov.za/Hydrology/Verified/HyStations.aspx?Region=B&StationType=rb>
River
- Domenico, P. R., and Schwartz, F. W. (1998). *Physical and Chemical Hydrogeology* (Second Edition ed.). New York: John Wiley & Sons.
- Durov, S. A. (1948). Classification of natural waters and graphic presentation of their composition. *Doklady Akademii Nauk SSSR*, 87-90.
- DWAF (Department Water Affairs and Forestry). (1999). Map Sheet titled, “Johannesburg 2526”, at a scale of 1:500000. Pretoria, Gauteng, South Africa.
- Ebrahim, G. Y. (2013). *Modelling Groundwater Systems: Understanding and Improving Groundwater quality management*. Delft: Delft University of Technology and of the Academic Board of the UNESCO-IHE Institute for Water Education.
- Edmunds, W. M., and Shand, P. (2008). *Natural Groundwater Quality* (1st ed.). Malden, USA: Blackwell Publishing Ltd.
- Engeolab. (2019). Hydrogeological overview of Arbor rural village. Hilton: Engeolab Pty (Ltd).
- Environmental Integrity Project. (2012, April). *Forty-Nine Coal-Fired Plants Acknowledge Groundwater Contamination in Response to EPA Data Collection*. Washington, DC, USA.
- Eriksson, E., and Khunakasem, V. (1969). Chloride concentration in groundwater, recharge rate and rate of deposition of chloride in the Israel Coastal Plain. *Journal of Hydrology*, 7(2), 178-197.
- Eriksson, P. G., Altermann, W., and Hartzler, F. J. (2006). The Transvaal Supergroup and its Precursor. In M. Johnson, C. Anhaeusser, and R. Thomas (Eds.), *The Geology of South Africa*. Pretoria.
- Fianko, J. R., Nartey, V. K., and Donkor, A. (2010). The hydrochemistry of groundwater in rural communities within the Tema District, Ghana. *Environ Monit Assess* (168), 441–449.
- Fitts, C. R. (2002). *Groundwater Science* (Second ed.). London: Academic Press.

- GCS. (2014). Kusile Power Station Hydrogeological Investigation. Johannesburg: Eskom.
- Gibbs, R. J. (1970). Mechanisms Controlling World Water Chemistry. *Science*, 170, 1088–1090.
- Gibrilla, A., Osae, S., Akiti, T. T., Adomako, D., Ganyaglo, S. Y., Bam, E. P., and Hadisu, A. (2010). Origin of Dissolve Ions in Groundwaters in the Northern Densu River Basin of Ghana Using Stable Isotopes of ^{18}O and ^2H . *Journal Water Resource and Protection*, 2, 1010-1019.
- Golder Associates Africa (Pty) Ltd. (2007). Project Bravo Power Station Site: Geophysical Survey and Groundwater Assessment. Johannesburg.
- Goussard, F. (2017). The Development of a pre-mining groundwater monitoring network for open pit mines in South Africa. Bloemfontein, Free State, South Africa.
- Groundwater Square. (2018). Vlakvarkfontein Coliery, Pilar Mining Project: Groundwater Impact Assessment. Delmas: Groundwater Square.
- Guilford, J. P. (1973). *Fundamental statistics in psychology and education*. New York: McGraw-Hill.
- Härdle, W., and Simar, L. (2007). *Applied Multivariate Statistical Analysis*. Berlin: Springer.
- Harter, T. (2003). *Basic Concepts of Groundwater Hydrology*. California: Regents of the University of California.
- Hiscock, K. M. (2005). *Hydrogeology: Principles and Practice*. Oxford: Blackwell Publishing.
- Hodgson, F., and Krantz, R. (1998). Groundwater quality deterioration in the Olifants River catchment above the Loskop Dam with specialised investigations in the Witbank Dam sub-catchment. Pretoria: Water Research Commission.
- Hossain, M. G., Reza, S., Lutfun-Nessa, M., and Ahmed, S. S. (2013). Factor and Cluster Analysis of Water Quality Data of the Groundwater Wells of Kushtia, Bangladesh: Implication for Arsenic Enrichment and Mobilization. *Journal Geological Society of India*, 81, 377 - 384.
- Hounslow, A. (1995). *Water Quality Data: Analysis and Interpretation*. Florida: CRC Press.

- International Groundwater Resources Assessment Centre (IGRAC). (2008). Guideline on: Groundwater monitoring for general reference purposes. Utrecht, Netherlands: International Groundwater Resources Assessment Centre (IGRAC).
- JG Afrika. (2016). Groundwater feasibility and implementation for monitoring boreholes at Kusile Power Station. Durban: JG Afrika Pty (Ltd).
- JMA Consulting. (2012). New Largo Geology specialist study report. Delmas: JMA Consulting.
- Johnson, M., Van Vuuren, C., Visser, J., Cole, D., Wickens, H., Christie, A., and Brandl, G. (2006). Sedimentary rocks of the Karoo Supergroup. In M. Johnson, C. Anhaeusser, and R. Thomas (Eds.), *The Geology of South*. Pretoria.
- Jothivenkatachalam, K., Nithya, A., and Mohan, C. S. (2010). Correlation Analysis of Drinking Water Quality in and around Perur Block of Coimbatore District, Tamil Nadu, India. *Rasayan Journal Chemistry*, 3(4), 649-654.
- Karmegam, U., Chidamabram, S., Sasidhar, P., Manivannan, R., Manikandan, S., and Anandhan, P. (2010). Geochemical Characterization of Groundwater's of Shallow Coastal Aquifer in and Around Kalpakkam, South India. *Research Journal of Environmental and Earth Sciences*, 170-177.
- Kaur, P., Stoltzfus, J., and Yellapu, V. (2018). Descriptive statistics. *Int J Acad Med* , 60-63.
- Kendall, M. G. (1955). *Rank correlation methods* (2nd ed.). London: Hafner Publishing Co.
- Kendall, M. G. (1975). *Rank correlation methods* (4th ed.). London: Griffin.
- Kresic, N. (2007). *Hydrogeology and Groundwater Modeling* (2nd ed.). Boca Raton: CRC Press.
- Kresic, N. (2009). *Groundwater Resources: Sustainability, Management, and Restoration* (eBook ed.). New York: The McGraw-Hill Companies, Inc.
- Kumar, P., Chandniha, S. K., Lohani, A. K., Krishan, G., and Nema, A. K. (2018). Trend analysis of groundwater level using non-parametric tests in alluvial aquifers of Uttar Pradesh, India. *Current World environment*, 13(1), 44-54.

- Kumar, S. P. (2013). Interpretation of groundwater chemistry using piper and chadha's diagrams: a comparative study from perambalur taluk. *Elixir Geoscience*, 54, 12208-12211.
- Law, A. G. (1974). Stochastic Analysis of Groundwater Level Time Series in the Western United States. *Hydrology Papers*, 68, 1-26.
- Ledwaba, L., Dingoko, O., and Havenga, M. (2009). Compilation of Survey Specifications for all the old regional airborne geophysical surveys conducted over South Africa. Pretoria: Council for Geoscience .
- Li, Y., and Migliaccio, K. (2011). *Water Quality Concepts, Sampling, and Analyses* (1st ed.). Florida: CRC Press.
- Lloyd, J. W., and Heathcote, J. A. (1985). *Natural inorganic hydrochemistry in relation to ground water*. Madison: Clarendon Press.
- Mabee, S. B., Hardcastle, K. C., and Wise, D. U. (1994). A Method of Collecting and Analyzing Lineaments for Regional-Scale Fractured-Bedrock Aquifer Studies. *Ground Water*, 884-894.
- Machiwal, D., and Jha, M. K. (2012). *Hydrologic Time Series Analysis: Theory and Practice* (1st ed.). Dordrecht: Springer.
- MacKella, N., New, M., and Jack, C. (2014, July/August). Observed and modelled trends in rainfall and temperature for South Africa: 1960–2010. *South African Journal of Science*, 10(7/8), 1-13.
- Mafamadi , M. A. (2017). Impacts of greenhouse gases from coal power stations on climatic trends in Witbank area, South Africa. Venda: University of Venda.
- Manders, D., Godfrey, L., and Hobbs, P. (2009, August). Acid Mine Drainage in South Africa: Briefing Note 2009/02. Pretoria: CSIR Natural Resources and the Environment.
- Manikandan, S. (2011, September). Measures of central tendency: Median and mode. *Journal of Pharmacology and Pharmacotherapeutics*, 2(3), 214-215.
- Mann, H. B. (1945). Nonparametric tests against trend. *Econometrica*, 13, 245–259.

- Manoj, K., Ghosh, S., and Padhy, P. K. (2013). Characterization and Classification of Hydrochemistry using Multivariate Graphical and Hydrostatistical Techniques. *Research Journal of Chemical Sciences*, Vol. 3(5), 32-42.
- Marghade, D., Malpe, D. B., and Zade, A. B. (2010). Geochemical characterization of groundwater from north-eastern part of Nagpur urban, Central India. *Environmental Earth Sciences*, 62, 1419–1430.
- Mazor, E. (2004). *Chemical and Isotopic Groundwater Hydrology* (Third Edition ed.). New York: Library of Congress.
- Mechlem, K. (2016). Groundwater Governance: The Role of Legal Frameworks at the Local and National Level—Established Practice and Emerging Trends. *Water*, 8(8), 1-16.
- Meng, S. X., and Maybard, B. J. (2001). Use of statistical analysis to formulate conceptual models of geochemical behaviour: water chemical data from the Botucatu aquifer in Sao Paulo state, Brazil. *Journal of Hydrology* (250), 78-97.
- Middlemis, H. (2001). *Murray-Darling Basin Commission: Groundwater Flow Modelling Guidelines*. Perth: Aquaterra Consulting Pty Ltd.
- Moolman, D. (2011, May). *Baseline Study of Kendal Power Station*. Bloemfontein, Free State, SouthAfrica.
- Mpenyana-Monyatsi, L., Onyango, M. S., and Momba, M. N. (2012). Groundwater Quality in a South Africa Rural Community: A Possible Threat to Public Health. *Pol. J. Environ. Stud*, 1349 -1358.
- Mustapha, A. (2013). Detecting surface water quality trends using Mann-Kendal Tests and Sen's Slope estimates. *International Journal of Advanced and Innovative Research*, 108-114.
- Parkhurst, D. L., and Appelo, C. A. (2013). *Description of input and examples for PHREEQC version 3—A computer program for speciation, batch-reaction, one-dimensional transport, and inverse geochemical calculations: U.S. Geological Survey Techniques and Methods* (Book 6 ed.). Denver: U.S. Geological Survey.
- Peplinski, B., and Czubak, W. (2021). The Influence of Opencast Lignite Mining Dehydration on Plant Production—A Methodological Study. *Energies*, 14(1917), 1-29.

- Pitkanen, P., Luukkonen, A., Ruotsalainen, P., Leino-Forsman, H., Vuorinen, U. (1998). Geochemical modelling of groundwater evolution and residence time at the Kivetty site. Mikonkatu: POSIVA OY.
- Plummer, N. L., Bexfield, L. M., Anderholm, S. K., Sanford, W. E., and Busenberg, E. (2004). Geochemical Characterization of Ground-water Flow in the Santa Fe Group Aquifer System, Middle Rio Grande Basin, New Mexico. Virginia: U.S. Geological Survey.
- Rehman, F., Cheema, T., Abuelnaga, H. S., Harbi, H. M., Atef, A. H., and Lisa, M. (2016). Interpretation of Groundwater Chemistry Data using Multivariate Statistical Techniques. Global NEST, 665-673.
- Ravikumar, P., Somashekar, R. K., and Prakash, K. L. (2015). A comparative study on usage of Durov and Piper diagrams to interpret hydrochemical processes in groundwater from SRLIS river basin, Karnataka, India. Earth Science, 80, 31073-31077.
- Rehman, F., Cheema, T., Abuelnaga, H. S., Harbi, H. M., Atef, A. H., and Lisa, M. (2016). Interpretation of Groundwater Chemistry Data using Multivariate Statistical Techniques. Global NEST, 665-673.
- Reimanna, C., Filzmoser, P., and Garrett, R. G. (2002). Factor analysis applied to regional geochemical data problems and possibilities. Applied Geochemistry, 17, 185–206.
- Rick Brassington. (2007). Field Hydrogeology (Third Edition ed.). Chichester: John Wiley & Sons, Ltd.
- Rovai, A. P. (2016). Using Microsoft Excel for Univariate and Bivariate Analysis (Third Edition ed.). Chesapeake: Watertree Press LLC.
- Sadashivaiah, C., Ramakrishnaiah, C. R., and Ranganna, G. (2008). Hydrochemical Analysis and Evaluation of Groundwater Quality in Tumkur Taluk, Karnataka State, India. International Journal of Environmental Research and Public Health, 5(3), 158-164.
- Saikia, M. M., and Sarma, H. P. (2011). Hydro-geochemical characterization of groundwater of Nagaon District Assam, India. Journal of Environmental Research and Development, 6(1), 41-50.
- Satyanarayana, P., Raju, N. A., Harikrishna, K., and Viswanath, K. (2013). Urban Groundwater Quality Assessment: A Case Study of Greater Visakhapatnam Municipal Corporation Area

- (Gvmc), Andhra Pradesh, India. *International Journal of Engineering Science Invention*, 2(5), 20-31.
- SAWS . (2018). South African Weather Services. Pretoria Weather Office-Meteorological Data. Pretoria.
- Sen, P. K. (1968). Estimates of the regression coefficient based on Kendall's tau. *Journal of the American Statistical Association*, 63, 1379-1389.
- Singh, K. C., Kumar, A., Shashtri, S., Kumar, A., Kumar, P., and Mallick, J. (2017). Multivariate statistical analysis and geochemical modeling for geochemical assessment of groundwater of Delhi, India. *Journal of Geochemical Exploration* (175), 59–71.
- Singhal, B. B., and Gupta, R. P. (2010). *Applied Hydrogeology of Fractured Rocks* (Second ed.). New York: Springer.
- Suma, C. S., Srinivasamoorthy, K., Saravanan, K., Faizalkhan, A., Prakash, R., and Gopinath, S. (2015). Geochemical Modeling of Groundwater in Chinnar River Basin: A Source Identification Perspective. *Aquatic Procedia*, 4, 986 – 992.
- Templ, M., Filzmoser, P., and Reimann, C. (2006). Cluster analysis applied to regional geochemical data: Problems and possibilities. *Wiedner Hauptstr: Forschungsberich*.
- Thakur, G. S., and Thomas, T. (2011). Analysis of Groundwater Levels for Detection of Trend in Sagar District, Madhya Pradesh. *Journal Geological Society of India*, 77, 303-308.
- Tikhomirov, V. V. (2016). *Hydrogeochemistry Fundamentals and Advances* (Vol. Volume 1: Groundwater Composition and Chemistry). Massachusetts: Scrivener Publishing LLC.
- Tiwary, A. R., and Sinha, S. (2006). Status of Surface and Groundwater Quality in Coal Mining and Industrial ares of Jharia Coalfields. *IJEP*, 905-910.
- Usman, U. N., Toriman, M. E., Juahir, H., Abdullahi, M. G., Rabi, A. A., and Isiyaka, H. (2014). Assessment of Groundwater Quality Using Multivariate Statistical Techniques in Terengganu. *Science and Technology*, 4(3), 42-49.
- Van Tonder, G. and Xu, Y., 2001. Recharge – Programme to estimate recharge and the groundwater reserve.

- van Wyk, E., van Tonder, G. J., and Vermeulen, D. (2011, April 2). Characteristics of local groundwater recharge cycles in South African semi-arid hard rock terrains – rainwater input. Retrieved October 15, 2020, from <http://www.wrc.org.za/wp-content/uploads/mdocs/2600.pdf>.
- Vegter, J. R. (1995). An explanation of a set of national groundwater maps. WRC Report No. TT 74/95. Pretoria: Water Research Commission.
- Vousoughi, F. D., Dinpashoh, Y., Aalami, M. T., Jhajharia, D. (2012). Trend analysis of groundwater using non-parametric methods (case study: Ardabil plain). *Stochastic Environmental Research and Risk Assessment*, 27, 547–559.
- Ward, J. J. (1963). Hierarchical grouping to optimize an objective function. *Journal of the American Statistical Association*, 236–244.
- Woodford, A. C., and Chevallier, L. (2002). Hydrogeology of the Main Karoo Basin: Current Knowledge and Future Research Needs. Pretoria: Water Research Commission (WRC) of South Africa. WRC Report No. TT 179/02.
- WWF-SA. (2017). Scenarios for the Future of Water in South Africa. Cape Town: WWF-SA.
- Zekai, S. (2014). *Practical and Applied Hydrogeology* (1st ed.). Amsterdam: Elsevier.
- Zhu, C., and Anderson, G. (2002). *Environmental Application of Geochemical Modeling* (First ed.). Cambridge: Cambridge University Press.
- Zitholele. (2014). Environmental Impact Assessment for the Kusile 60 year Ash Disposal Facility at the Kusile Power Station. Johannesburg: Eskom Holdings SCO (Ltd).

APPENDIX A: FIELD MEASURED PARAMETERS AND CALCULATED ELECTRONEUTRALITY

Sample Point ID	Sample ID	Sample Date	Latitude	Longitude	Resource Type	Sample Method	Groundwater Level (m bgl)	Temp (°C)	pH	EC (mS/m)	TDS (mg/L)	CBE (%)
10490-08	K6-40	15/06/2018	-25.9099	28.91759	Borehole	Submersible	22.73	17.8	5.59	94.2	66.7	-3.8
10490-09	K6-31	14/06/2018	-25.9274	28.91664	Borehole	Submersible	5.2	20	6.3	134.5	95.7	-3.2
10490-10	K6-39	15/06/2018	-25.9274	28.896	Borehole	Submersible	0.08	16.4	6.56	587	415	0.4
10490-14	K6-37	15/06/2018	-25.93476	28.91506	Borehole	Submersible	5.7	20.1	4.95	63	44.5	-3.6
10490-17	K6-36	15/06/2018	-25.93989	28.90533	Borehole	Submersible	2.56	18.5	4.93	62.1	44.2	-4.9
10490-21	K6-34	14/06/2018	-25.94277	28.92259	Borehole	Submersible	10.39	18.5	7.28	206	146	-2.2
10490-25	K6-06	12/06/2018	-25.9233	28.88393	Borehole	Submersible	1.17	18.2	6.98	371	265	-2.7
10490-27	K6-25	14/06/2018	-25.9128	28.93232	Borehole	Submersible	10.64	20.1	5.94	68.9	48.9	1.3
BH02	K6-11	12/06/2018	-25.9026	28.90675	Borehole	Submersible	6.12	19	6.19	124.1	88.1	-1.4
BH11	K6-01	12/06/2018	-25.9502	28.93147	Borehole	Submersible	-	20.3	6.11	82	42	-4.5
BH24	K6-09	12/06/2018	-25.9	28.89945	Borehole	Submersible	11.16	19.3	6.11	117.7	83.7	-3.3
BH25	K6-05	12/06/2018	-25.9045	28.89334	Borehole	Submersible	13.67	20.2	5.05	68.2	48.3	-3.1
BH27 (LGW-B4)	K6-16	13/06/2018	-25.93319	28.94313	Borehole	Submersible	5.09	19.4	5.11	30.2	21.3	0.9
BH30 (LGW-B11)	K6-15	13/06/2018	-25.9161	28.95413	Borehole	Submersible	2.52	20	5.9	101.1	71.6	-4.5
DWBH-06	K6-27	14/06/2018	-25.92171	28.92613	Borehole	Submersible	10.26	20.2	5.19	59.1	42.1	-4.3
DWBH-36	K6-24	14/06/2018	-25.91445	28.91236	Borehole	Submersible	6.54	20.4	6.19	105.7	74.4	-4.2
KP05	K6-26	14/06/2018	-25.91958	28.93214	Borehole	Submersible	14.51	19.4	5.76	50.7	36.2	-4.4
MP14-001	K6-38	15/06/2018	-25.9298	28.89699	Borehole	Submersible	9	19.8	6.11	150.1	107	-3.8
MP14-002	K6-32	14/06/2018	-25.91896	28.89642	Borehole	Submersible	2.14	19.1	9.1	317	226	-3.7
MP14-003	K6-29	14/06/2018	-25.92724	28.92193	Borehole	Submersible	4.58	19	6.38	238	169	-2.6
Spring01	K6-14	12/06/2018	-25.9056	28.92831	Spring	Grab		13.8	6.85	115.7	82.6	-3.0
Spring03	K6-04	12/06/2018	-25.97322	28.90632	Spring	Grab		15.9	5.96	105.4	75.5	4.8
Spring04	K6-18	13/06/2018	-25.94449	28.88893	Spring	Grab		16.7	4.05	134.4	94.7	-2.2

Sample Point ID	Sample ID	Sample Date	Latitude	Longitude	Resource Type	Sample Method	Groundwater Level (m bgl)	Temp (°C)	pH	EC (mS/m)	TDS (mg/L)	CBE (%)
Spring06	KOV6-2-01	13/06/2018	-25.9476	28.92797	Spring	Grab		8.6	6.12	394	279	-0.6
Spring11	K6-17	13/06/2018	-25.9311	28.9346	Spring	Grab		16	5.59	93.6	66.5	-4.0
Spring12	K6-35	15/06/2018	-25.94236	28.91466	Spring	Grab		10	7.64	36.6	26.2	4.4
CSW08	KOV6-2-05	13/06/2018	-25.87199	28.86529	Surface water	Grab		10.4	7.7	593	421	-2.8
NCSW01	K6-13	12/06/2018	-25.90743	28.92214	Surface water	Grab		16.1	6.41	163.8	116	-4.9
NCSW03	K6-33	14/06/2018	-25.9234	28.90512	Surface water	Grab		13.8	8.48	445	313	-2.2
NCSW08	K6-28	14/06/2018	-25.92858	28.92297	Surface water	Grab		13	5.74	145	103	-3.7
NCSW09	K6-30	14/06/2018	-25.92697	28.91531	Surface water	Grab		10.2	6.36	130.7	92.8	-3.8
SW01	K6-07	12/06/2018	-25.92	28.88306	Surface water	Grab		10	7.28	454	323	-4.0
SW02	K6-23	14/06/2018	-25.8533	28.86847	Surface water	Grab		8.7	7.69	577	409	-0.9
SW03	KOV6-2-03	13/06/2018	-25.8881	28.88915	Surface water	Grab		15.3	6.17	116	82.4	-3.6
SW04	K6-08	12/06/2018	-25.8909	28.89269	Surface water	Grab		10.8	7.12	119.1	84.3	-4.7
SW05	K6-03	12/06/2018	-25.94323	28.9022	Surface water	Grab		9.1	7.37	505	368	-4.6
SW06	K6-19	13/06/2018	-25.88797	28.88723	Surface water	Grab		11.1	6.58	122.3	86.9	-4.2
SW07	KOV6-2-02	13/06/2018	-25.92578	28.89394	Surface water	Grab		9.9	6.29	238	167	4.0
SW08	K6-10	12/06/2018	-25.89552	28.90084	Surface water	Grab		9.7	6.78	121.5	86.1	-2.4
SW09	K6-12	12/06/2018	-25.90245	28.91739	Surface water	Grab		12	6.24	111.3	79.2	-4.7
SW10	K6-20	13/06/2018	-25.87853	28.86982	Surface water	Grab		11.6	7.05	122.9	87.3	-4.0
SW11	KOV6-2-04	13/06/2018	-25.88439	28.8617	Surface water	Grab		8.7	7.23	500	352	-0.9
SW16	K6-22	14/06/2018	-25.90237	28.85132	Surface water	Grab		9.3	7.9	610	432	-1.0
SW17	K6-21	13/06/2018	-25.87476	28.86313	Surface water	Grab		9.8	7.68	589	416	-4.4
SW18	K6-02	12/06/2018	-25.94699	28.91201	Surface water	Grab		9.8	6.77	599	422	-3.1

APPENDIX B: LABORATORY MEASURED PHYSICAL AND CHEMICAL PARAMETERS OF THE SURFACE WATER AND GROUNDWATER SAMPLES.

All values in mg/L unless otherwise stated

Count	Location	Sample Type	Sample Date	pH	EC (mS/m)	Turbidity as N.T.U.	Ca ²⁺	Mg ²⁺	Na ⁺	HCO ₃ ⁻	Cl ⁻	SO ₄ ⁻²	DO
1	10490-08	Borehole	15/06/2018	6.14	8.75	166.00	2.97	2.53	7.89	25.62	3.08	1.72	4.97
2	10490-09		14/06/2018	7.25	13.70	38.50	8.60	4.29	8.42	70.76	3.21	1.00	4.66
3	10490-10		15/06/2018	6.83	67.20	101.00	54.60	26.30	42.60	62.22	19.60	250.00	4.27
4	10490-17		15/06/2018	6.12	7.45	46.70	2.18	1.20	5.78	24.40	4.09	4.75	4.29
5	10490-21		14/06/2018	7.30	21.90	77.00	13.40	9.18	18.30	122.00	5.28	9.78	4.66
6	10490-25		12/06/2018	7.99	38.90	18.20	20.60	10.10	45.80	248.88	2.89	3.39	5.28
7	10490-27		14/06/2018	6.80	6.32	133.00	2.03	1.50	3.97	32.94	3.19	0.09	4.07
8	BH02		12/06/2018	7.12	10.40	178.00	5.82	3.72	7.44	61.00	1.42	1.10	4.95
9	BH11		12/06/2018	6.68	6.84	0.50	2.87	2.96	3.83	28.06	2.71	1.00	5.55
10	BH24		12/06/2018	7.12	11.80	45.30	7.81	4.69	7.80	73.20	1.25	1.00	5.74
11	BH25		12/06/2018	6.49	7.43	3.88	1.76	2.28	4.13	24.40	3.71	1.00	5.55
12	BH27		13/06/2018	6.21	3.27	9.46	0.85	0.98	1.53	12.20	1.69	1.00	5.56
13	BH30		13/06/2018	6.63	10.30	25.00	6.31	4.34	2.10	24.40	3.41	1.00	5.67
14	DWBH-06		14/06/2018	6.64	5.79	6.55	2.83	2.29	3.19	26.84	1.72	0.90	5.16
15	DWBH-36		14/06/2018	7.17	11.80	61.70	5.16	7.92	6.21	68.32	2.63	6.84	4.35
16	KP05		14/06/2018	6.56	6.60	27.20	1.81	2.22	2.91	24.40	1.65	0.90	4.98

Count	Location	Sample Type	Sample Date	pH	EC (mS/m)	Turbidity as N.T.U.	Ca ²⁺	Mg ²⁺	Na ⁺	HCO ₃	Cl ⁻	SO ₄ ⁻	DO
17	10490-14		15/06/2018	6.43	8.26	3.80	1.66	1.43	5.75	17.08	1.98	1.00	5.24
18	MP14-001		15/06/2018	6.98	14.90	234.00	8.85	6.27	11.30	96.38	1.85	1.00	4.44
19	MP14-002		14/06/2018	9.59	30.40	15.30	2.47	1.24	62.60	150.06	1.99	4.38	4.68
20	MP14-003		14/06/2018	6.75	17.50	275.00	14.50	7.17	9.54	98.82	8.02	1.06	4.21
21	LGW B14		30/03/2018	7.56	33.92	-	1.59	1.60	-	101.99	3.49	-	-
22	KSP 1		30/03/2018	6.56	30.54	-	1.26	2.32	6.59	24.40	2.88	4.44	-
23	KSP 3		30/03/2018	6.39	8.46	-	1.81	1.70	4.14	17.08	5.37	3.52	-
24	KSP 4		30/03/2018	6.85	14.31	-	0.66	2.58	7.16	5.49	24.51	-	-
25	KSP 5		30/03/2018	6.08	14.58	-	4.73	4.74	8.20	48.80	7.13	5.20	-
26	SPRING01	Spring	12/06/2018	7.47	12.70	65.60	4.12	1.83	12.30	26.84	4.09	22.30	5.87
27	SPRING03		12/06/2018	6.79	9.43	39.40	2.88	3.69	4.50	35.38	7.34	4.36	5.46
28	SPRING04		13/06/2018	5.21	12.50	0.31	3.12	3.41	9.05	20.74	17.20	1.00	5.48
29	SPRING06		13/06/2018	7.17	38.80	8.72	56.90	9.75	5.64	46.36	4.47	152.00	5.83
30	SPRING11		13/06/2018	7.20	10.90	2.00	8.66	2.46	3.61	36.60	3.52	4.86	5.86
31	SPRING12		15/06/2018	6.49	6.61	62.60	0.60	0.53	8.77	42.70	6.88	6.39	4.21
32	CSW08	Surface Water	13/06/2018	7.94	57.60	2.73	40.50	17.30	53.50	115.90	14.60	188.00	5.70
33	NCSW01		12/06/2018	7.67	15.80	89.40	16.50	3.64	4.60	48.80	4.87	32.50	6.03
34	NCSW03		14/06/2018	8.10	47.20	46.90	41.40	9.82	31.80	111.02	14.90	109.00	5.37
35	NCSW08		14/06/2018	7.27	13.90	3.69	11.80	5.25	6.57	63.44	4.58	8.60	5.19
36	NCSW09		14/06/2018	7.55	14.20	4.18	7.69	5.91	6.71	58.56	7.97	5.36	5.56
37	SW01		12/06/2018	7.70	46.50	4.83	58.60	12.60	12.20	73.20	8.55	168.00	5.75

Count	Location	Sample Type	Sample Date	pH	EC (mS/m)	Turbidity as N.T.U.	Ca ²⁺	Mg ²⁺	Na ⁺	HCO ₃ ⁻	Cl ⁻	SO ₄ ⁻²	DO
38	SW02		14/06/2018	7.76	58.50	3.25	40.20	17.70	54.10	111.02	14.30	181.00	5.65
39	SW03		13/06/2018	7.61	10.70	21.20	4.66	3.00	12.10	58.56	3.62	8.19	5.82
40	SW04		12/06/2018	7.66	12.90	52.00	5.61	3.47	9.85	43.92	6.66	12.60	5.72
41	SW05		12/06/2018	7.38	54.30	6.75	75.60	13.30	7.50	59.78	6.37	220.00	5.49
42	SW06		13/06/2018	7.52	13.60	12.60	5.71	3.40	9.95	48.80	6.71	8.76	2.79
43	SW07		13/06/2018	7.66	22.50	5.99	18.20	7.42	15.40	89.06	10.10	34.40	5.85
44	SW08		12/06/2018	7.58	11.20	10.70	6.25	3.65	9.21	51.24	6.14	6.92	6.30
45	SW09		12/06/2018	7.50	10.30	29.30	5.56	3.17	9.67	48.80	7.52	6.71	6.08
46	SW10		13/06/2018	7.53	11.20	9.39	6.32	3.51	9.86	58.56	5.92	7.17	5.76
47	SW11		13/06/2018	7.70	48.90	5.01	65.70	13.50	14.60	71.98	9.62	181.00	5.61
48	SW16		14/06/2018	7.67	62.90	3.11	38.40	19.10	68.70	119.56	14.80	206.00	5.83
49	SW17		13/06/2018	7.87	58.50	2.51	39.40	16.90	51.90	109.80	14.60	192.00	5.86
50	SW18		12/06/2018	7.52	62.80	1.99	94.70	16.50	7.68	65.88	6.01	271.00	5.78

APPENDIX C: LABORATORY MEASURED CONCENTRATIONS OF TRACE ELEMENTS

All results in µg/L except for Al, Fe and Mn which are reported in mg/L

Count	Location	Sample Type	Al	As	Cd	Co	Cr	Cu	Fe	Mn	Hg	Pb	Zn	Sb	Ni
1	10490-08	Borehole	0.23	<1.0	<1.0	1.34	60.4	1.89	8.95	0.09	<1.0	2.75	6.03	<1.0	2.82
2	10490-09		<0.01	<1.0	<1.0	<1.0	2.76	<1.0	9.09	0.12	<1.0	<1.0	7.41	<1.0	1.61
3	10490-10		0.02	<1.0	<1.0	2.45	<1.0	1.04	37.2	0.25	<1.0	<1.0	18.7	<1.0	8.09
4	10490-17		0.24	<1.0	<1.0	9.41	10.1	21.1	20.0	1.26	<1.0	9.26	10.4	<1.0	8.42
5	10490-21		0.08	<1.0	<1.0	1.05	5.77	<1.0	11.3	0.15	<1.0	<1.0	1.85	<1.0	3.04
6	10490-25		0.01	<1.0	<1.0	<1.0	7.26	<1.0	3.21	0.04	<1.0	<1.0	2.37	<1.0	5.67
7	10490-27		<0.01	<1.0	<1.0	1.73	12.8	<1.0	14.8	0.13	<1.0	<1.0	2.46	<1.0	2.26
8	BH02		0.16	<1.0	<1.0	1.66	6.85	1.63	15.6	0.78	<1.0	<1.0	8.08	<1.0	7.47
9	BH11		0.01	<1.0	<1.0	<1.0	3.88	4.63	0.25	<0.01	<1.0	<1.0	7.89	<1.0	5.78
10	BH24		0.11	<1.0	<1.0	1.00	9.51	36.8	7.31	0.20	<1.0	4.22	229	1.19	6.04
11	BH25		0.12	<1.0	<1.0	<1.0	3.45	1.88	0.84	0.01	<1.0	<1.0	6.46	<1.0	7.13
12	BH27 (LGW-B4)		<0.01	<1.0	<1.0	<1.0	5.25	<1.0	4.35	0.03	<1.0	<1.0	4.57	<1.0	3.37
13	BH30 (LGW-B11)		0.17	<1.0	<1.0	8.3	4.88	2.6	7.22	0.23	<1.0	1.56	6.55	<1.0	8.94
14	DWBH-06		0.02	<1.0	<1.0	<1.0	1.30	<1.0	0.48	0.02	<1.0	<1.0	2.04	<1.0	1.78
15	DWBH-36		0.15	<1.0	<1.0	<1.0	38.3	1.55	3.31	0.19	<1.0	2.74	3.57	<1.0	2.33
16	KP05		0.08	<1.0	<1.0	<1.0	<1.0	1.47	3.22	0.04	<1.0	1.70	5.77	<1.0	3.20
17	10490-14		0.03	<1.0	<1.0	<1.0	4.41	<1.0	0.46	0.13	<1.0	<1.0	5.35	<1.0	3.53
18	MP14-001		0.02	<1.0	<1.0	<1.0	4.44	<1.0	29.1	0.20	<1.0	<1.0	2.20	<1.0	2.36
19	MP14-002		0.15	2.58	<1.0	<1.0	<1.0	<1.0	2.86	0.04	<1.0	<1.0	2.62	<1.0	2.05
20	MP14-003		0.01	<1.0	<1.0	<1.0	3.80	<1.0	33.2	0.42	<1.0	<1.0	1.90	<1.0	1.58
21	LGW B14		-	-	-	-	-	-	0.4	0.01	-	-	0.01	-	-
22	KSP 1		-	-	-	-	-	-	0.36	0.01	-	-	0.02	-	-

Count	Location	Sample Type	Al	As	Cd	Co	Cr	Cu	Fe	Mn	Hg	Pb	Zn	Sb	Ni
23	KSP 3		-	-	-	-	-	-	0.15	-	-	-	0.02	-	-
24	KSP 4		-	-	-	-	-	-	0.02	0.02	-	-	0.05	-	-
25	KSP 5		-	-	-	-	-	-	-	0.14	-	-	-	0.02	-
26	SPRING 01	Spring	0.47	<1.0	<1.0	<1.0	10.1	1.9	3.54	0.01	<1.0	<1.0	4.16	<1.0	5.82
27	SPRING 03		0.50	<1.0	<1.0	1.36	18.9	5.06	13.2	0.10	<1.0	3.13	47.1	<1.0	31.7
28	SPRING 04		0.05	<1.0	<1.0	1.88	<1.0	1.22	0.22	0.07	<1.0	<1.0	6.81	<1.0	8.32
29	SPRING 06		0.07	<1.0	<1.0	<1.0	4.59	<1.0	1.24	0.07	<1.0	<1.0	3.58	<1.0	3.60
30	SPRING 11		0.07	<1.0	<1.0	<1.0	1.18	<1.0	0.45	0.03	<1.0	<1.0	2.73	<1.0	2.39
31	SPRING 12		5.55	<1.0	<1.0	5.67	<1.0	2.42	2.32	0.08	<1.0	1.28	8.29	<1.0	4.15
32	CSW08	Surface water	0.13	<1.0	<1.0	<1.0	16.9	<1.0	0.42	0.03	<1.0	<1.0	2.56	<1.0	4.01
33	NCSW01		0.48	<1.0	<1.0	<1.0	9.82	3.43	3.84	0.03	<1.0	1.11	15.2	<1.0	5.87
34	NCSW03		0.34	1.00	<1.0	1.15	9.69	3.05	3.00	0.24	<1.0	1.40	19.1	<1.0	3.69
35	NCSW08		0.12	<1.0	<1.0	<1.0	<1.0	1.94	0.32	0.02	<1.0	<1.0	2.04	<1.0	1.85
36	NCSW09		0.05	<1.0	<1.0	<1.0	4.72	<1.0	0.47	0.09	<1.0	<1.0	1.44	<1.0	1.69
37	SW01		0.18	<1.0	<1.0	<1.0	3.86	1.25	0.53	0.05	<1.0	<1.0	2.43	<1.0	5.57
38	SW02		0.09	<1.0	<1.0	<1.0	2.39	1.15	0.36	0.02	<1.0	<1.0	3.94	<1.0	2.60
39	SW03		0.34	1.44	<1.0	<1.0	4.66	1.16	1.87	0.03	<1.0	<1.0	3.21	<1.0	3.66
40	SW04		0.46	<1.0	<1.0	<1.0	9.32	2.12	2.61	0.07	<1.0	<1.0	3.11	<1.0	6.44
41	SW05		0.06	<1.0	<1.0	<1.0	<1.0	1.12	1.12	0.11	<1.0	<1.0	2.25	<1.0	5.22
42	SW06		0.32	<1.0	<1.0	<1.0	<1.0	<1.0	1.05	0.03	<1.0	<1.0	2.73	<1.0	2.94
43	SW07		0.11	<1.0	<1.0	<1.0	<1.0	<1.0	0.68	0.14	<1.0	<1.0	3.63	<1.0	3.24
44	SW08		0.47	<1.0	<1.0	<1.0	<1.0	1.55	1.55	0.03	<1.0	<1.0	2.53	<1.0	5.85
45	SW09		0.54	<1.0	<1.0	<1.0	7.47	1.75	1.92	0.06	<1.0	<1.0	3.83	<1.0	5.92
46	SW10		0.45	<1.0	<1.0	<1.0	5.60	<1.0	1.00	0.04	<1.0	<1.0	4.35	1.58	3.68
47	SW11		0.25	<1.0	<1.0	<1.0	6.56	176	0.56	0.02	<1.0	<1.0	113	<1.0	3.49
48	SW16		0.09	<1.0	<1.0	<1.0	<1.0	1.17	0.56	0.05	<1.0	<1.0	2.01	<1.0	2.88
49	SW17	0.11	<1.0	<1.0	<1.0	1.35	<1.0	0.40	0.03	<1.0	<1.0	3.89	1.14	4.21	

Count	Location	Sample Type	<i>Al</i>	<i>As</i>	<i>Cd</i>	<i>Co</i>	<i>Cr</i>	<i>Cu</i>	<i>Fe</i>	<i>Mn</i>	<i>Hg</i>	<i>Pb</i>	<i>Zn</i>	<i>Sb</i>	<i>Ni</i>
50	SW18		0.05	<1.0	<1.0	<1.0	8.51	1.14	0.36	0.10	<1.0	<1.0	1.59	<1.0	5.51

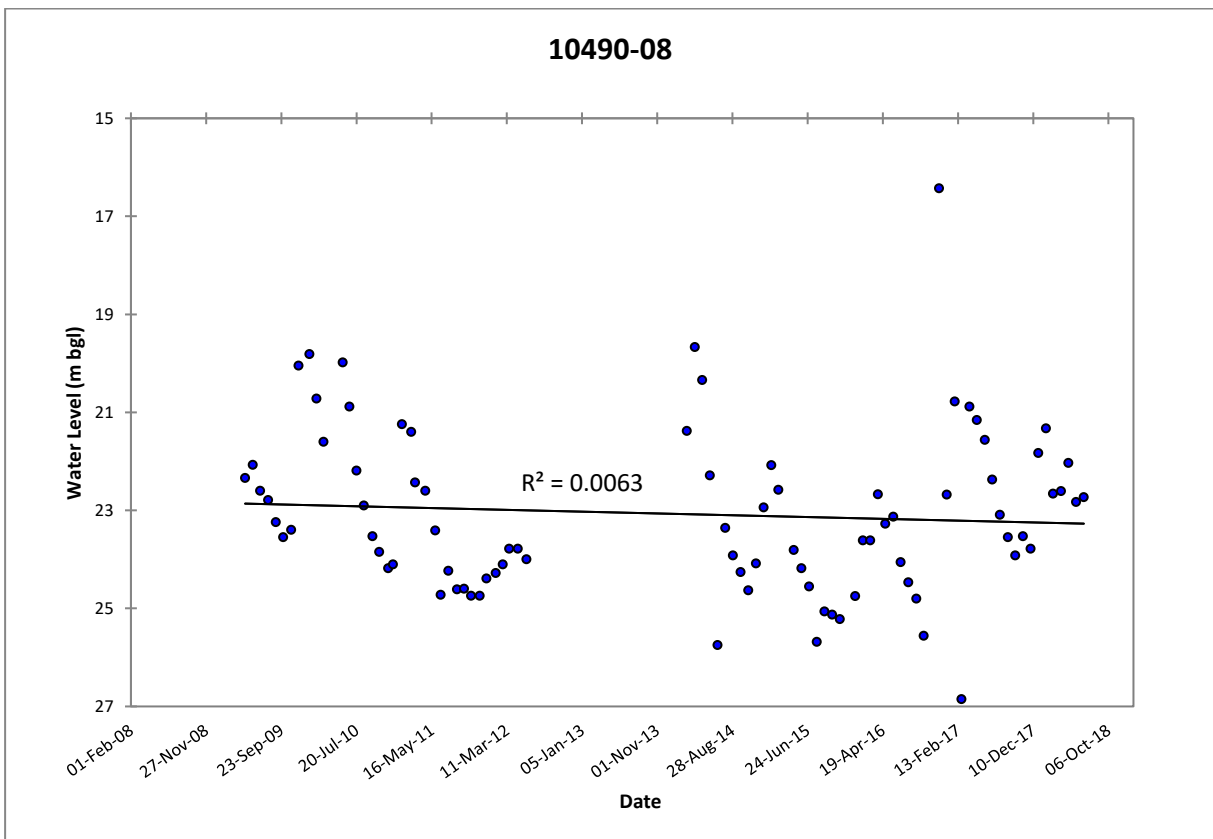
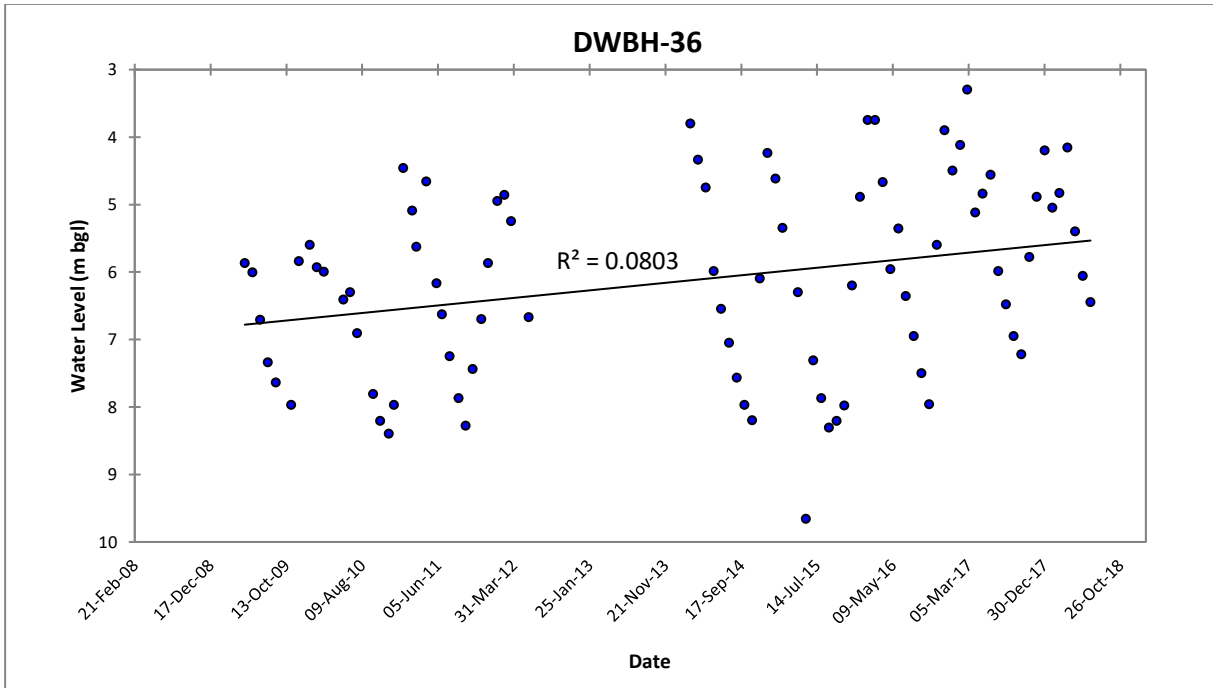
APPENDIX D: IONIC RATIOS USED IN HYDROCHEMICAL PROCESSES

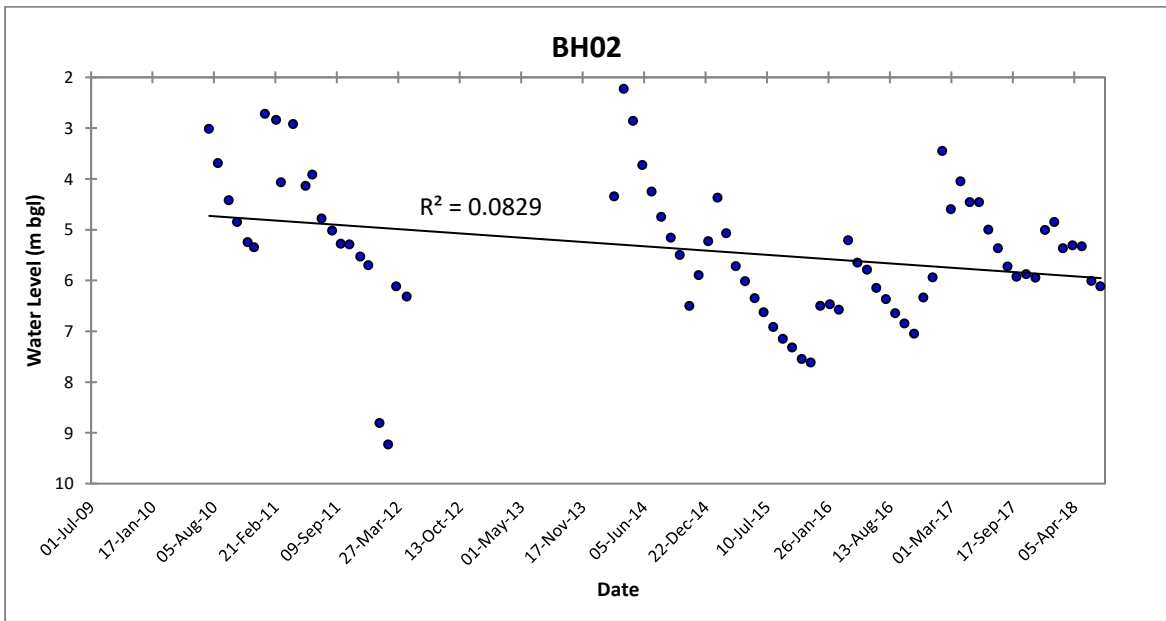
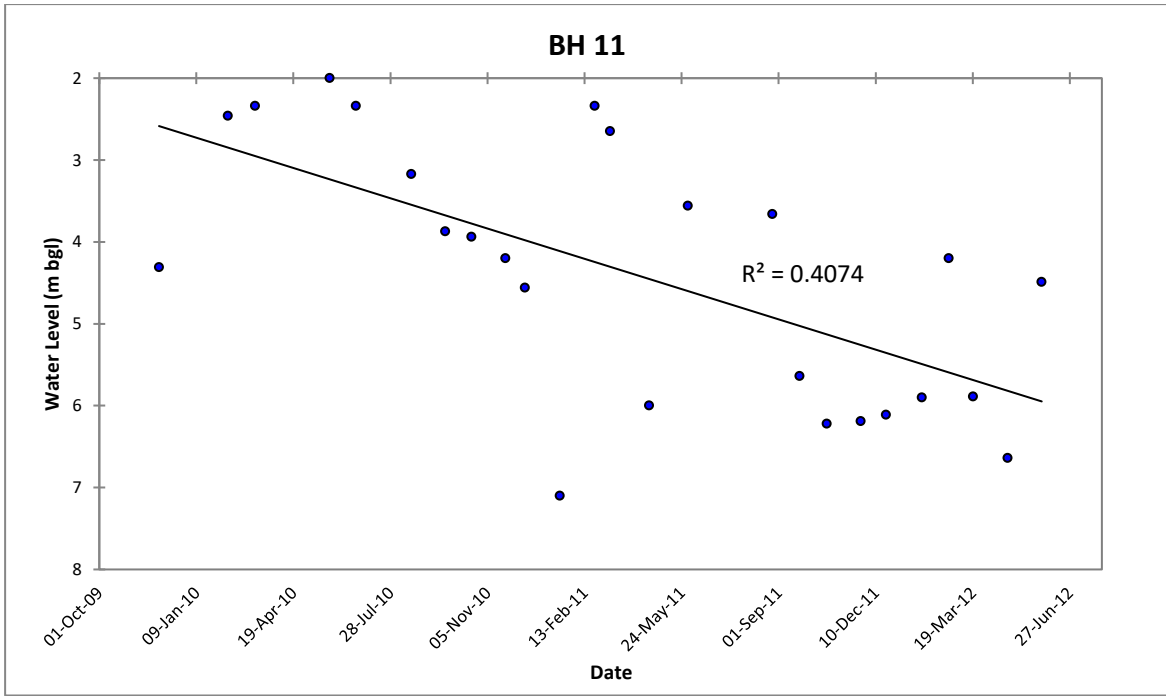
All results in (meq/l)

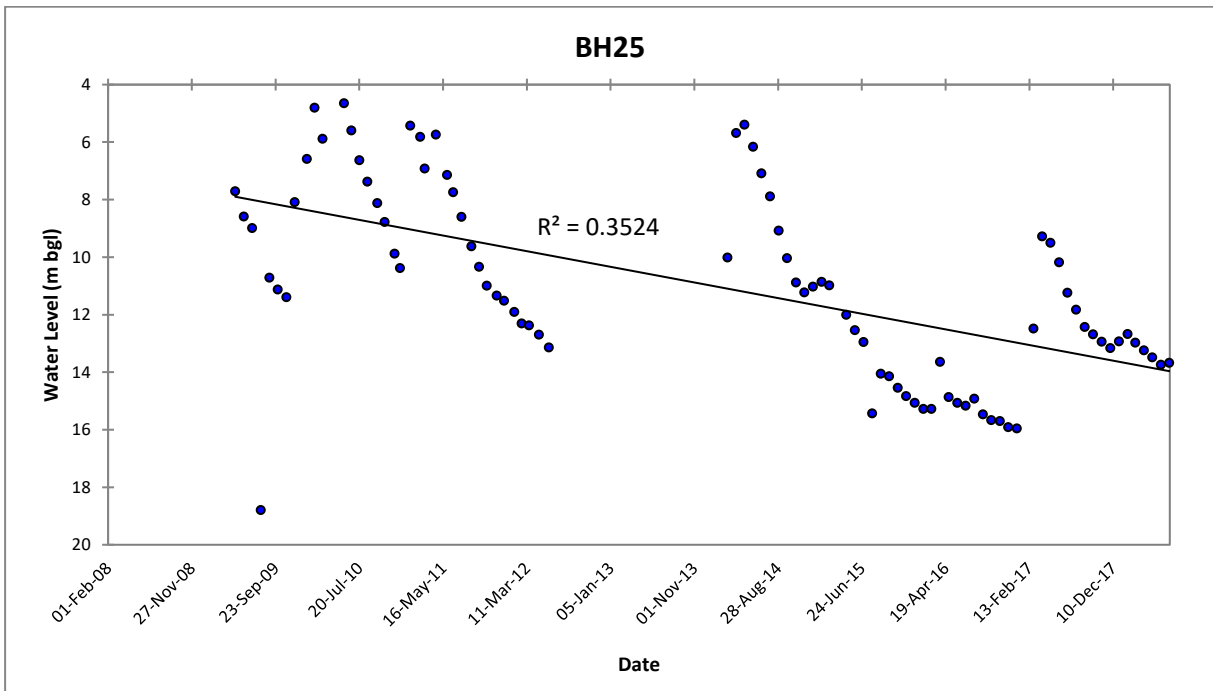
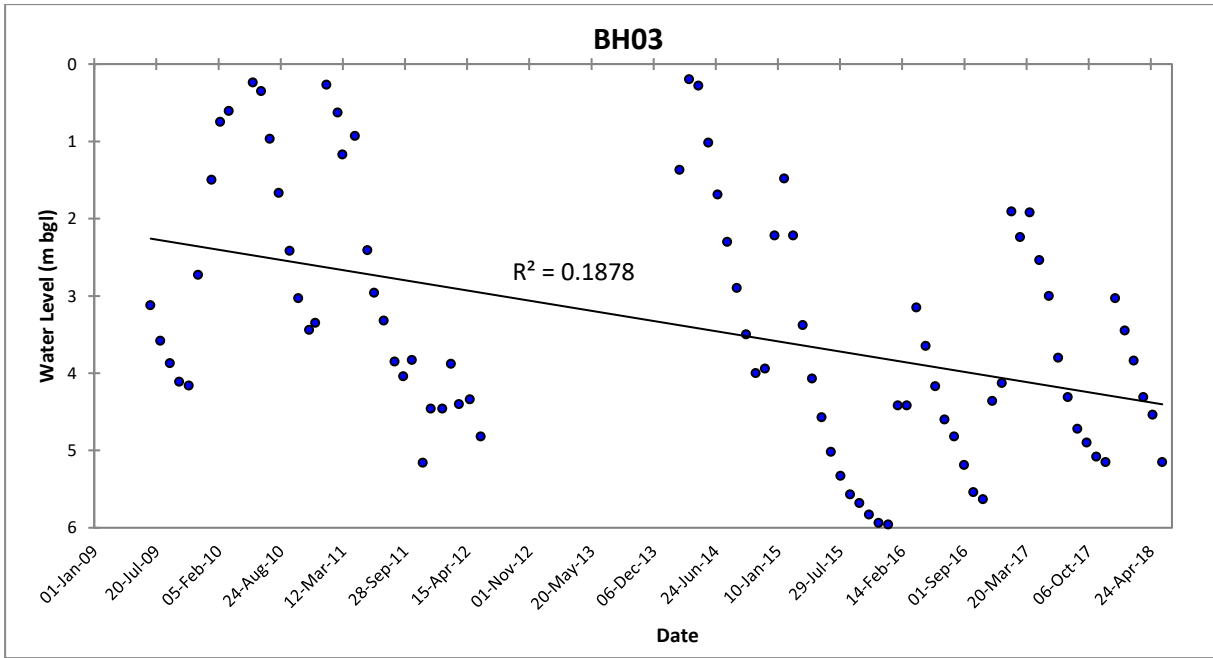
Sample Point ID	Na/Cl	Ca/Mg	Ca+Mg	HCO ₃ +SO ₄	Na+K-Cl/Na+K-Cl+Ca	Cl/Cl+HCO ₃
10490-08	3.954	0.711	0.178	0.438	0.813	0.171
10490-09	4.049	1.215	0.391	1.168	0.607	0.072
10490-10	3.355	1.258	2.444	3.621	0.503	0.351
10490-17	2.181	1.101	0.104	0.449	0.754	0.224
10490-21	5.350	0.885	0.712	2.098	0.664	0.069
10490-25	24.461	1.236	0.929	4.076	0.794	0.020
10490-27	1.921	0.820	0.112	0.540	0.697	0.143
BH02	8.087	0.948	0.298	1.010	0.708	0.039
BH11	2.181	0.588	0.193	0.470	0.656	0.142
BH24	9.631	1.009	0.388	1.209	0.656	0.029
BH25	1.718	0.468	0.138	0.410	0.799	0.207
BH27(LGW-B4)	1.397	0.526	0.062	0.210	0.611	0.192
BH30(LGW-B11)	0.951	0.881	0.336	0.410	0.195	0.194
DWBH-06	2.863	0.749	0.165	0.440	0.642	0.099
DWBH-36	3.644	0.395	0.455	1.190	0.649	0.062
KP05	2.722	0.494	0.136	0.400	0.698	0.104
10490-14	4.482	0.703	0.100	0.290	0.869	0.166
MP14-001	9.428	0.855	0.479	1.589	0.698	0.032
MP14-002	48.554	1.207	0.113	1.815	0.977	0.031
MP14-003	1.836	1.225	0.657	1.630	0.374	0.122
SPRING01	4.642	1.364	0.178	0.671	0.813	0.208
SPRING03	0.946	0.473	0.224	0.625	0.192	0.263
SPRING04	0.812	0.554	0.218	0.350	-0.468	0.588
SPRING06	1.947	3.536	1.820	2.341	0.113	0.142
SPRING11	1.583	2.133	0.317	0.650	0.276	0.142
SPRING12	1.967	0.686	0.037	0.766	0.939	0.217
CSW08	5.656	1.419	1.722	3.840	0.665	0.179
NCSW01	1.458	2.747	0.561	1.134	0.333	0.147
NCSW03	3.294	2.555	1.437	2.932	0.533	0.189
NCSW08	2.214	1.362	0.510	1.128	0.382	0.111
NCSW09	1.299	0.788	0.435	1.012	0.362	0.190
SW01	2.202	2.818	1.980	2.942	0.202	0.168
SW02	5.839	1.376	1.731	3.693	0.670	0.182
SW03	5.159	0.941	0.240	1.041	0.807	0.096
SW04	2.283	0.980	0.283	0.848	0.677	0.207
SW05	1.817	3.445	2.433	3.267	0.105	0.155
SW06	2.289	1.018	0.282	0.889	0.677	0.192
SW07	2.353	1.486	0.759	1.811	0.491	0.164
SW08	2.315	1.038	0.306	0.909	0.639	0.171

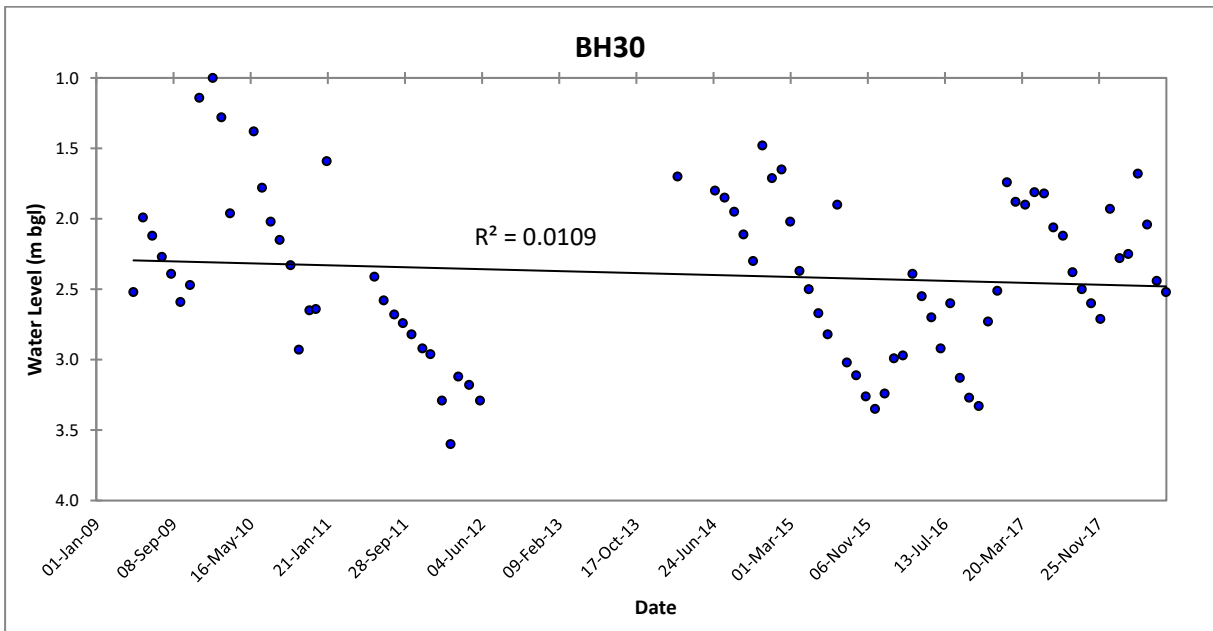
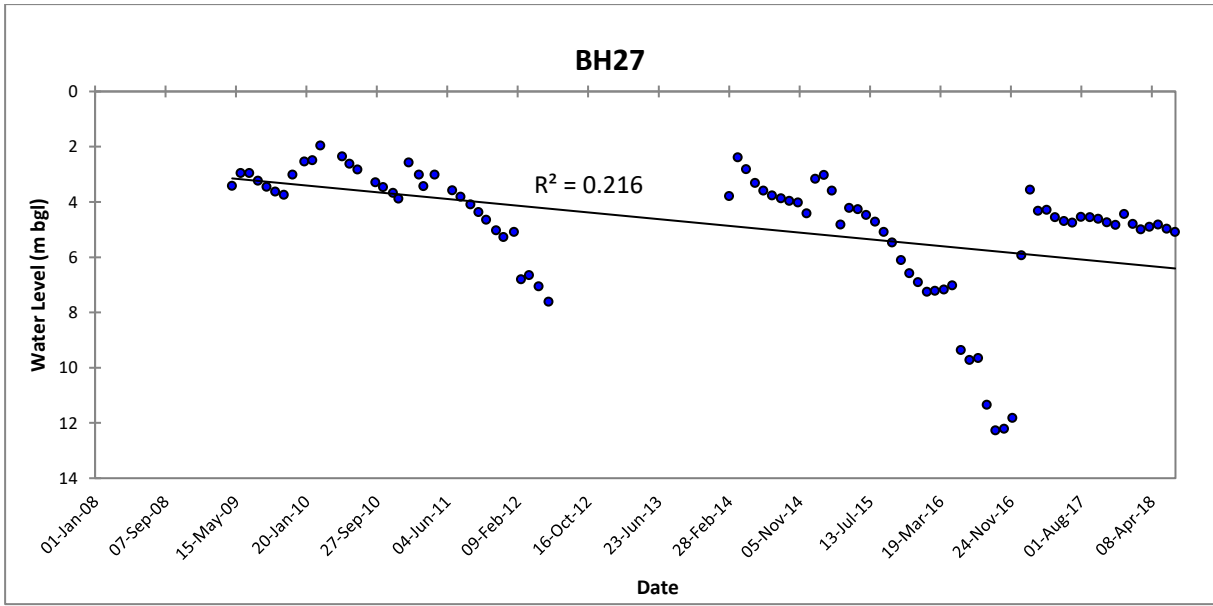
Sample Point ID	Na/Cl	Ca/Mg	Ca+Mg	HCO ₃ +SO ₄	Na+K-Cl/Na+K-Cl+Ca	Cl/Cl+HCO ₃
SW09	1.985	1.063	0.269	0.867	0.645	0.210
SW10	2.571	1.091	0.302	1.031	0.669	0.148
SW11	2.342	2.949	2.194	3.058	0.221	0.188
SW16	7.165	1.218	1.744	4.094	0.735	0.176
SW17	5.487	1.413	1.678	3.785	0.663	0.187
SW18	1.972	3.478	3.041	3.896	0.096	0.136

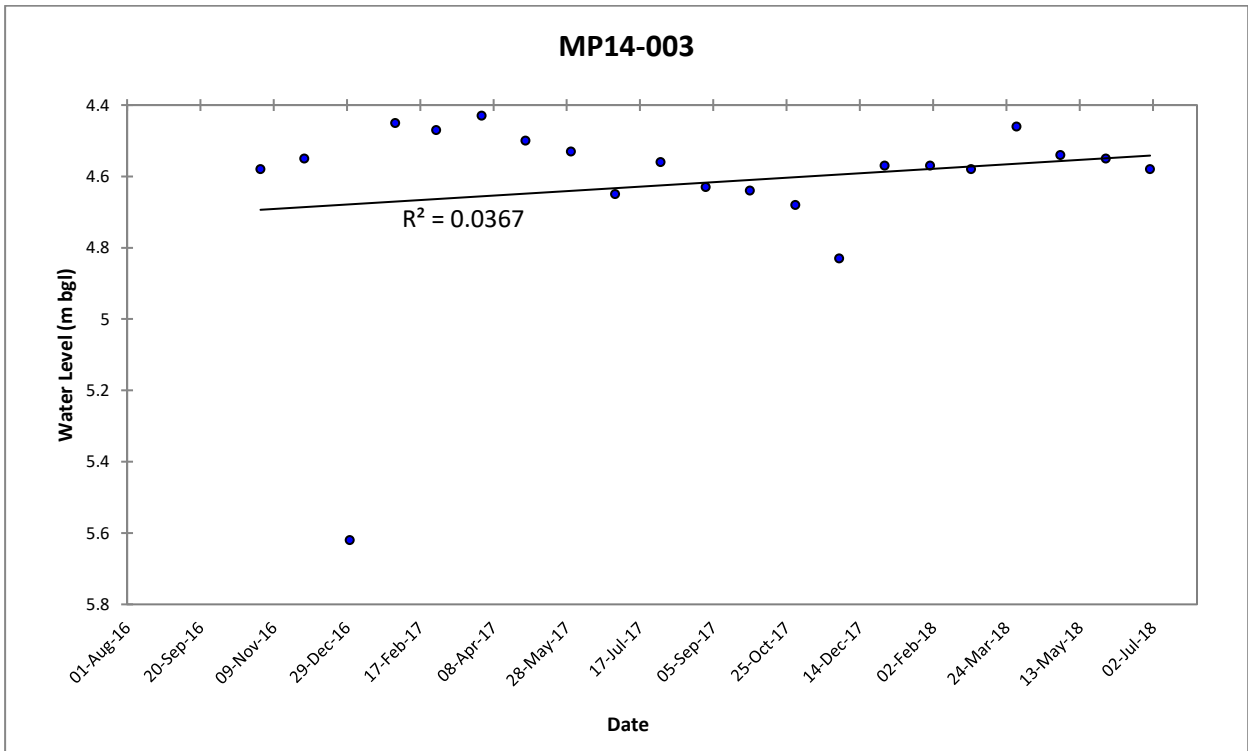
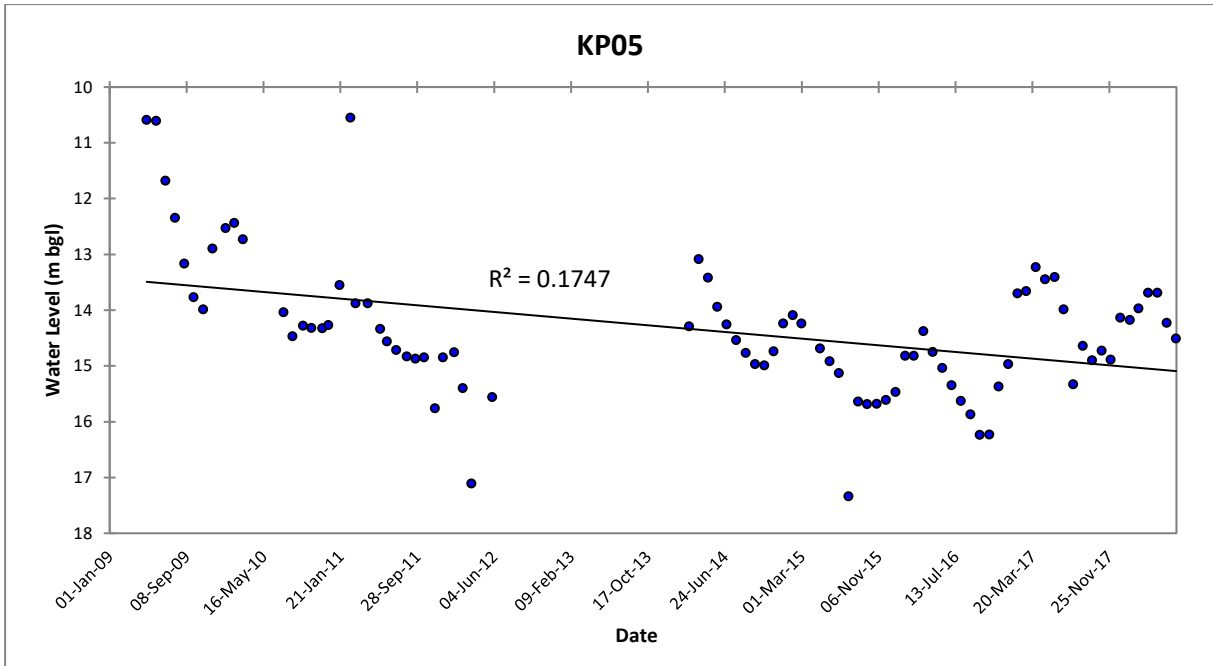
APPENDIX E: GRAPHS OF VARIATIONS IN GROUNDWATER LEVELS











APPENDIX F: TREND ANALYSIS OF HYDROCHEMICAL DATA

P values at 95%

Count	Sample Point ID	pH	EC mS/m	Turbidity NTU	MAIk mg/L	Ca mg/L	Cl mg/L	Mg mg/L	K mg/L	Na mg/L	SO4 mg/L
1	10490-08	0.00001	0.03987	0.44095	0.00284	0.00001	0.00000	0.00025	0.03664	0.00000	0.00001
2	10490-09	0.56191	1.00000	0.00009	0.84310	0.02380	0.00000	0.20451	0.06590	0.01043	0.00578
3	10490-10	0.06736	0.48975	0.32487	0.04146	0.02188	0.17655	0.27025	0.00288	0.42790	0.00202
4	10490-14	0.76726	0.17146	0.01496	0.59333	1.00000	1.00000	0.13463	0.00020	1.00000	0.08532
5	10490-17	0.19197	0.00000	0.27714	0.00141	0.00000	0.00000	0.00002	0.35462	0.00000	0.63968
6	10490-21	0.02086	0.00787	0.21730	0.00047	0.00087	0.00008	0.00019	0.00719	0.00025	0.07446
7	10490-25	0.80128	0.00422	0.03406	0.00036	0.00905	0.00000	0.24343	0.06360	0.07773	0.00191
8	10490-27	0.64437	0.47614	0.00000	0.00032	0.00089	0.00000	0.00004	0.00098	0.00030	0.00035
9	BH02	0.03657	0.00027	0.00007	0.00741	0.69696	0.00906	0.07417	0.01459	0.00000	0.06674
10	BH03	0.98118	0.00098	0.02140	0.52491	0.00008	0.00383	0.00036	0.00078	0.00000	0.00138
11	BH11	0.49579	0.00213	0.15655	0.37624	0.00349	0.46908	0.00105	0.28793	0.00000	0.00243
13	BH24	0.03721	0.01609	0.24402	0.50370	0.36767	0.00006	0.00013	0.54274	0.00000	0.51622
14	BH25	0.27175	0.00029	0.00169	0.00001	0.19921	0.02572	0.15977	0.32448	0.00000	0.05705
15	BH27	0.00022	0.01266	0.00004	0.00010	0.20336	0.00000	0.13130	0.11962	0.22775	0.00006
16	BH30	0.00005	0.00000	0.02266	0.00002	0.00070	0.00000	0.00000	0.00005	0.19527	0.00001
17	CSW08	0.76887	0.00021	0.07373	0.09974	0.00028	0.00156	0.53103	0.10938	0.94435	0.00000
18	DWBH-06	0.16917	0.00978	0.02756	0.13625	0.36604	0.00000	0.31836	0.11069	0.89010	0.01044
19	DWBH-07	1.00000	0.01472	0.22574	0.00853	0.86103	0.30077	0.01253	0.18164	0.00507	0.04131
20	DWBH-36	0.00965	0.15825	0.00001	0.01385	0.01765	0.00000	0.05667	0.85926	0.00006	0.13354
21	KP05	0.00000	0.00000	0.00002	0.00001	0.17104	0.00000	0.00003	0.45885	0.00000	0.58172
22	MP14-001	0.89493	0.13591	0.03267	0.36193	0.05428	0.31222	0.08600	0.00027	0.00105	0.03545
23	MP14-002	0.16867	0.00037	0.04759	0.03267	0.00624	0.47010	0.00142	0.00099	0.04361	1.00000

Count	Sample Point ID	pH	EC mS/m	Turbidity NTU	MAIk mg/L	Ca mg/L	Cl mg/L	Mg mg/L	K mg/L	Na mg/L	SO4 mg/L
24	MP14-003	0.52164	1.00000	0.81656	0.75003	0.33918	0.67137	0.18542	0.81971	0.07102	0.04361
25	NCSW01	0.26400	0.20055	0.46395	0.40112	0.15561	0.13253	0.40226	0.34209	0.09403	0.16112
26	NCSW03	0.00405	0.14793	0.54435	0.57443	0.01981	0.27445	0.95825	0.00030	0.57210	0.39796
27	NCSW08	0.34117	0.00000	0.06756	0.00006	0.00000	0.05813	0.14989	0.94211	0.24542	0.10155
28	NCSW09	0.00586	0.17583	0.00010	0.40604	0.80951	0.51461	1.00000	0.03009	0.03175	0.00034
29	Spring01	0.89974	0.75868	0.97770	0.15945	0.85851	0.01763	0.37106	0.13201	0.64862	0.02103
30	Spring02	0.00025	0.00237	0.36558	0.00712	0.00018	0.00147	0.00139	0.73914	0.43105	0.10325
31	Spring03	0.04139	0.05919	0.25425	0.62399	0.00414	0.02884	0.90641	0.95651	0.41122	0.00012
32	Spring04	0.00000	0.00000	0.04623	0.91295	0.00000	0.00000	0.00000	0.00057	0.74824	0.16144
33	Spring06	0.72493	0.00927	0.37177	0.00144	0.04380	0.00000	0.01709	0.02374	0.00008	0.02628
34	Spring11	0.08581	0.00000	0.61452	0.00001	0.00000	0.00000	0.16964	0.11606	0.00496	0.00399
35	Spring12	0.00029	0.00000	0.00011	0.00000	0.00000	0.00001	0.00000	0.00000	0.00000	0.00419
36	SW01	0.12691	0.00758	0.00184	0.00000	0.10035	0.00000	0.05226	0.00000	0.00000	0.05050
37	SW02	1.00000	0.00644	0.01777	0.05237	0.07114	0.00015	0.74006	0.00085	0.00804	0.00001
38	SW03	0.36780	0.00014	0.00768	0.00014	0.00000	0.31506	0.00000	0.00022	0.00225	0.16403
39	SW04	0.55205	0.00090	0.01733	0.32544	0.00132	0.76513	0.00000	0.86111	0.00015	0.01324
40	SW05	0.00040	0.00102	0.19082	0.23269	0.00124	0.00000	0.00149	0.00050	0.00209	0.00035
41	SW06	0.98618	0.05567	0.22100	0.51561	0.65358	0.00068	0.77993	0.23886	0.69933	0.20238
42	SW07	0.63781	0.00001	0.09402	0.00074	0.00000	0.00000	0.58001	0.02026	0.00000	0.00012
43	SW08	0.23753	0.03692	0.00583	0.03734	0.46281	0.00521	0.61630	0.04226	0.15084	0.00083
44	SW09	0.00139	0.17571	0.13617	0.71541	0.04360	0.00232	0.62390	0.00054	0.30546	0.08534
45	SW10	0.55305	0.78520	0.60427	0.95203	0.00091	0.06880	0.09536	0.51184	0.65959	0.12955
46	SW11	0.00197	0.00000	0.03164	0.00018	0.00000	0.00000	0.00000	0.00015	0.00000	0.00000
47	SW16	0.08167	0.00145	0.44800	0.05788	0.00005	0.00273	0.18038	0.00058	0.00398	0.00000
48	SW17	0.85067	0.00015	0.01533	0.08142	0.05198	0.00065	0.30342	0.00026	0.00583	0.00000
49	SW18	0.41752	0.93710	0.41657	0.10659	0.49390	0.31086	0.85245	0.35698	0.09971	0.32503

Summary of Hydrochemical data MK Trend Test

Count	Sample Point ID	pH	EC (mS/m)	Turbidity (NTU)	Total Alkalinity mg/L	Ca mg/L	Cl mg/L	Mg mg/L	K mg/L	Na mg/L	SO4 mg/L
1	10490-08	Decreasing	Decreasing	No Trend	Decreasing	Decreasing	Increasing	Decreasing	Increasing	Decreasing	Increasing
2	10490-09	No Trend	No Trend	Decreasing	No Trend	Decreasing	Increasing	No Trend	No Trend	Decreasing	Increasing
3	10490-10	No Trend	No Trend	No Trend	Increasing	Decreasing	No Trend	No Trend	Increasing	No Trend	Increasing
4	10490-14	No Trend	No Trend	Decreasing	No Trend	No Trend	No Trend	No Trend	Decreasing	No Trend	No Trend
5	10490-17	No Trend	Decreasing	No Trend	Decreasing	Decreasing	Increasing	Decreasing	No Trend	Decreasing	No Trend
6	10490-21	Decreasing	Decreasing	No Trend	Decreasing	Decreasing	Increasing	Decreasing	Decreasing	Decreasing	No Trend
7	10490-25	No Trend	Increasing	Increasing	Increasing	Increasing	Increasing	No Trend	No Trend	No Trend	Decreasing
8	10490-27	No Trend	No Trend	Increasing	Decreasing	Decreasing	Increasing	Decreasing	Decreasing	Decreasing	Increasing
9	BH02	Increasing	Increasing	Increasing	Increasing	No Trend	Increasing	No Trend	Increasing	Decreasing	No Trend
10	BH03	No Trend	Decreasing	Decreasing	No Trend	Decreasing	Decreasing	Decreasing	Decreasing	Decreasing	Increasing
11	BH11	No Trend	Decreasing	No Trend	No Trend	Decreasing	No Trend	Decreasing	No Trend	Decreasing	Increasing
13	BH24	Decreasing	Increasing	No Trend	No Trend	No Trend	Increasing	Decreasing	No Trend	Decreasing	No Trend
14	BH25	No Trend	Decreasing	Decreasing	Increasing	No Trend	Decreasing	No Trend	No Trend	Decreasing	No Trend
15	BH27	Decreasing	Increasing	Decreasing	Decreasing	No Trend	Increasing	No Trend	No Trend	No Trend	Increasing
16	BH30	Decreasing	Increasing	Decreasing	Decreasing	Increasing	Increasing	Increasing	Increasing	No Trend	Increasing
17	CSW08	No Trend	Increasing	No Trend	No Trend	Increasing	Increasing	No Trend	No Trend	No Trend	Increasing
18	DWBH-06	No Trend	Increasing	Decreasing	No Trend	No Trend	Increasing	No Trend	No Trend	No Trend	Increasing
19	DWBH-07	No Trend	Increasing	No Trend	Increasing	No Trend	No Trend	Increasing	No Trend	Decreasing	Increasing
20	DWBH-36	Decreasing	No Trend	Decreasing	Decreasing	Decreasing	Increasing	No Trend	No Trend	Decreasing	No Trend
21	KP05	Increasing	Increasing	Decreasing	Increasing	No Trend	Increasing	Increasing	No Trend	Decreasing	No Trend

Count	Sample Point ID	pH	EC (mS/m)	Turbidity (NTU)	Total Alkalinity mg/L	Ca mg/L	Cl mg/L	Mg mg/L	K mg/L	Na mg/L	SO4 mg/L
22	MP14-001	No Trend	No Trend	Increasing	No Trend	No Trend	No Trend	No Trend	Decreasing	Decreasing	Decreasing
23	MP14-002	No Trend	Increasing	Decreasing	Increasing	Decreasing	No Trend	Decreasing	Decreasing	Increasing	No Trend
24	MP14-003	No Trend	No Trend	No Trend	No Trend	No Trend	No Trend	No Trend	No Trend	No Trend	Decreasing
25	NCSW01	No Trend	No Trend	No Trend	No Trend	No Trend	No Trend	No Trend	No Trend	No Trend	No Trend
26	NCSW03	Decreasing	No Trend	No Trend	No Trend	Increasing	No Trend	No Trend	Decreasing	No Trend	No Trend
27	NCSW08	No Trend	Increasing	No Trend	Increasing	Increasing	No Trend	No Trend	No Trend	No Trend	No Trend
28	NCSW09	Decreasing	No Trend	Decreasing	No Trend	No Trend	No Trend	No Trend	Decreasing	Decreasing	Decreasing
29	Spring01	No Trend	No Trend	No Trend	No Trend	No Trend	Increasing	No Trend	No Trend	No Trend	Increasing
30	Spring02	Decreasing	Increasing	No Trend	Increasing	Increasing	Increasing	Increasing	No Trend	No Trend	No Trend
31	Spring03	Decreasing	No Trend	No Trend	No Trend	Decreasing	Increasing	No Trend	No Trend	No Trend	Decreasing
32	Spring04	Decreasing	Increasing	Increasing	No Trend	Increasing	Increasing	Increasing	Increasing	No Trend	No Trend
33	Spring06	No Trend	Increasing	No Trend	Increasing	Increasing	Increasing	Increasing	Increasing	Increasing	Increasing
34	Spring11	No Trend	Increasing	No Trend	Increasing	Increasing	Increasing	No Trend	No Trend	Decreasing	Increasing
35	Spring12	Decreasing	Decreasing	Increasing	Decreasing	Decreasing	Increasing	Decreasing	Decreasing	Decreasing	Increasing
36	SW01	No Trend	Increasing	Decreasing	Increasing	No Trend	Increasing	No Trend	Increasing	Increasing	No Trend
37	SW02	No Trend	Increasing	Decreasing	No Trend	No Trend	Increasing	No Trend	Increasing	Increasing	Increasing
38	SW03	No Trend	Decreasing	Increasing	Decreasing	Decreasing	No Trend	Decreasing	Increasing	Decreasing	No Trend
39	SW04	No Trend	Decreasing	Decreasing	No Trend	Decreasing	No Trend	Decreasing	No Trend	Decreasing	Increasing
40	SW05	Decreasing	Increasing	No Trend	No Trend	Increasing	Increasing	Increasing	Increasing	Increasing	Increasing
41	SW06	No Trend	No Trend	No Trend	No Trend	No Trend	Increasing	No Trend	No Trend	No Trend	No Trend
42	SW07	No Trend	Increasing	No Trend	Increasing	Increasing	Increasing	No Trend	Increasing	Increasing	Increasing
43	SW08	No Trend	Increasing	Decreasing	Increasing	No Trend	Increasing	No Trend	Decreasing	No Trend	Decreasing

Count	Sample Point ID	pH	EC (mS/m)	Turbidity (NTU)	Total Alkalinity mg/L	Ca mg/L	Cl mg/L	Mg mg/L	K mg/L	Na mg/L	SO4 mg/L
44	SW09	Decreasing	No Trend	No Trend	No Trend	Decreasing	Increasing	No Trend	Decreasing	No Trend	No Trend
45	SW10	No Trend	No Trend	No Trend	No Trend	Decreasing	No Trend	No Trend	No Trend	No Trend	No Trend
46	SW11	Increasing	Increasing	Decreasing	Increasing	Increasing	Increasing	Increasing	Increasing	Increasing	Increasing
47	SW16	No Trend	Increasing	No Trend	No Trend	Increasing	Increasing	No Trend	Increasing	Increasing	Increasing
48	SW17	No Trend	Increasing	Decreasing	No Trend	No Trend	Increasing	No Trend	Increasing	Increasing	Increasing
49	SW18	No Trend	No Trend	No Trend	No Trend	No Trend	No Trend	No Trend	No Trend	No Trend	No Trend